Accelerator perspectives for Synchrotron Light Sources

M. E. Couprie
Synchrotron SOLEIL

EUCARD, EUCARD2 and and Workshop on Visions for accelertor future, CERN, June 11-13, 2013

Synchrotron Radiation

- *J. Larmor, Phil. Mag. 44, 503 (1897)*
- 1898 : First correct calculation of the emitted power by an accelerated charged particule $(E/mc^2)^4/R^2$, *A. Liénard, L' Eclairage électrique, 16, 5 (1898)*
- 1907-1912 : angular and spectral distribution and polarization properties, *G.A. Schott, Ann. Phys. 24, 635 (1907), G. A. Schott, Electromagentic Radiation, Cambridge University Press (1912)*
- 1944 : energy limit (0.5 GeV) due to losses due to radiating electrons in a beatraton, *D. Ivanenko and I. Pomeranchuk, Phys. Rev. 65, 343 (1944)*
- 1945-46: phase stability *E. M. McMillan, PRL 68, 1434 (1945), V. Veksler J. Phys. USSR 9, 153 (1946)*
- 1946 : synchrotron construction *F. K. Gloward et al;, Nature 158, 413 (1946)* particle energy loss measurement on the 100 MeV betatron, attempt to observe synchrotron radiation in the micro-waves failed, *J. P. Blewett, Phys. Rev. 69, 87 (1946)*
- 1946 : theory on peak spectrum and higher photon energies, *J. Schwinger, Phys. Rev. 70, 798 (1946)*
- 1947 : first observation of synchrotron radiation *F. R. Elder, A.M. Gurewitsch, R.V. Langmuir, H. C. Pollock, Radiation from Electrons in a Synchrotron, Physical Review, 71, 11, (1947), 829-830*

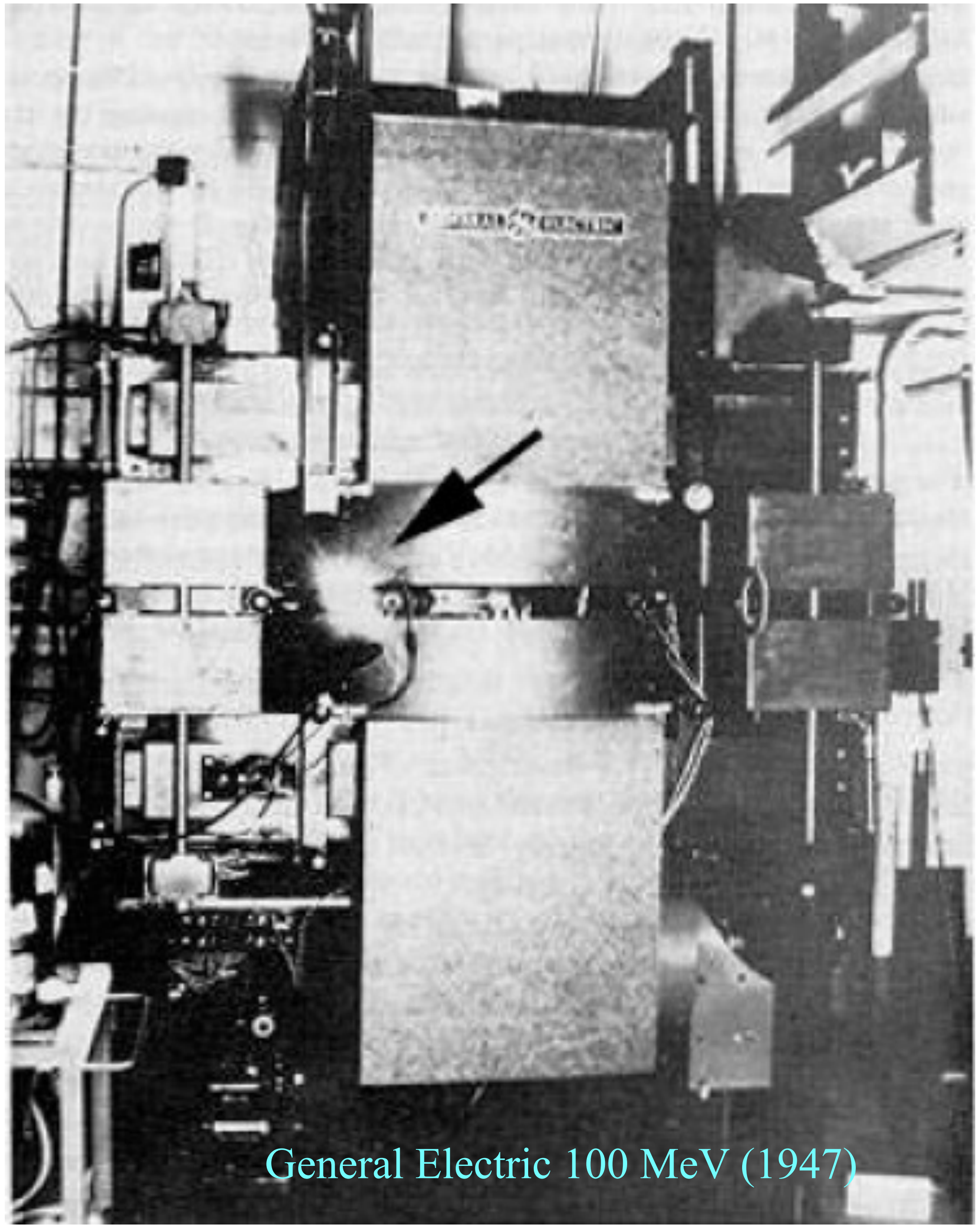
General Electric 100 MeV (1947)

50 years spent for the observation of SR !

J. P. Blewett, 50 years of synchrotron radiation, J. Synchrotron Rad. , 5, 135-139 (1998)

Undulator Radiation

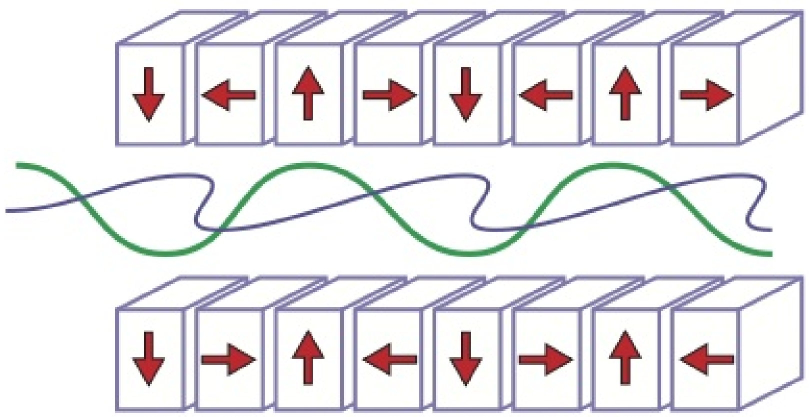

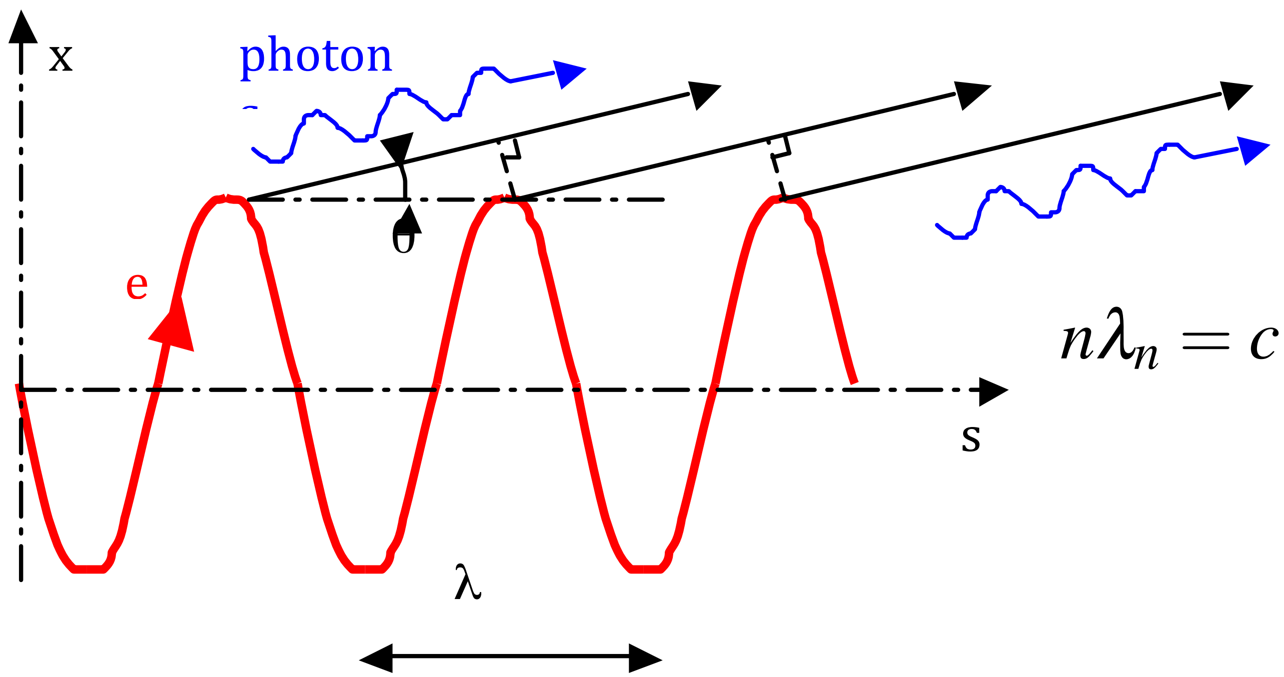

$$n\lambda_n = c(1-\beta_s)t$$

$$\vec{B_u} = B_u \cos(\frac{2\pi}{\lambda_u}s)\vec{z} \qquad K_u = \frac{eB_u\lambda_u}{2\pi m_o c}$$

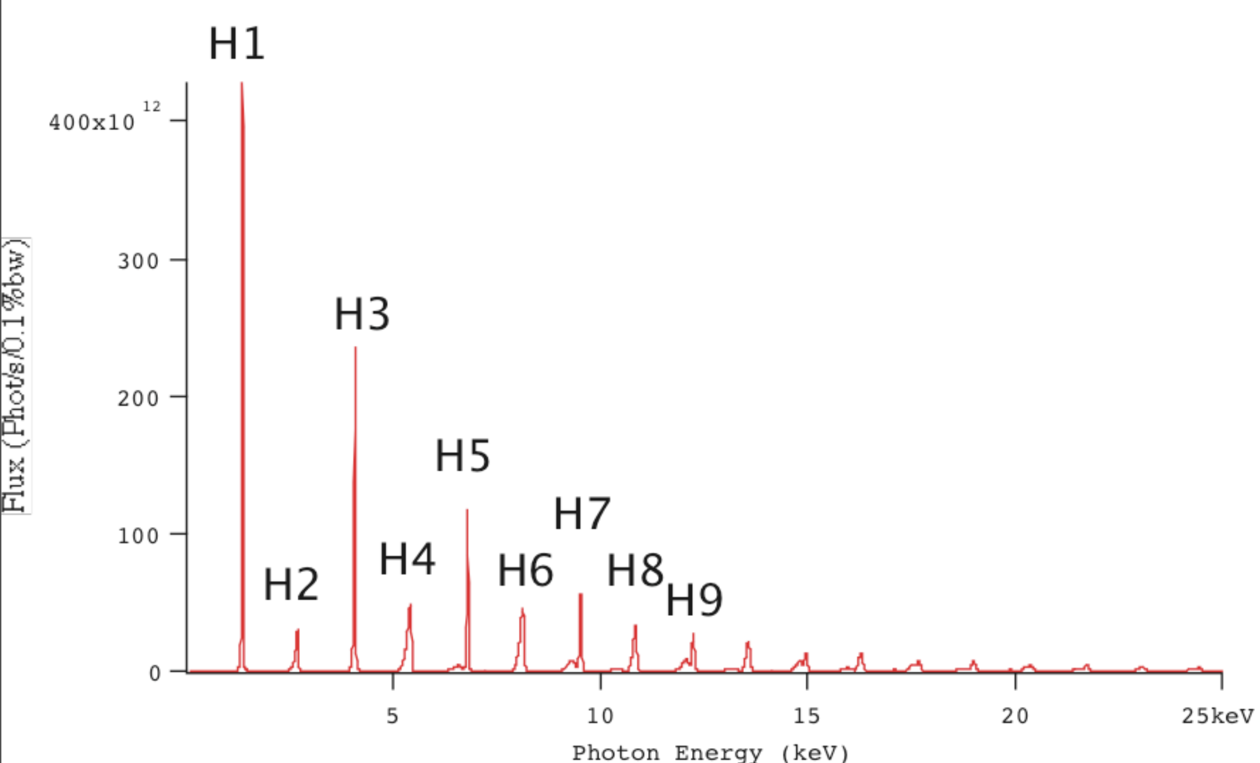

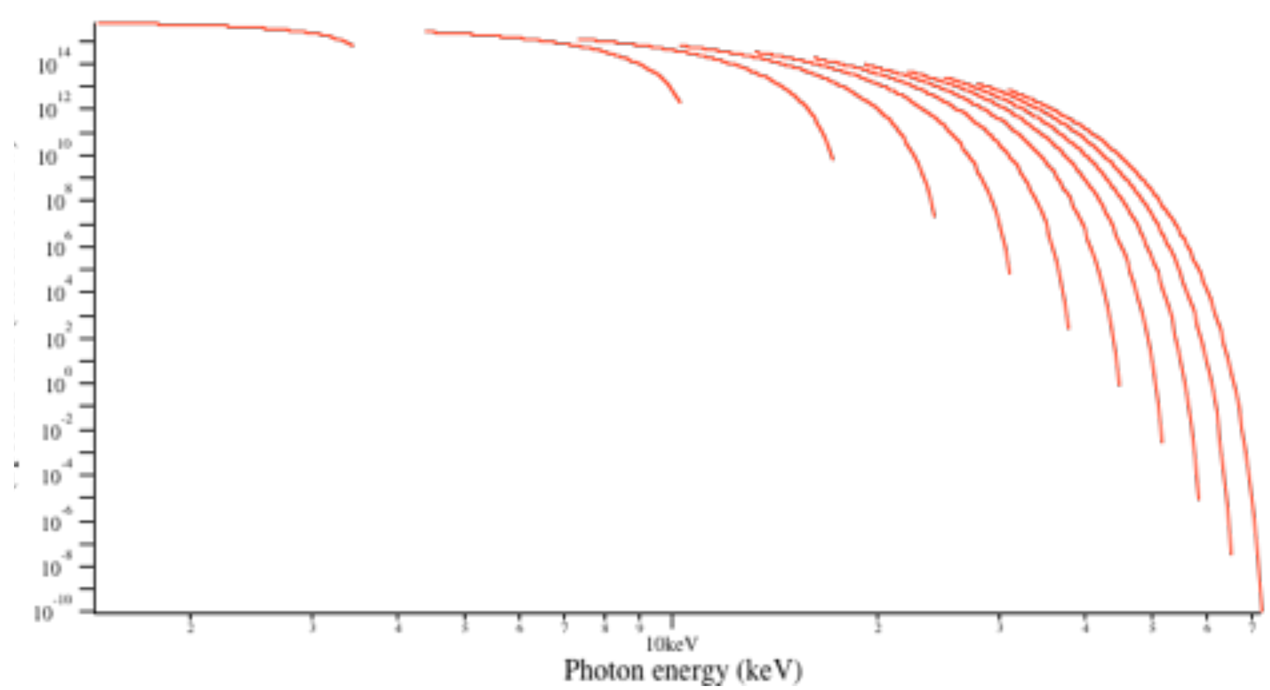

SOLEIL @ 2.75 GeV, U20, K=1.81, Gap 5.5 mm
300 µmx300 µm at 15 m observation

Undulator Radiation : divergence

$$\lambda_n = \frac{\lambda_u}{2\gamma^2 n}\left(1 + \frac{K_{ux}^2}{2} + \frac{K_{uz}^2}{2} + \gamma^2\theta_x^2 + \gamma^2\theta_z^2\right)$$

ACO

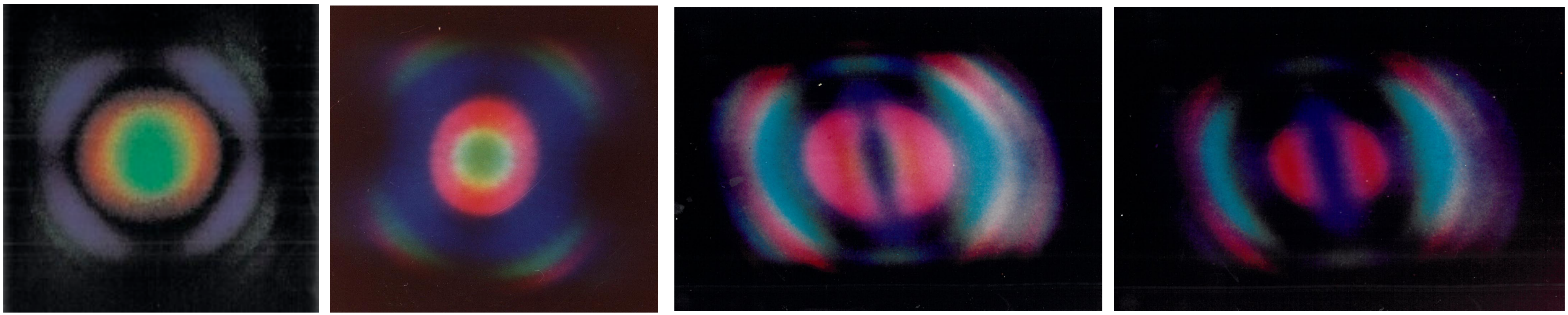

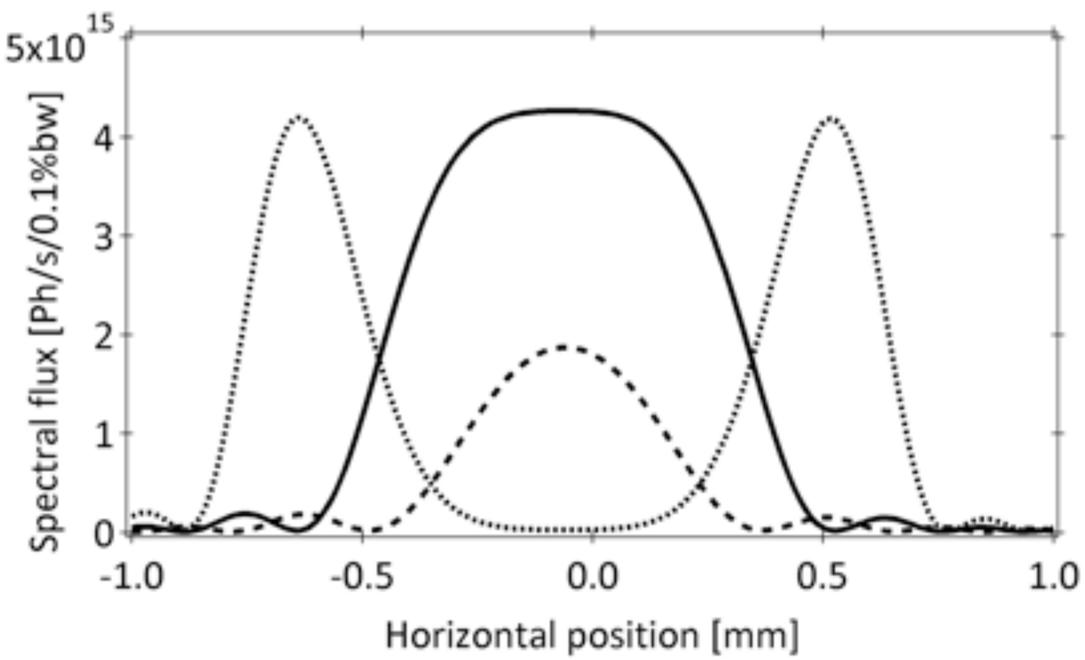

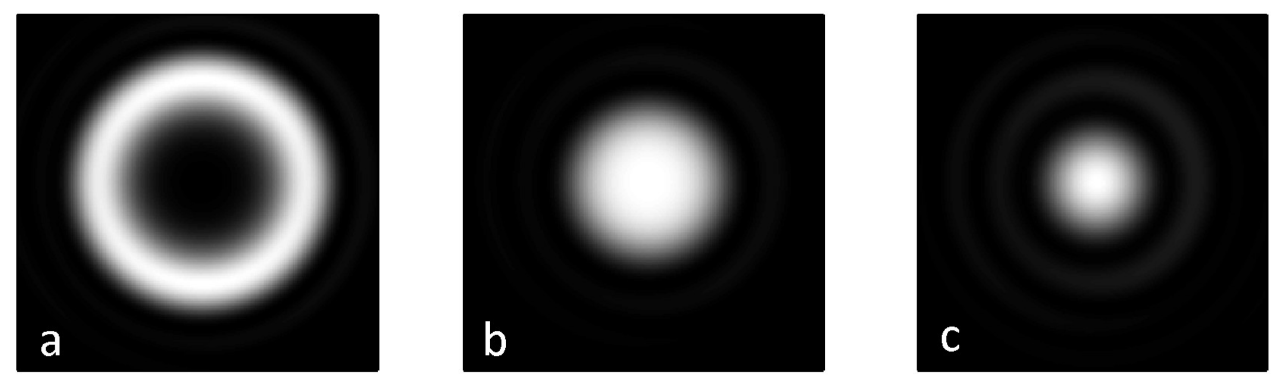

1470 eV

1480 eV : resonant wavelength

1487 eV

$$\sigma_{ph} = 0.69\sqrt{\frac{\lambda_n}{2L}} = \frac{0.69}{2\gamma}\sqrt{\frac{(1+\frac{K_{ux}^2}{2}+\frac{K_{uz}^2}{2})}{nN}}$$

5th harmonic radiation

- $\lambda < \lambda_r$: minimum divergence, lower flux
- $\lambda = \lambda_r$: intermediate
- $\lambda > \lambda_r$: larger divergence, larger flux; non Gaussian

Influence of energy spread and emittance on the undulator spectrum

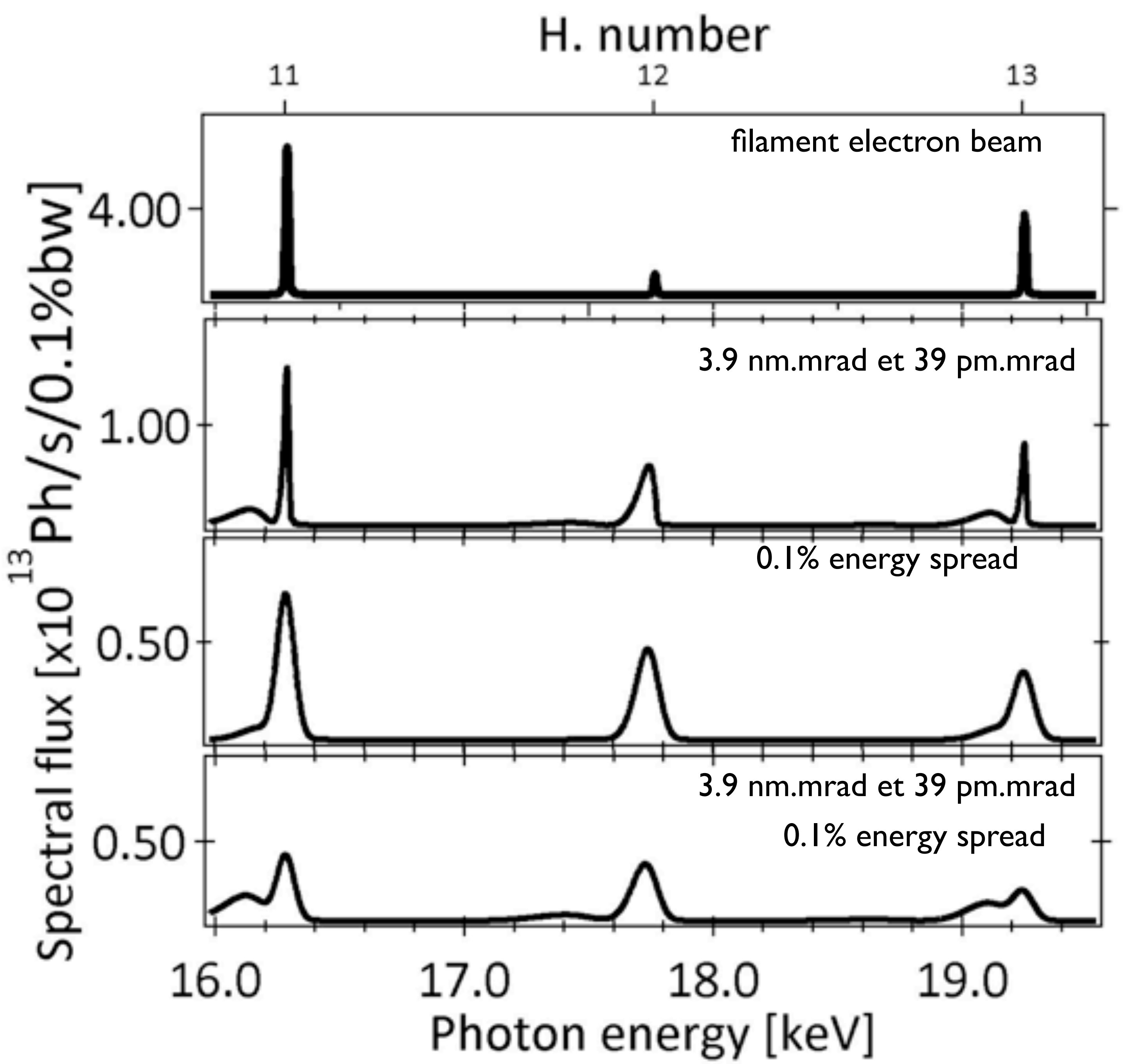

U20 case, 0.97 T, 2.75 GeV

$$\lambda_n = \frac{\lambda_u}{2\gamma^2 n}\left(1 + \frac{K_{ux}^2}{2} + \frac{K_{uz}^2}{2} + \gamma^2\theta_x^2 + \gamma^2\theta_z^2\right)$$

- Homogeneous linewidth :

$$\frac{\Delta\lambda}{\lambda_n} = \frac{1}{nN_u}$$

- Inhomogeneous linewidth :

  - Emittance : via $\gamma^2\theta_x^2 + \gamma^2\theta_z^2$

  - Energy spread $\Delta\lambda/\lambda = 2\sigma_\gamma$

Brilliance

Wigner distribution : general case — *K. J. Kim, Nucl. Instr. Meth. A 246, 71 (1986)* *I. Bazanov, PRSTAB 15 (2012) 050703*

$$B(x,z,x',z',s,w,\vec{u}) = \frac{\varepsilon_0 w^2}{2\pi^2 hc}\frac{I}{E}\int_{-\infty}^{+\infty}\int_{-\infty}^{+\infty}\left(\vec{E}\left(x'+\frac{b_x}{2},s,w\right)\vec{u}^*\right)$$

$$\times\left(\vec{E}^*\left(x'-\frac{b_x}{2},s,w\right)\vec{u}\right)\exp\left(-i\frac{w}{c}\vec{x}\,\vec{b}_x\right)db_x db_z$$

B: Nber of photons per cell phase space

$\nu = \Delta x\ \Delta x'\ \Delta z\ \Delta z'\ \Delta t\ \ \Delta\omega / \omega$

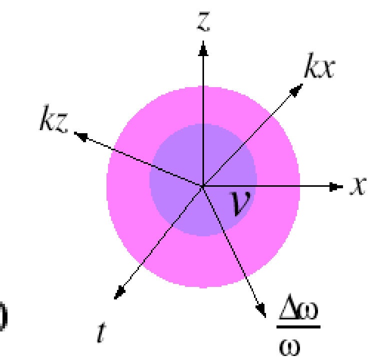

APPROXIMATION of Gaussian beam

$$B = \left(\frac{w}{\pi c}\right)^2 \Phi(w,\vec{u})\exp\left(-\frac{\theta_x^2}{2\sigma_{x'ph}} - \frac{\theta_z^2}{2\sigma_{z'ph}} - \frac{x^2}{2\sigma_{xph}} - \frac{z^2}{2\sigma_{zph}}\right)$$

$\sigma_{x'ph}$ $\sigma_{z'ph}$ Convolution of the electron and photon distributions

$$\sigma_i = \sqrt{\varepsilon_i\beta_i + \eta_i^2\sigma_\gamma^2}$$

$$\sigma_i' = \sqrt{\varepsilon_i(1+\beta_i^2/4)/\beta_i + \eta_i'^2\sigma_\gamma^2}$$

$$\Sigma_{ph} = 2.74\sqrt{\lambda_n L}/4\pi = \frac{1.89\lambda_u}{4\pi\gamma}\sqrt{\frac{N}{2}\frac{(1+\frac{K_{ux}^2}{2}+\frac{K_{uz}^2}{2})}{nN}}$$

$$\Sigma_{ph}' = 0.69\sqrt{\frac{\lambda_n}{2L}} = \frac{0.69}{2\gamma}\sqrt{\frac{(1+\frac{K_{ux}^2}{2}+\frac{K_{uz}^2}{2})}{nN}}$$

emission matching:

$\sigma_i / \sigma_i' = \Sigma_{ph} / \Sigma_{ph}'$

$\beta = L/ 4\pi$

Fourier limit : Δω. Δτ ~ 1

Case of Gaussian beams : c Δt.Δλ/λ²=0.44

Diffraction limit:

Δx. Δx' ~ 1.34 λ/ 4π

Coherence

Transverse coherence

$$M(x,z,x',z',b_x,s,\omega,\vec{u}) = \sum_i \left(\vec{E_i}\left(x+\frac{b_x}{2},s,\omega\right)\vec{u}^*\right)\left(\vec{E_i^*}\left(x-\frac{b_x}{2},s,\omega\right)\vec{u}\right)$$

$$M(x,z,x',z',b_x,s,\omega,\vec{u}) = \frac{h}{2\pi\varepsilon_0 c}\frac{e}{I}\int_{-\infty}^{+\infty}\int_{-\infty}^{+\infty} B(x,z,x',z',s,\omega,\vec{u})\exp\left(-\frac{\omega}{c}\vec{x'}\,\vec{bx}\right)dxdz$$

K.J. Kim, Nucl. Instr. Meth. A 246, 71–76 (1986),; Bazanovl.V.:.Phys.Rev.Spec.Topics AB 15, 050703 (2012)

Longitudinal coherence

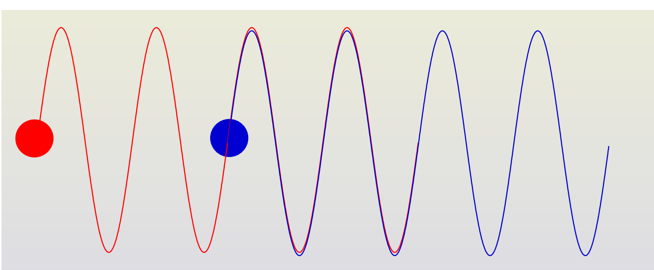

in phase

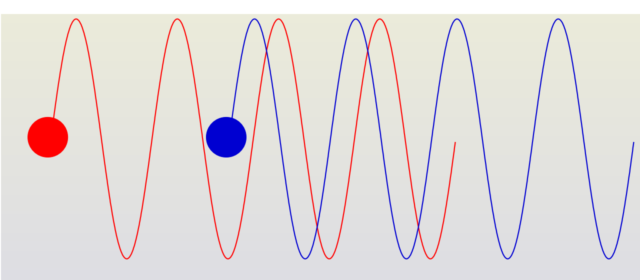

random emission

$$P(\lambda) = P_{inc} + P_{coh} = P_{1e}(\lambda)\left[\overbrace{N}^{incoherent} + \overbrace{(N-1)N|\tilde{\rho}(\lambda)|^2}^{coherent}\right]$$

Texte

P_{1e} : power emitted by one electron

N: number of electrons

$\tilde{\rho}(\lambda)$: Fourier transform of the bunch longitudinal charge distribution $\rho(z)$

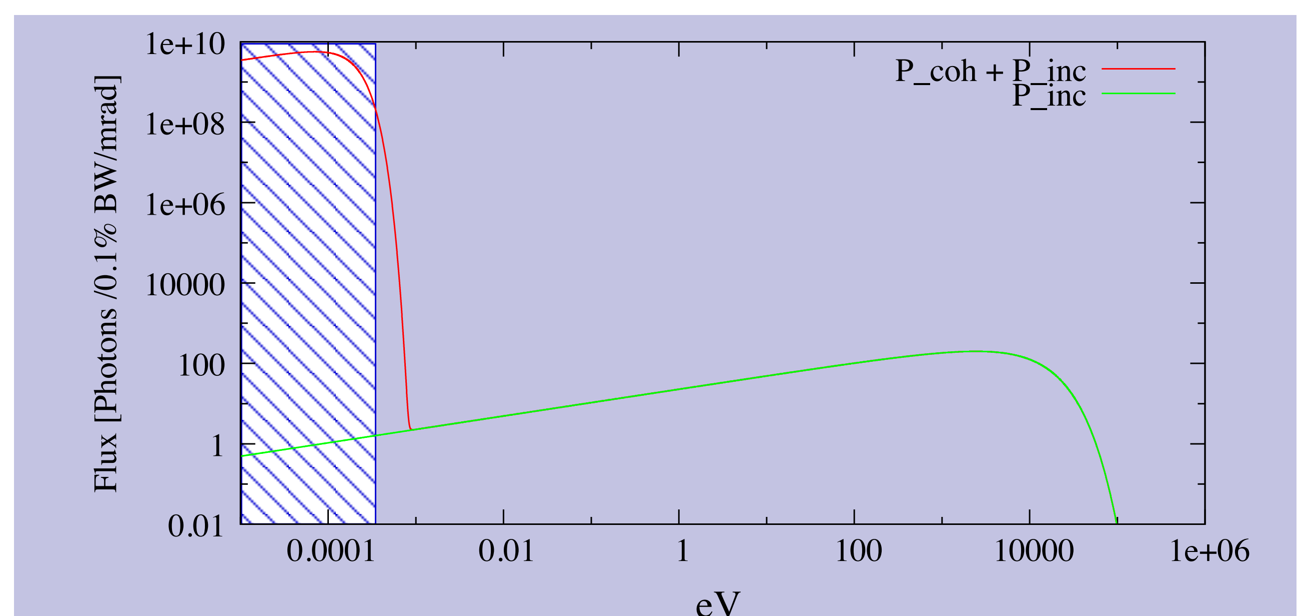

Free Electron Laser

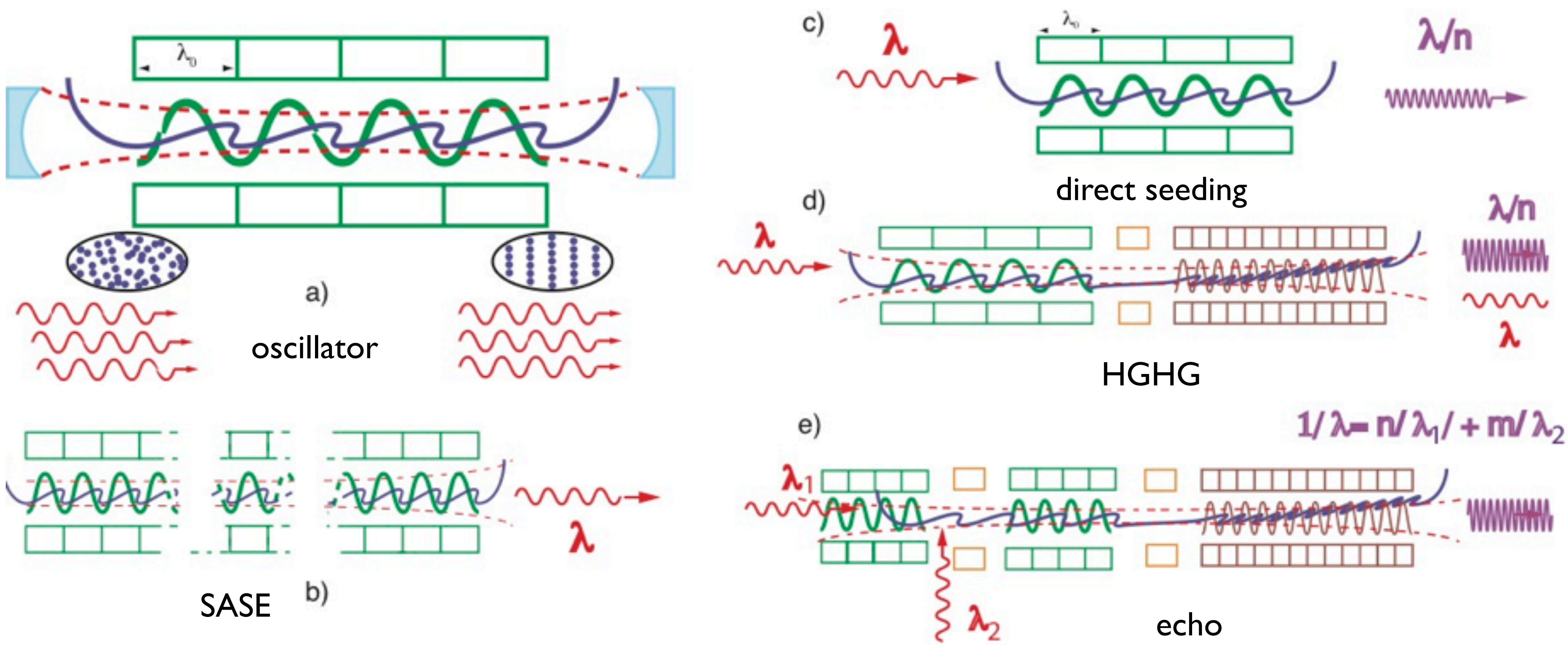

$$\lambda = \frac{\lambda_0}{2n\gamma^2}\left(1+\frac{K^2}{2}\right) \qquad K = 0.94\,\lambda_0\,(\mathrm{cm})\,B_0\,(\mathrm{T}) \qquad G \alpha L_{ond}^2/\Upsilon^3$$

- electron beam-optical wave interaction (spontaneous, stored spontaneous emission, external laser tuned on the fundamental wavelength λ of the undulator)
- energy exchange between the optical wave and the electrons
- microbunching (λ separation)
- coherent emission
- saturation (enhancement of energy spread, unsatisfied resonance condition)

Accelerator type

Storage ring

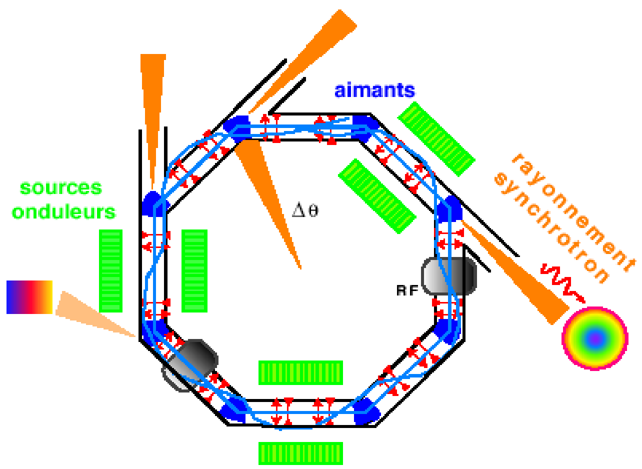

10–30ps, εαE²
Energy spread : 0.1 %

Linear accelerator

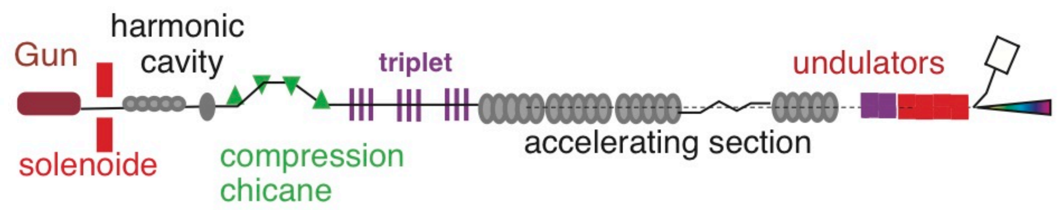

10 fs–10 ps, εα1/E

Energy spread : 0.01 %

Repetition rate : depending on the linac (room temperature or superconducting)

Energy recovery Linac (ERL)

M.Tigner Nuovo Cimento 1965

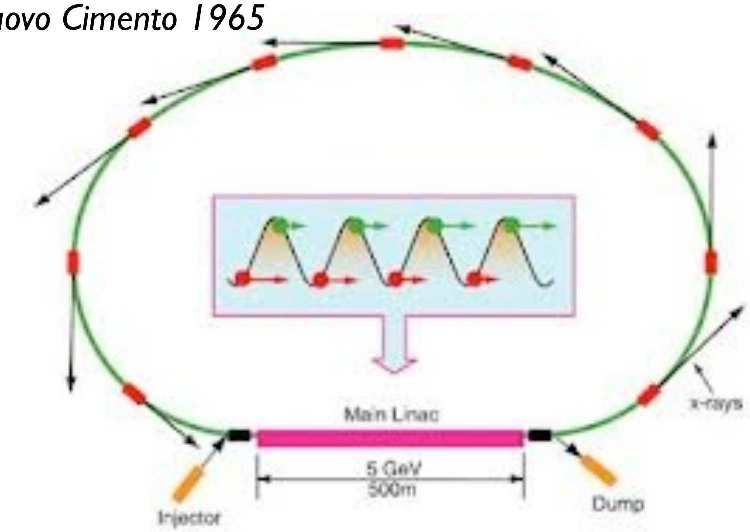

Ex ALS

Ex FLASH

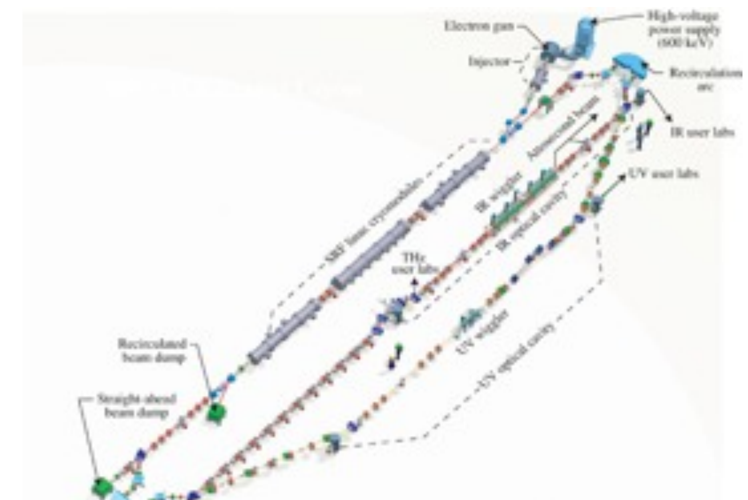

Ex Jefferson Lab

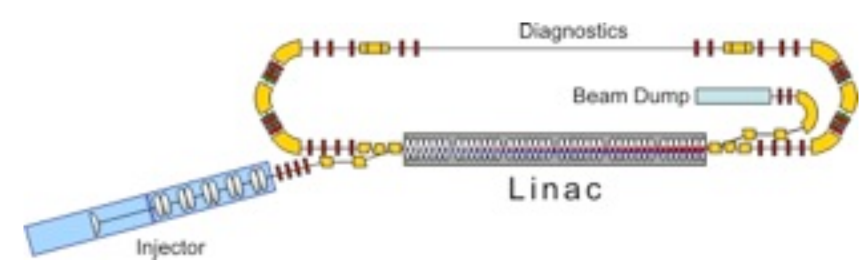

Ex Berlin Pro

Towards short period / high field undulators

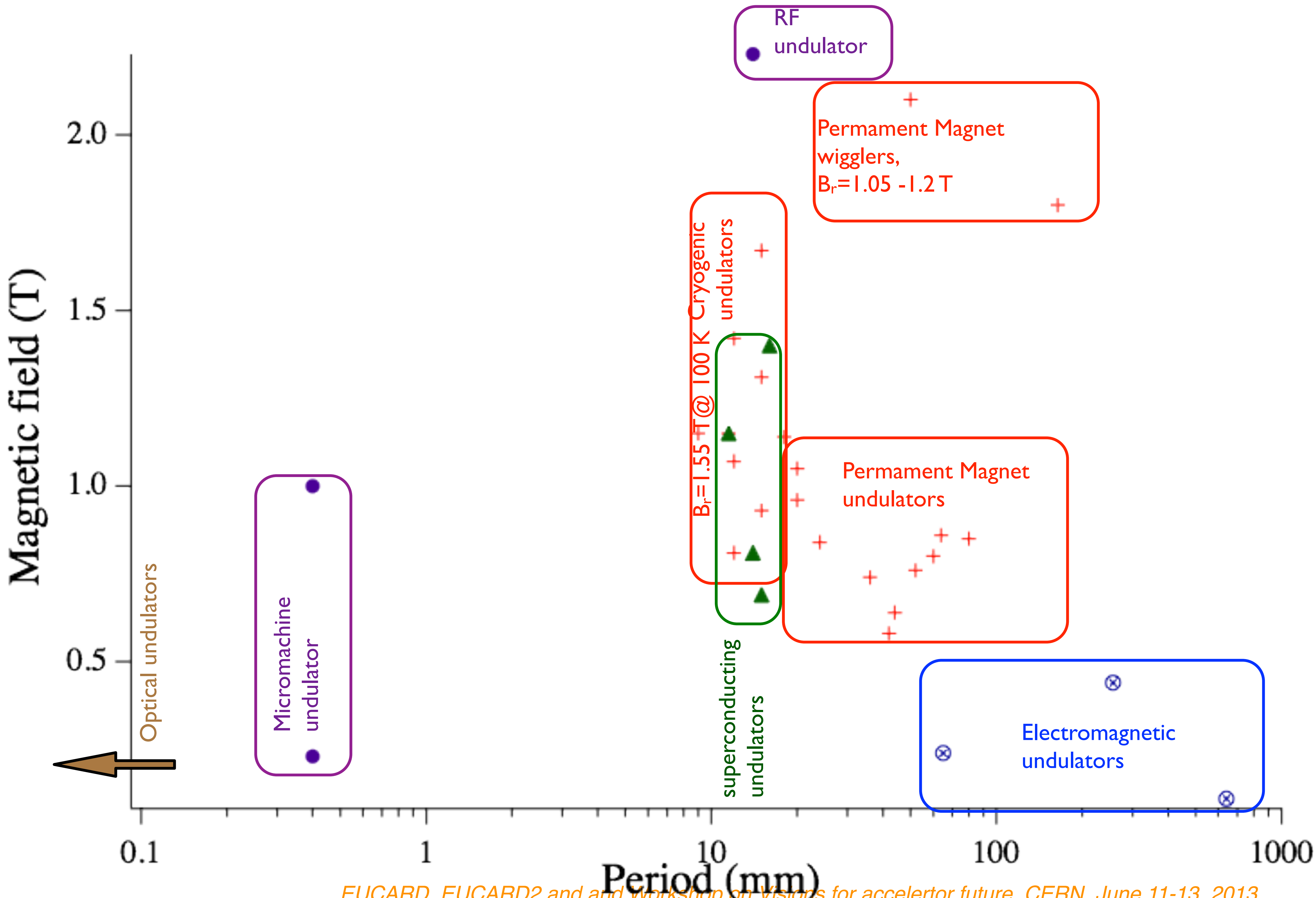

EUCARD, EUCARD2 and and Workshop on Visions for accelertor future, CERN, June 11-13, 2013

II-Generation of light sources and recent developments

Towards short period / high field undulators

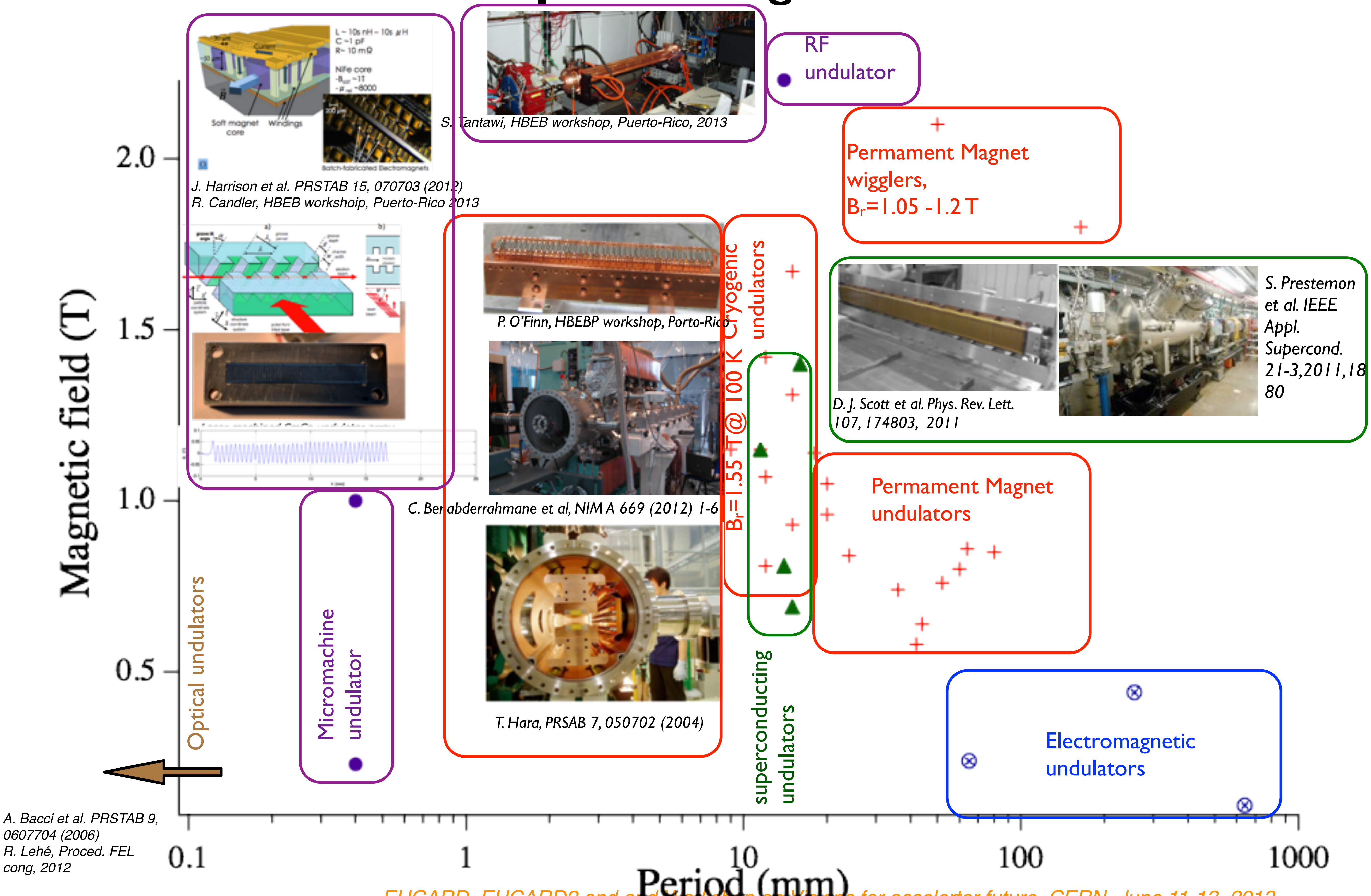

EUCARD, EUCARD2 and and Workshop on Visions for accelertor future, CERN, June 11-13, 2013

EUCARD, EUCARD2 and and Workshop on Visions for accelertor future, CERN, June 11-13, 2013

Towards high field permanent magnets EPU

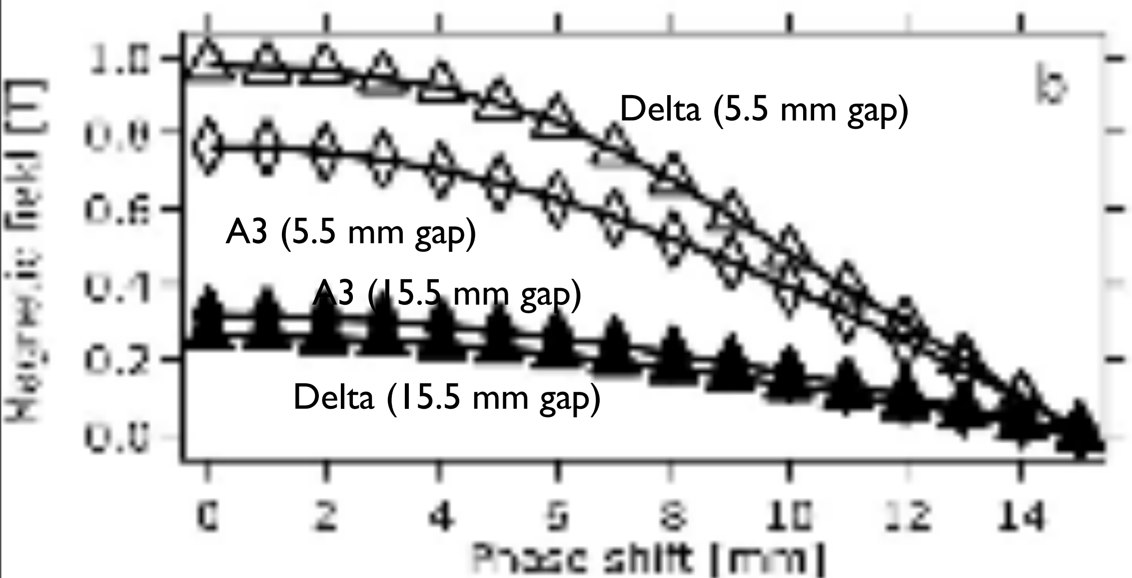

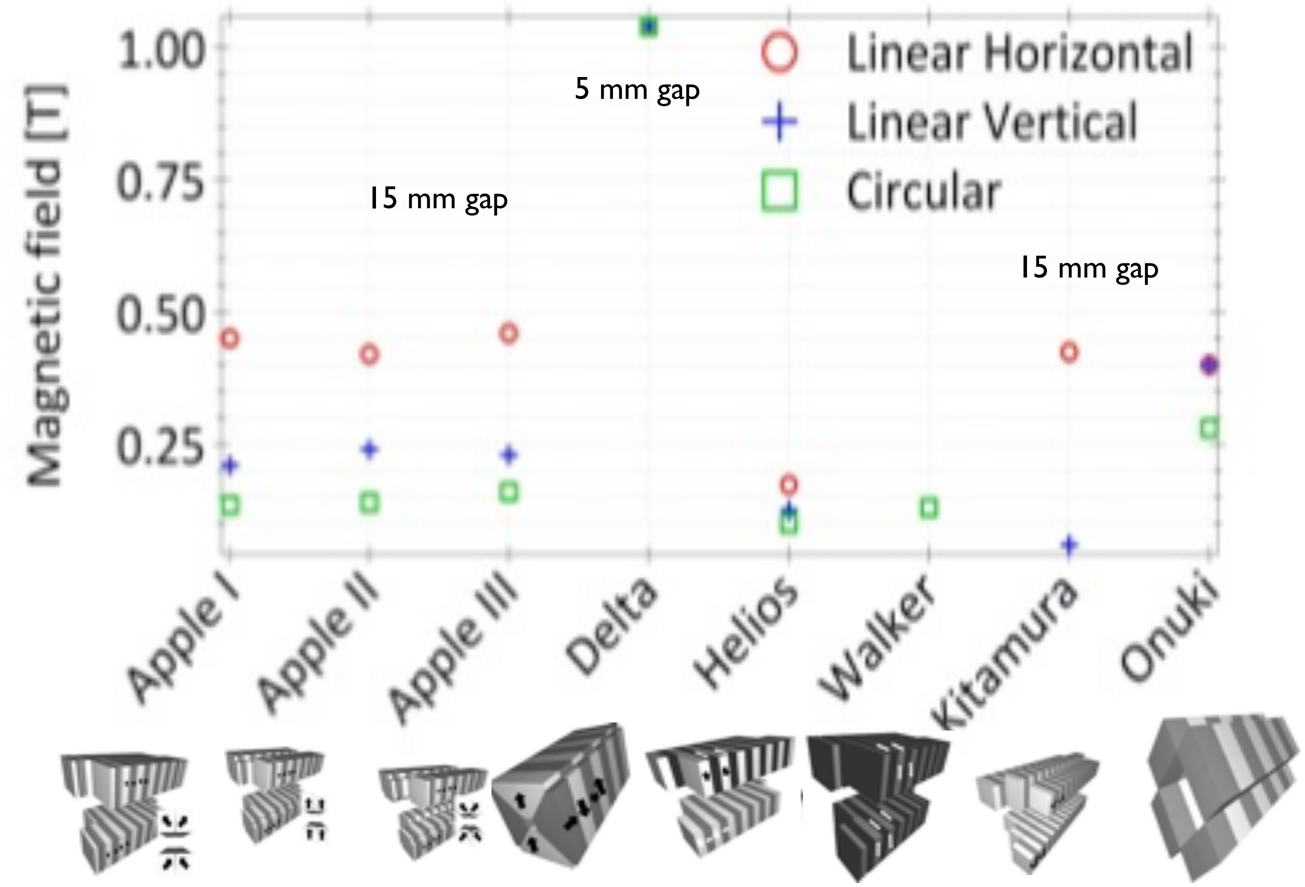

Period : 30 mm, gap 15,5mm/5 mm, Br = 1.26 T, 45 mmx45 mm

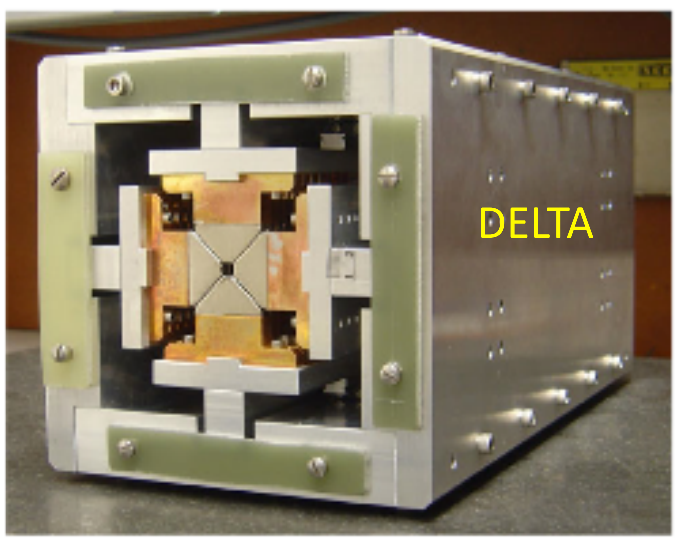

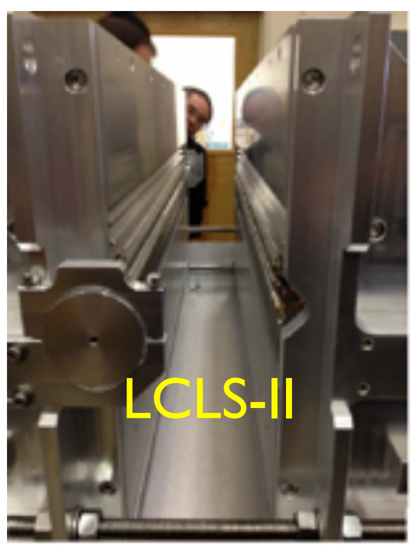

T. Raubenheimer HBEBP workshop, 2013, Puerto Rico

Courtesy F. Ciocci

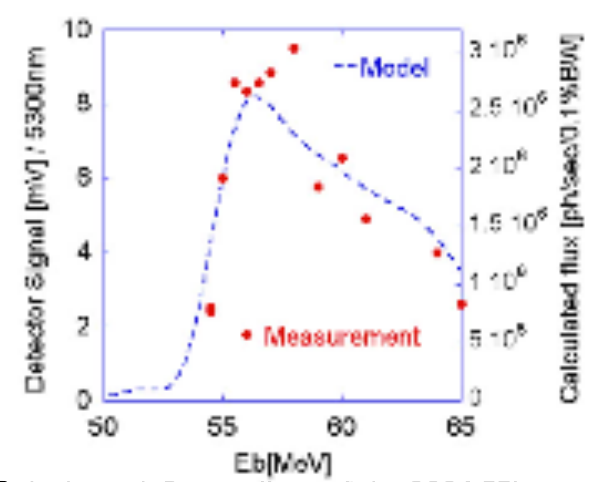

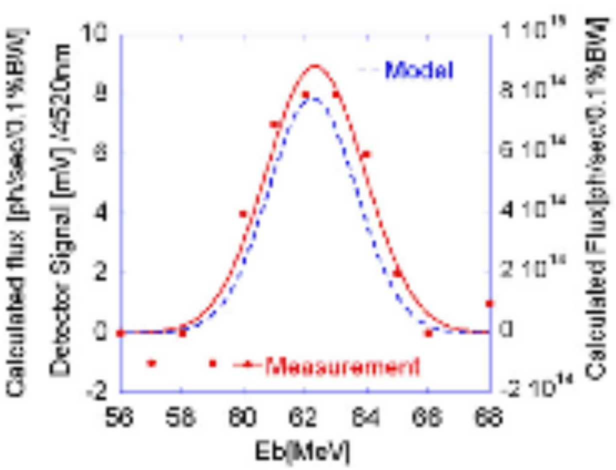

S. Sasaki et al,, Jpn. J. Appl. Phys., 31, L194 (1992)
S. Sasaki et al, Nucl. Instr. Meth., A331, 763 (1993)
S. Sasaki et al, Nucl. Instr. Meth., A347,87 (1994)

P. Elleaume, Nucl. Instr. Meth., A291, 371 (1990)
P. Elleaume, J. Synch. Rad.,1, 19 (1994)

R. Carr , Nucl. Instr. Meth., A306, 391 (1991)
R. Carr et al , Rev. Sci. Instrum., 63, 3564 (1992)
R. Carr, Proceedings of 1992 EPAC, p489 (1992)

B. Diviacco and R. P. Walker, Nucl. Instrum. Meth., A292, 517 (1990)

Bahrdt et al, Proceedings of the 2004 FEL Conference, Triestre, ITALY, p610 (2004)

H. Kitamura et al, J. Electron Spectr. Relate Phenom., 80 ,437, (1996)
A. Hiraya et al, J. Synchr. Rad., 5, 445, (1998)

A. B. Temnykh, PRSTAB, 11,120702 (2008)
A. B. Temnykh,. A 649 (2011) 42-45

M. Moissev et al. Sov. Phys. J. 21, 332, 1978
K. J. Kim NIMA219, 426 (1986)

H. Onuki, Nucl. Instr. Meth., A246, 94, (1986)
H. Onuki et al, Appl. Phys. Lett., 52, 173, (1988)

Light source generations

First generation (~1980) : Parasitic use

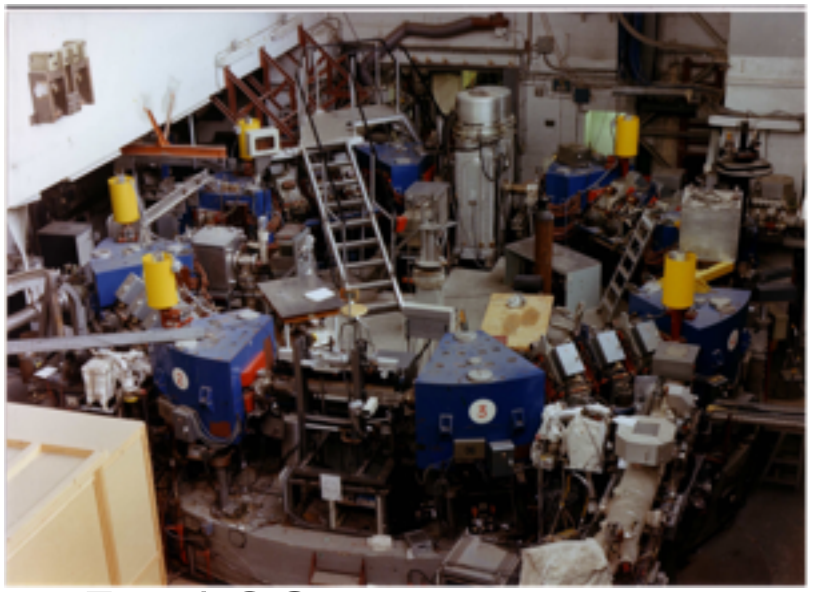

Ex : ACO

Second generation (~1985-2020?...) : Dedicated storage rings built for synchrotron radiation, few undulators and wigglers, emittance of few

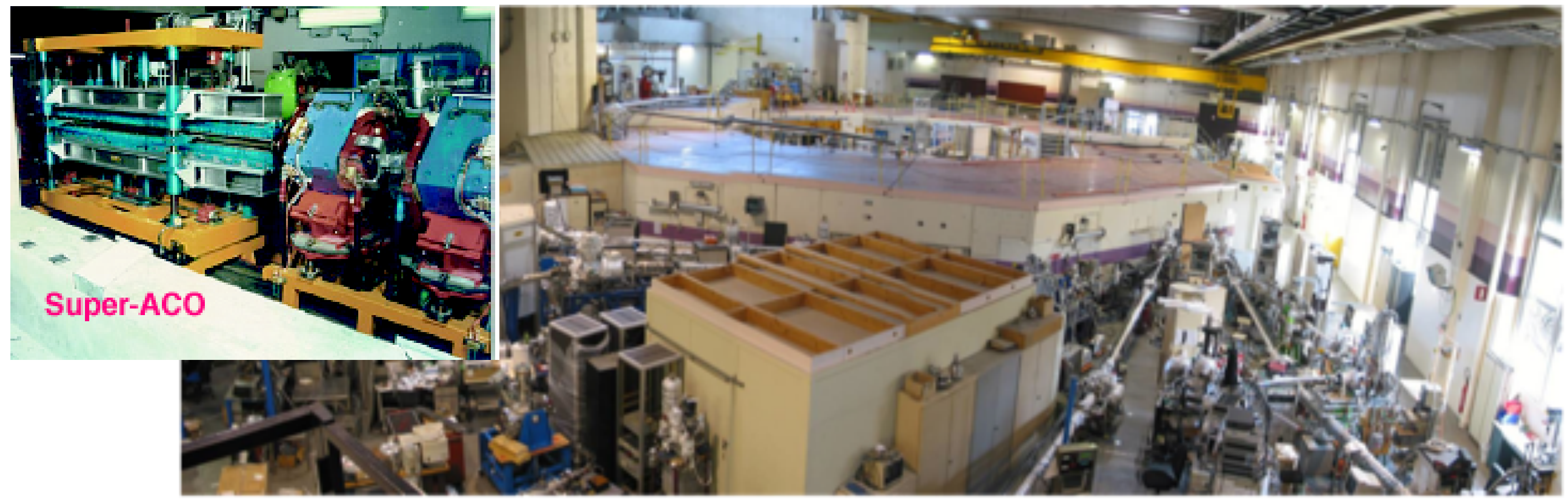

Third generation (~1990-?..) : low emittance, high number undulators, partial transverse coherence

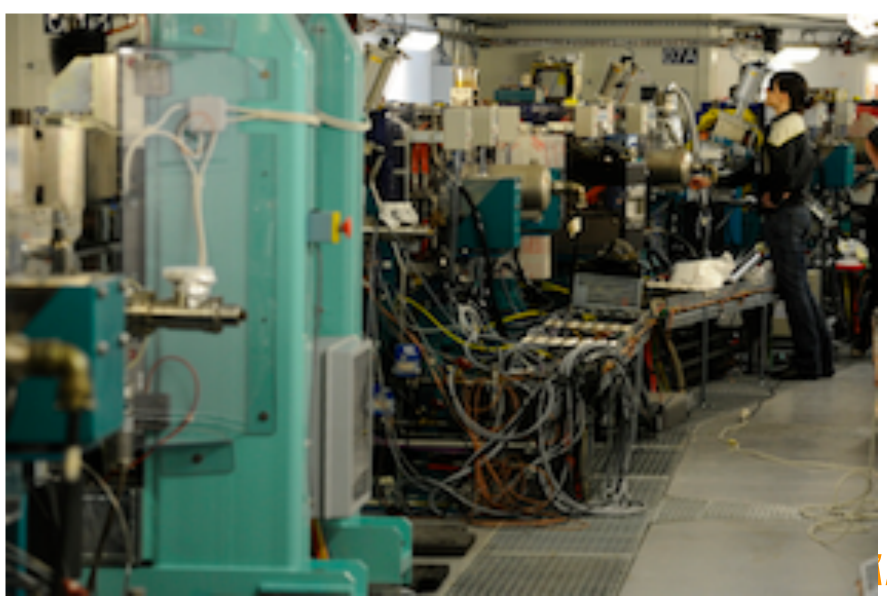

Fourth generation (2000-...) : short pulses with ERLs and Linacs, longitudinal coherence thanks to FELs

Evolution of brilliance

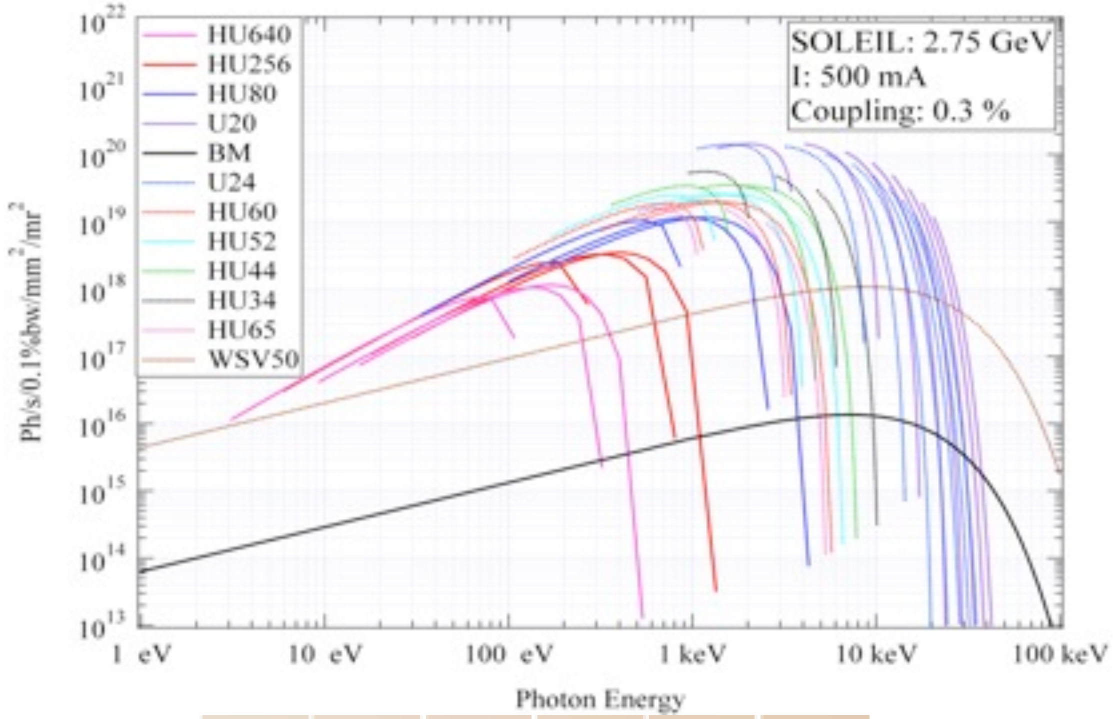

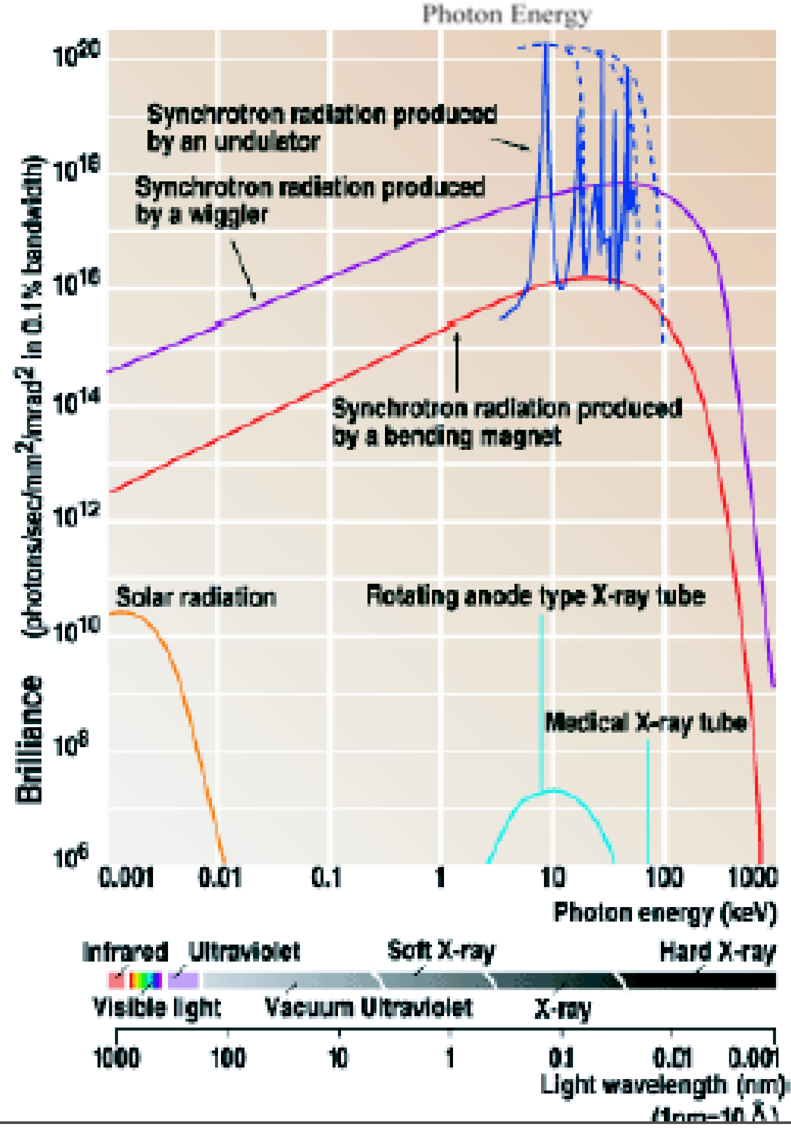

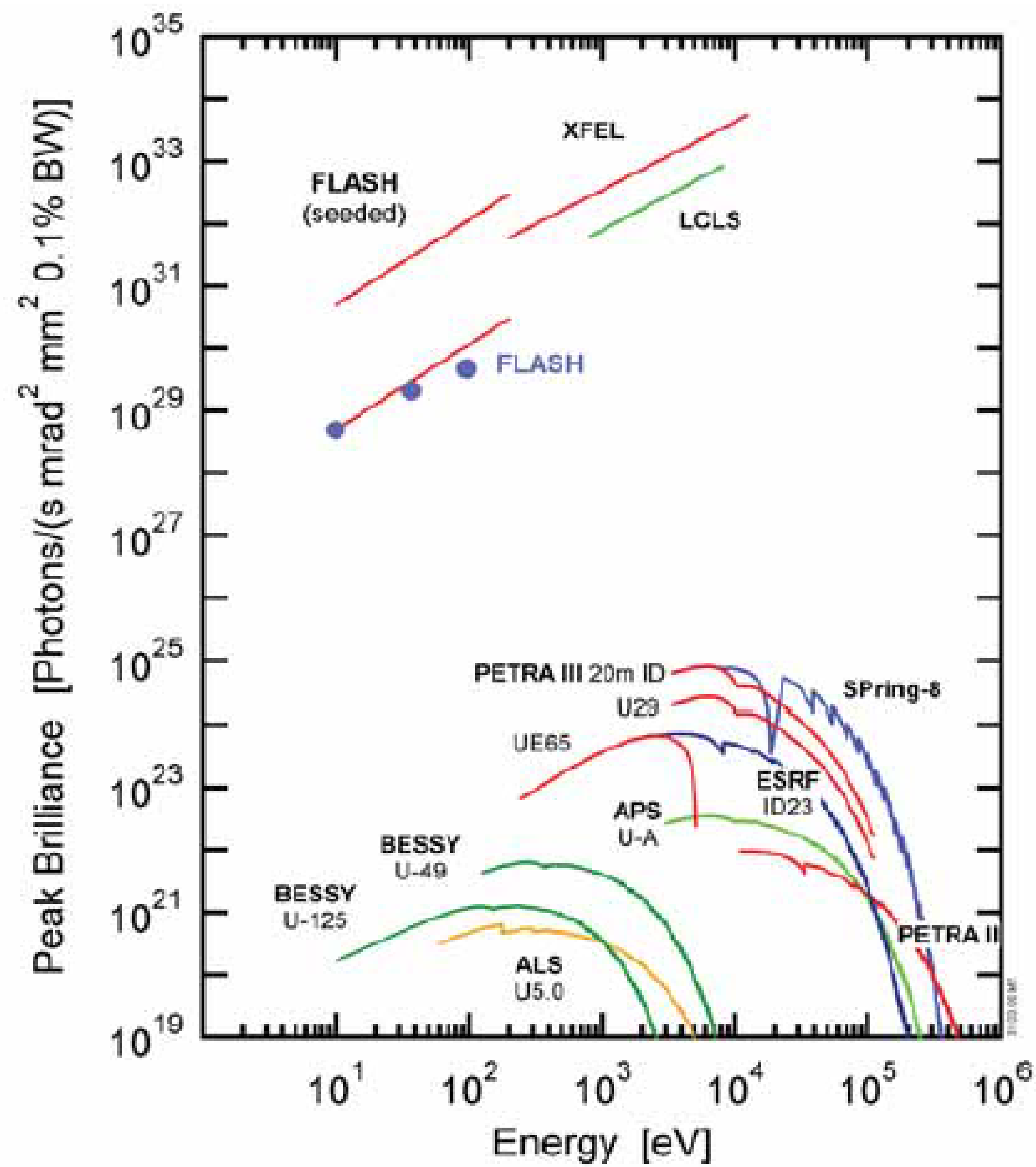

What is the fifth generation?

Approach diffraction limit and Fourier- transform limit with larger spectral range and flexibility for the user

- Diffraction limit => Ultimate strage rings, ERL, FELs
- Fourier transform limit : from as pulse to high energy resolution
- High level of stability
- Properties manipulations
- Higher flux
- Single / Multi-user
- Repetition rate : high with recirculating machines, superconducting linacs
- Combinations with other sources (e.g. pump-probe experiments)

...

or reduce the cost and make it more compact by replacing constituting elements?

What is the fifth generation?

Physics and applications of High Brightness Beams : towards a fifth generation light source
Puerto-Rico, March 25-28, 2013

Beyond present SASE based FELs : Better photon performances and further flexibility

- higher photon energy
- larger photon flux, brightness, coherence
- smaller bandwidth : 10^{-6}

=> ridiculously low emittance and energy spread required

- energy spread / wakefields
- modified SASE process, single spike, seeding, oscillator
- ultrafast : attosecond....
- synchronisation with THz sources
- more user friendly

=> «dramatic increase of X-ray spectrum specialised for experiments»

- multi-users

Towards more compact, university-scale for physics or medecine :

- use of «compact accelerators»
- use of laser as interacting medium : Compton / Thomson backscattering
- compact FEL proccess
- compact undulators

=> proof-of-principle required, critical measurements
technical up-grades
synergy among the different approaches

?

Source comparison

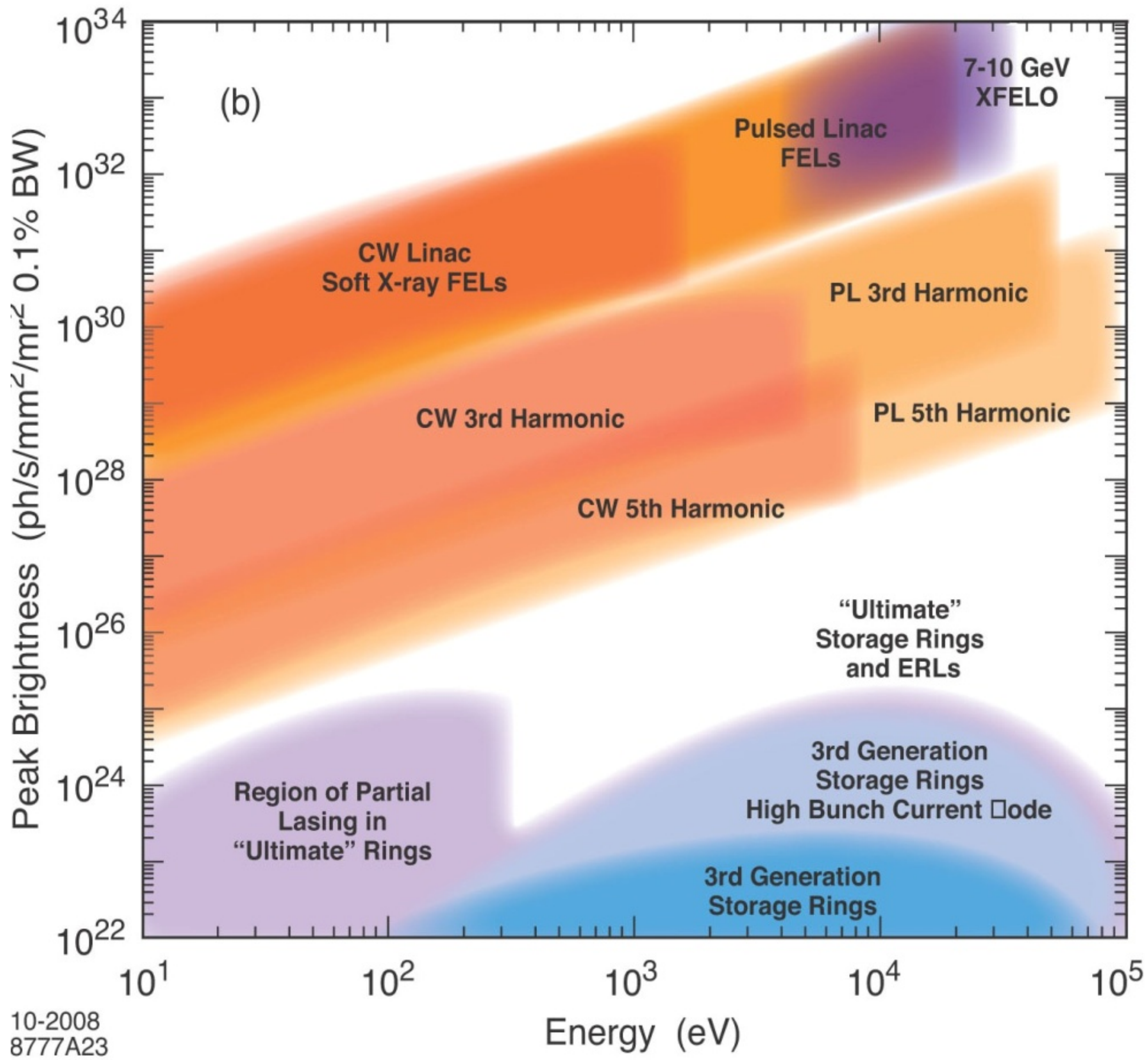

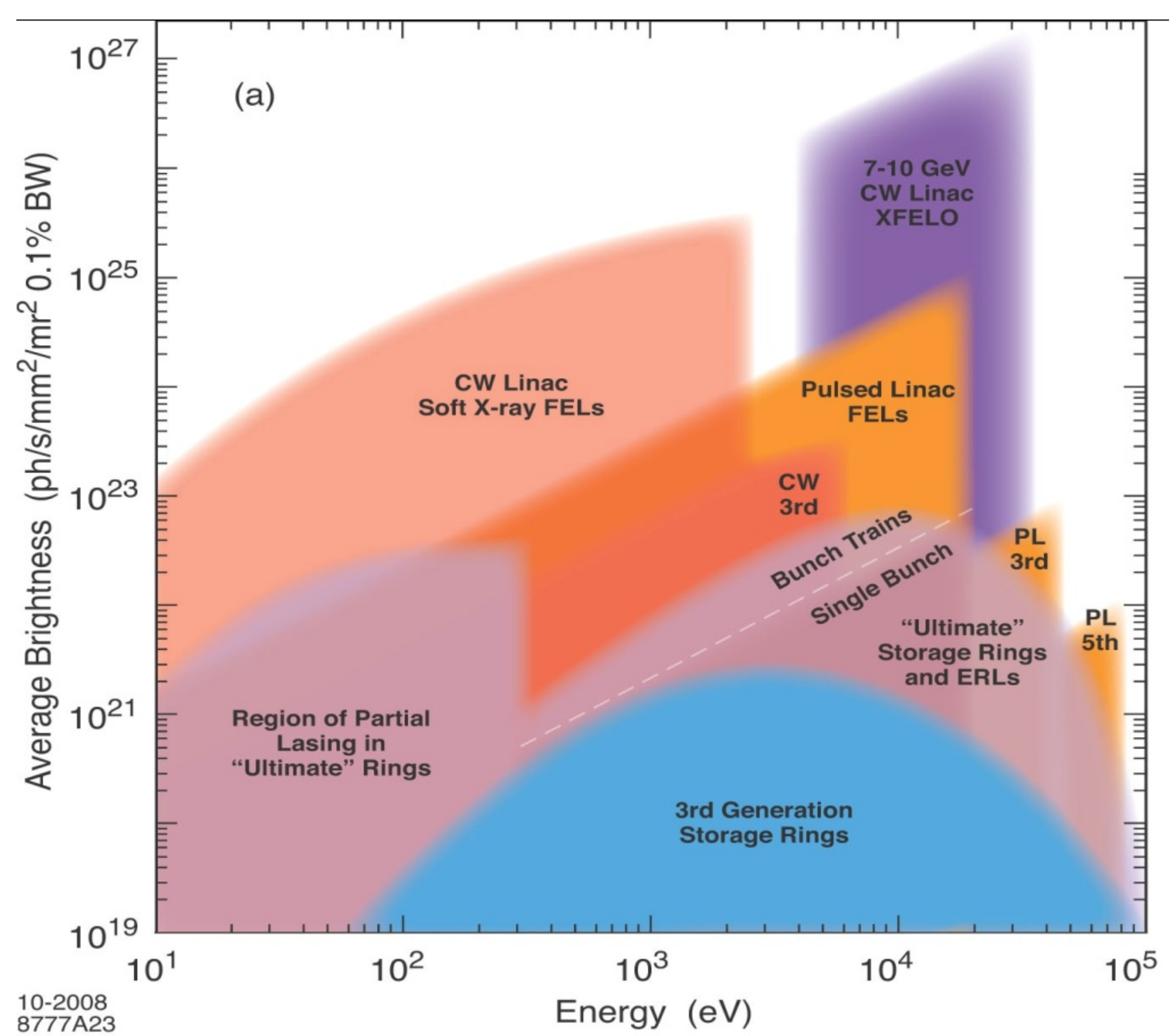

B. Hettel, Ultimate storage ring light sources, design and performances objectives, *USR Accelerator R&D Workshop, Huairou (Beijing), China, October 30, 2012*

Synchrotron radiation centers

Synchrotron radiation centers

Ultimate storage rings : towards transverse coherence

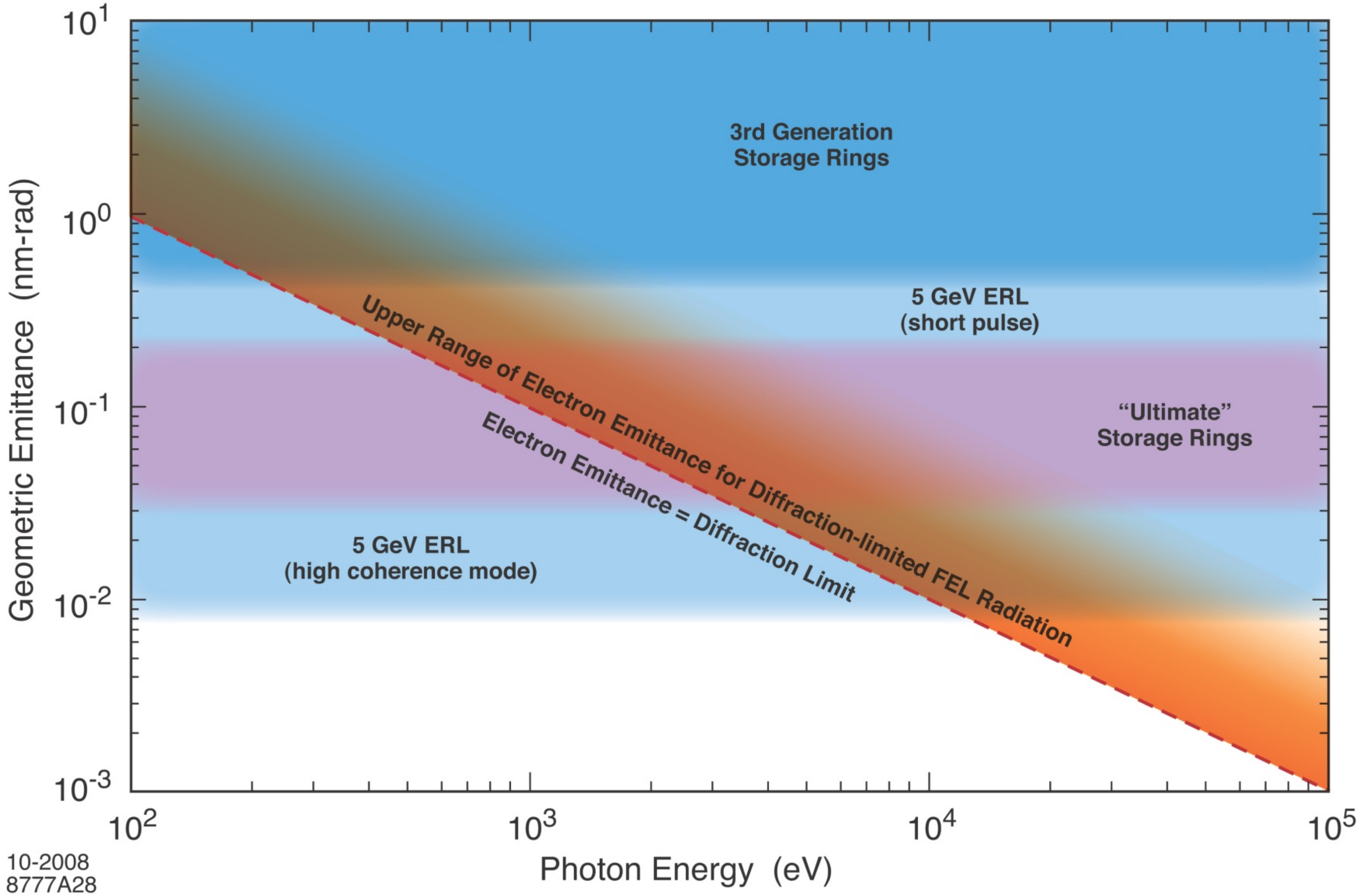

B. Hettel, Ultimate storage ring light sources, design and performances objectives, USR Accelerator R&D Workshop, Huairou (Beijing), China, October 30, 2012

Ultimate storage rings : how?

Emittance

$$\epsilon_0 \approx F(\nu_x, \text{lattice}) \frac{E^2\theta^3}{J_x} \frac{I_{2,d}}{I_{2,d} + I_{2,w}}$$

θ : bending angle per dipole
J_x =1-D, with D partition number due to radiation damping
$I_{2,d}$ $I_{2,w}$ dipole/ wiggler energy loss per tern

strategies for low emittance :

- high number of dipoles / minimization of the H function (stronger focusing) => figure of merit => MBA lattices

$$M = \epsilon_0 C^3 / E^2$$

- damping wiggler but with an increase of the energy spread

- partition number : Generally, D ~ 0 and J_x ~ 1, Robinson theorem : $J_x + J_z + J_s = 4$

PETRA III : 6 GeV, 1 nm
large circumference with damping wigglers

K. Balevski et al.

NSLS II : 3 GeV, 0.5 nm
large circumference, DBA, with damping wigglers

NLSL II CDR

MAX IV : 3 GeV, 0.24 nm
7BA with damping wigglers

S. Leemans et al. PRSTAB 12, 120701 (2009)

Ultimate storage rings : how?

Emittance

$$\epsilon_0 \approx F(\nu_x, \text{lattice}) \frac{E^2\theta^3}{J_x} \frac{I_{2,d}}{I_{2,d} + I_{2,w}}$$

θ : bending angle per dipole
J_x =1-D, with D partition number due to radiation damping $J_x = 1 - D$
$I_{2,d}$ $I_{2,w}$ dipole/ wiggler energy loss per tern

strategies for low emittance :

- high number of dipoles / minimization of the H function (stronger focusing) => figure of merit => MBA lattices $M = \epsilon_0 C^3 / E^2$

- damping wiggler but with an increase of the energy spread

- partition number : Generally, D ~ 0 and J_x ~ 1, Robinson theorem : $J_x + J_z + J_s = 4$

PETRA III : 6 GeV, 1 nm
large circumference with damping wigglers

K. Balevski et al.

NSLS II : 3 GeV, 0.5 nm
large circumference, DBA, with damping wigglers

NLSL II CDR

MAX IV : 3 GeV, 0.24 nm
7BA with damping wigglers

S. Leemans et al. PRSTAB 12, 120701 (2009)

III-Storage rings based light sources

Emittance reduction via lattice

MAX IV : 3 GeV, 0.24 nm
7BA with damping wigglers
D : 9T/m, Q: 40T/m, S: 2 kT/m^2, O : 30 kT/m^3

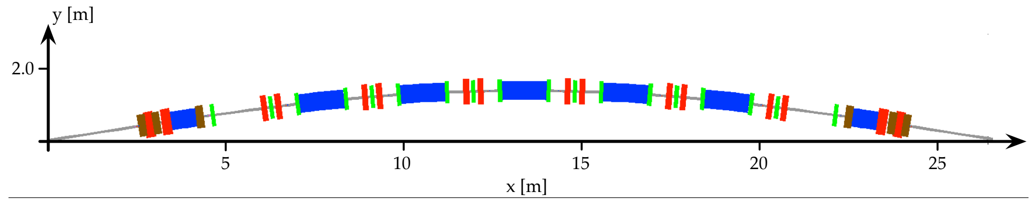

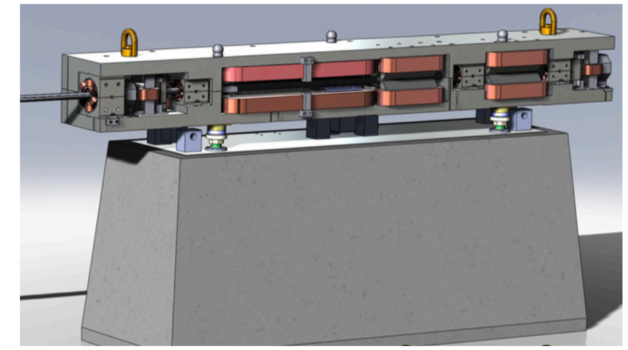

- Example of USR 7, 7 GeV
  40 sectors x 10BA
  0.028 nm emittance
  0.079 % energy spread

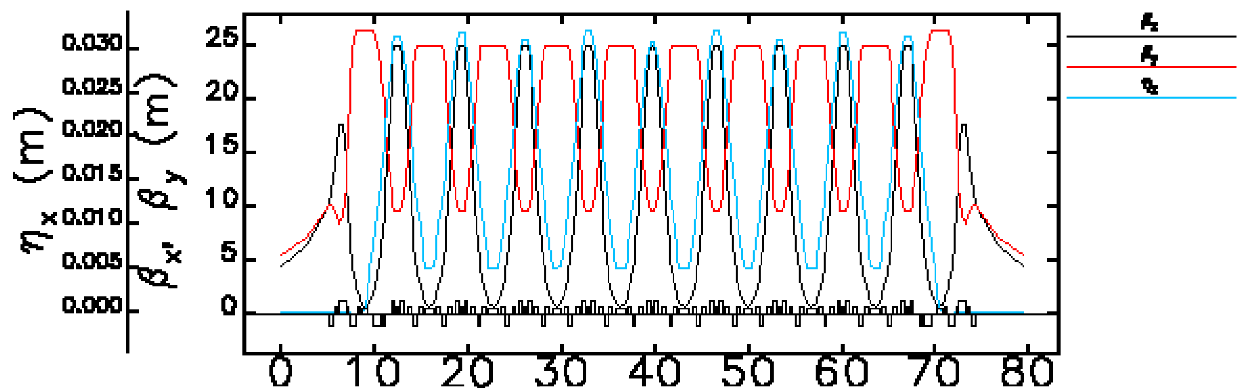

- Example of ESRF
  from DBA : 4 nm to 7BA :0.13 nm
  with strong focusing, better und. matching, tight tolerances
  First planning: commissioning 2019

P. Raimondi USR Accelerator R&D Workshop, Huairou (Beijing), China, October 30, 2012

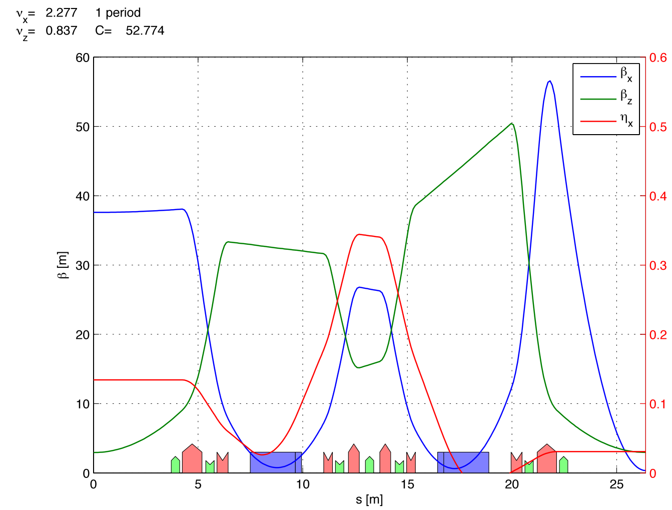

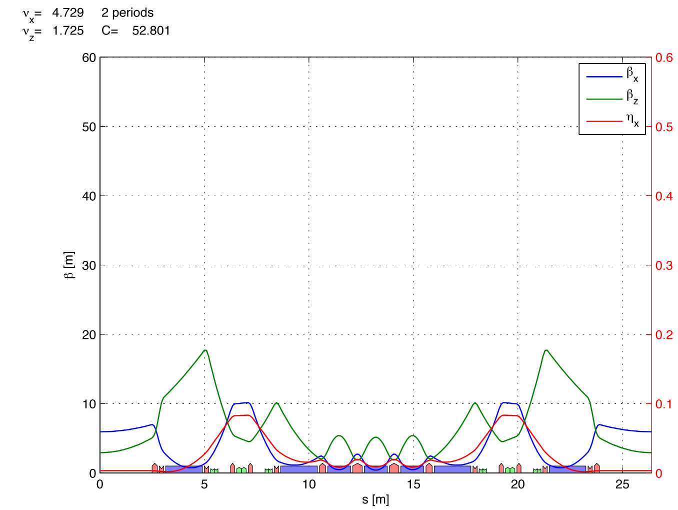

M. Bei et al. NIMA 622 (2010) 518-535

Issues and challenges :

- small dynamical aperture =>
  * beam lifetime (mitigation by top-up,)
  * injection (pulse pultipole, on-axis injection, reduced separation between inejcted and stored beam
- Intra Beam Scattering (mitigation by high beam energy, high damping time, round beam)
- low collective instability thresholds (TMCI, microwave isntability, Resistive wall instability...)
- Instrumentation (BPMs, strong quadrupoles and sextupoles, vacuum chambers...)

Emittance reduction via partition number

- partition number reduction by combined magnet scheme, Robinon wiggler

$$\varepsilon_x = \frac{C_q \gamma^2 \langle H \rangle_{dipole}}{J_x \rho_x}$$

D=-1 => $\varepsilon_x/2$ and energy spread x$\sqrt{2}$

B*dB/dx ≠0 and η_x≠0

SOLEIL case, horizontal emittance : 3.7 nmrad⇒1.85 nmrad

D=-1 =>

H. Abualrob, P. Brunelle, M-E. Couprie, O. Marcouillé, A. Nadji, L. Nadolski, R. Nagaoka, SOLEIL emittance reduction using a Robinson wiggler, IPAC12:, New Oerlans, Louisiana, 2012

- partition number reduction with a pair of coupling cavities driven in TM210 mode and set in π betatron phase difference in a mirror symmetrical optics

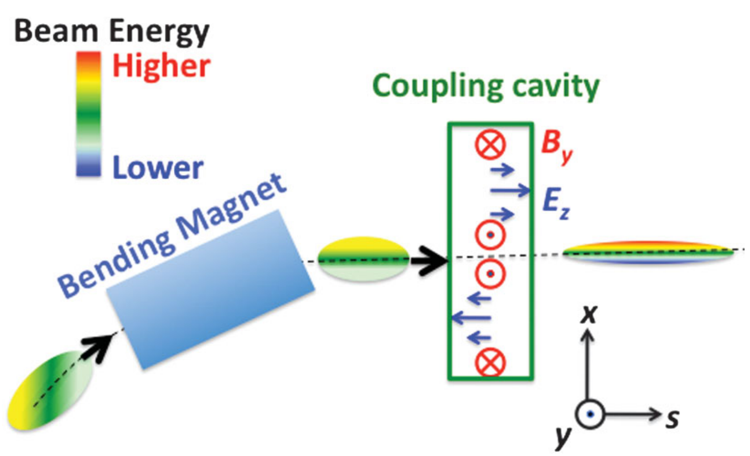

$\theta_c = 2\pi V \eta_x / \alpha U_o$

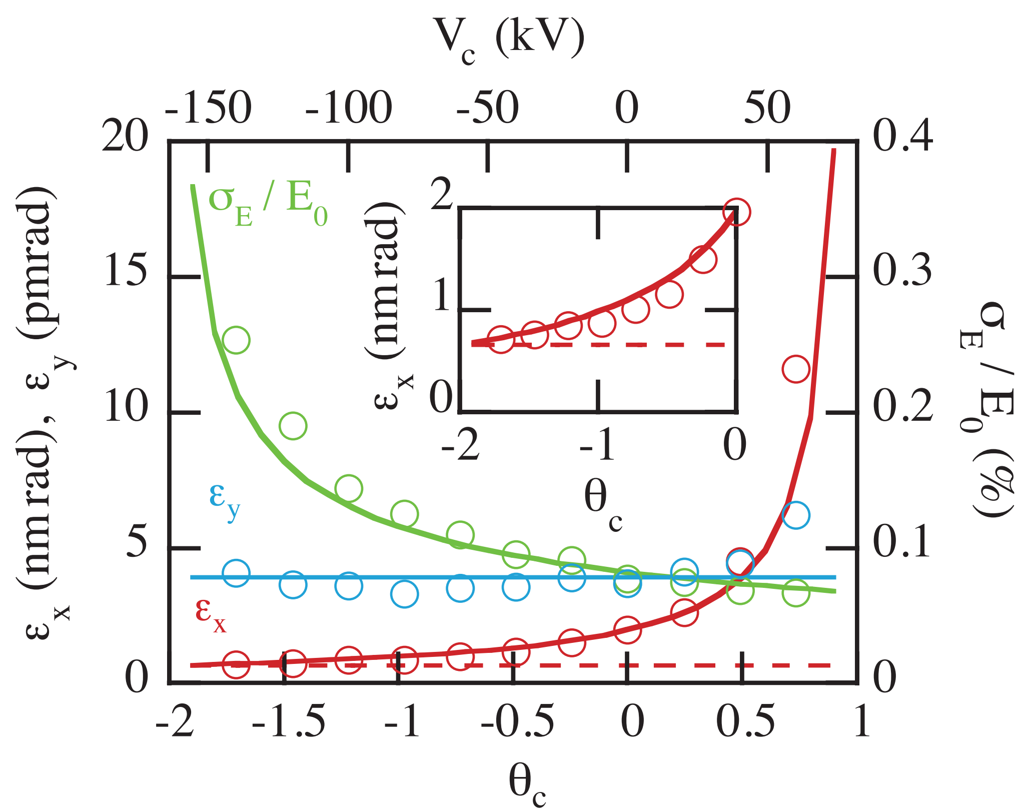

Y. Shimosaki, H. tanaka, Control of damping parititon numbers in a Ring Accelerator with rf Electromagnetic Fields, PRL 110, 154802 (2013) 154802

Emittance reduction via partition number

- partition number reduction by combined magnet scheme, Robinon wiggler

$$\varepsilon_x = \frac{C_q \gamma^2 \langle H \rangle_{dipole}}{J_x \rho_x} \qquad J_x = 1 - D \qquad \varepsilon_x = \varepsilon_{x,0} \frac{1}{1-D} \qquad \left(\frac{\sigma_E}{E_0}\right)^2 = \frac{2}{2+D}\left(\frac{\sigma_{E,0}}{E_0}\right)^2$$

D=-1 => $\varepsilon_x/2$ and energy spread $\times\sqrt{2}$

B*dB/dx ≠0 and $\eta_x \neq 0$

SOLEIL case, horizontal emittance : 3.7 nmrad⇒1.85 nmrad

D=-1 =>

H. Abualrob, P. Brunelle, M-E. Couprie, O. Marcouillé, A. Nadji, L. Nadolski, R. Nagaoka, SOLEIL emittance reduction using a Robinson wiggler, IPAC12:, New Oerlans, Louisiana, 2012

- partition number reduction with a pair of coupling cavities driven in TM210 mode and set in π betatron phase difference in a mirror symmetrical optics

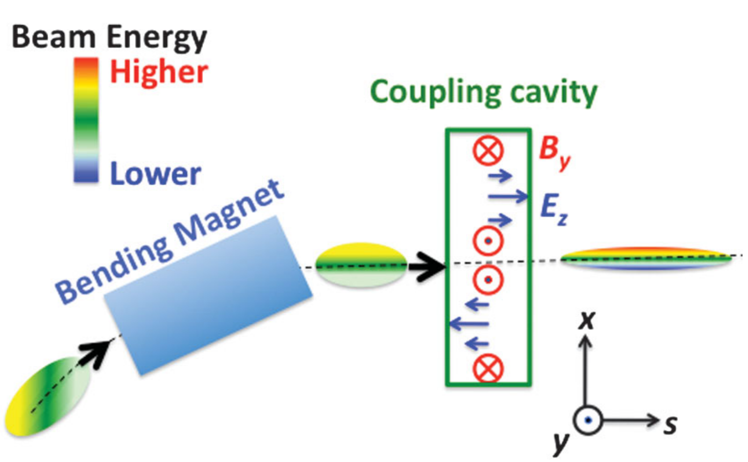

$\theta_c = 2\pi V \eta_x / \alpha U_o$

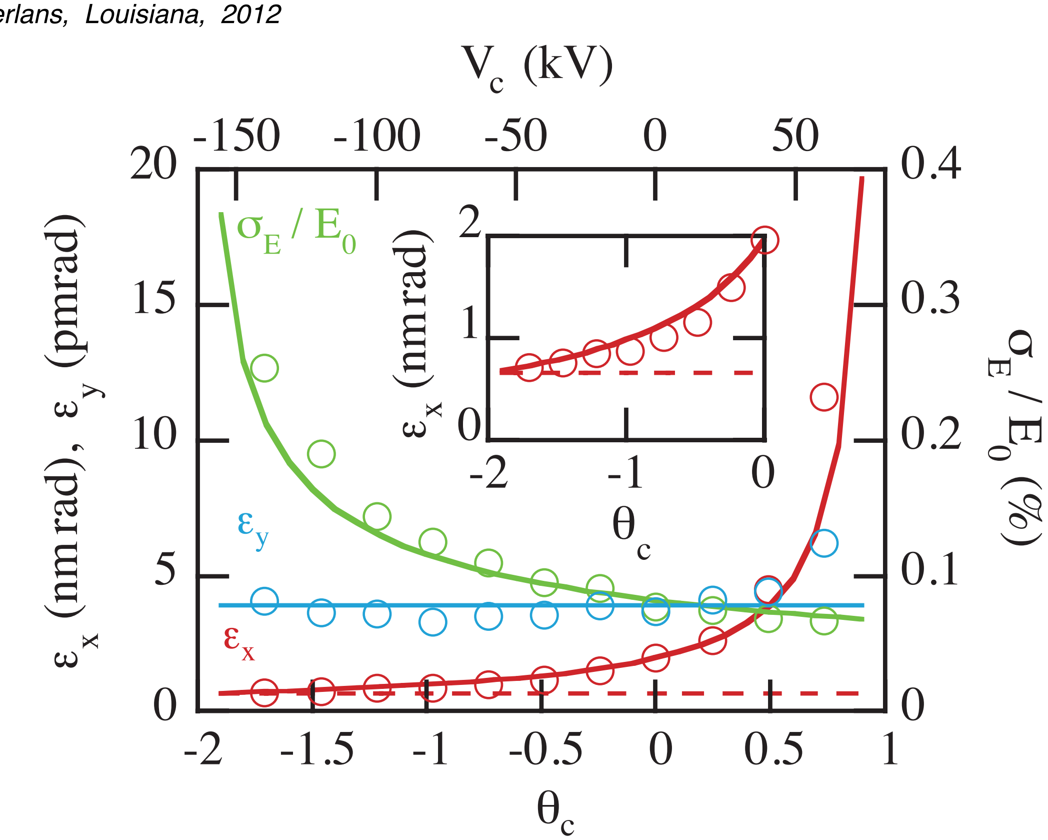

Y. Shimosaki, H. tanaka, Control of damping parititon numbers in a Ring Accelerator with rf Electromagnetic Fields, PRL 110, 154802 (2013) 154802

Emittance reduction via partition number

- partition number reduction by combined magnet scheme, Robinon wiggler

$$\varepsilon_x = \frac{C_q \gamma^2 \langle H \rangle_{dipole}}{J_x \rho_x} \qquad J_x = 1 - D \qquad \varepsilon_x = \varepsilon_{x,0} \frac{1}{1-D} \qquad \left(\frac{\sigma_E}{E_0}\right)^2 = \frac{2}{2+D} \left(\frac{\sigma_{E,0}}{E_0}\right)^2$$

D=-1 => $\varepsilon_x/2$ and energy spread x$\sqrt{2}$

B*dB/dx ≠0 and $\eta_x \neq 0$

SOLEIL case, horizontal emittance : 3.7 nmrad⇒1.85 nmrad

$$D = \frac{\oint \frac{\eta_x}{\rho_x^3} ds + \frac{2}{B^2 \rho_x^2} \oint \eta_x B \frac{dB}{dx} ds}{\oint \frac{ds}{\rho_x^2}}$$

D=-1 =>

H. Abualrob, P. Brunelle, M-E. Couprie, O. Marcouillé, A. Nadji, L. Nadolski, R. Nagaoka, SOLEIL emittance reduction using a Robinson wiggler, IPAC12:, New Oerlans, Louisiana, 2012

- partition number reduction with a pair of coupling cavities driven in TM210 mode and set in π betatron phase difference in a mirror symmetrical optics

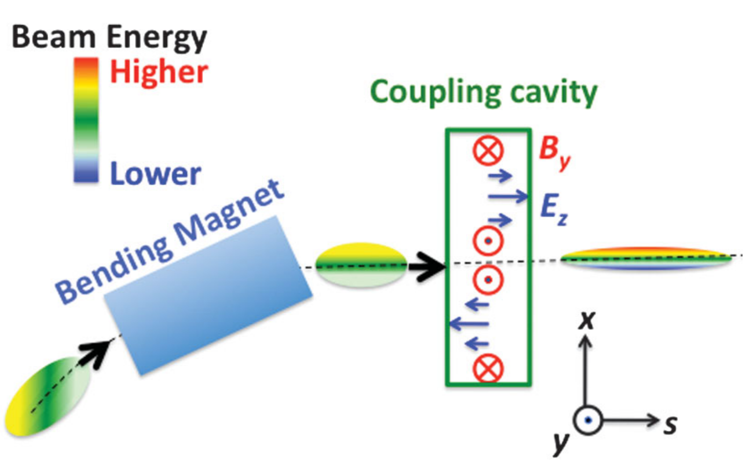

$\theta_c = 2 \pi V \eta_x / \alpha U_o$

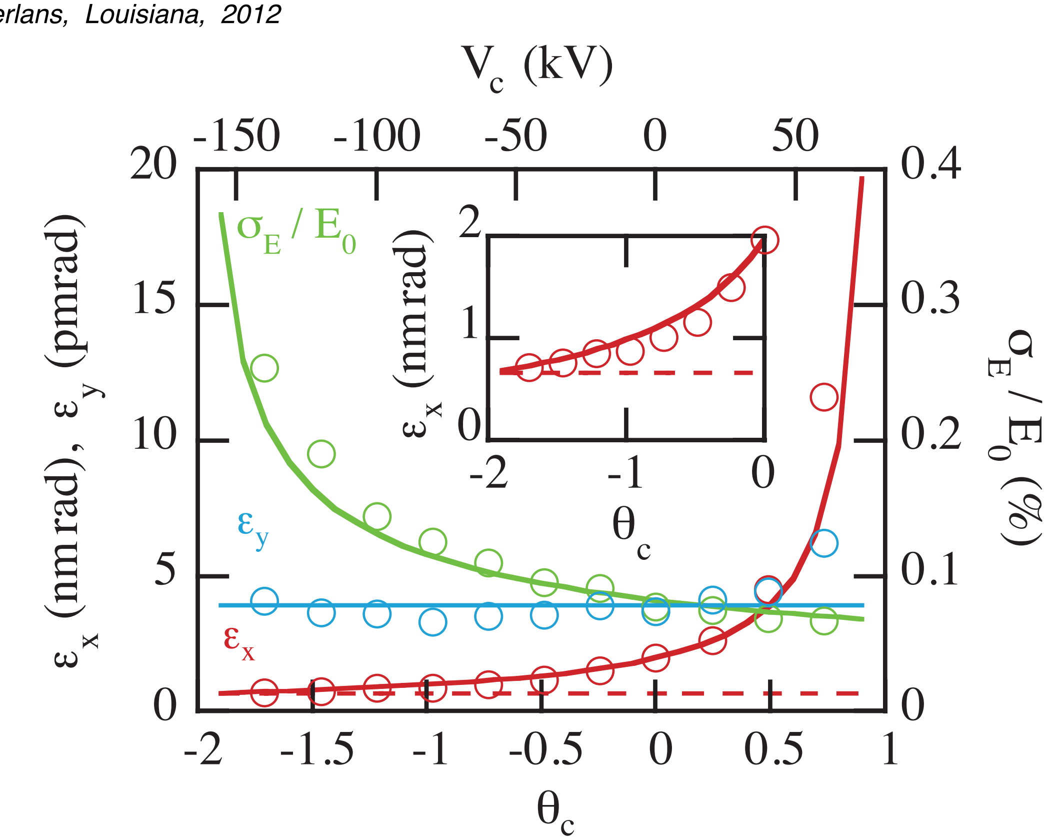

Y. Shimosaki, H. tanaka, Control of damping parititon numbers in a Ring Accelerator with rf Electromagnetic Fields, PRL 110, 154802 (2013) 154802

Emittance reduction via partition number

- partition number reduction by combined magnet scheme, Robinon wiggler

$$\varepsilon_x = \frac{C_q \gamma^2 \langle H \rangle_{dipole}}{J_x \rho_x} \qquad J_x = 1 - D \qquad \varepsilon_x = \varepsilon_{x,0} \frac{1}{1-D} \qquad \left(\frac{\sigma_E}{E_0}\right)^2 = \frac{2}{2+D}\left(\frac{\sigma_{E,0}}{E_0}\right)^2$$

D=-1 => $\varepsilon_x/2$ and energy spread x$\sqrt{2}$

B*dB/dx ≠0 and η_x≠0

SOLEIL case, horizontal emittance : 3.7 nmrad⇒1.85 nmrad

$$D = \frac{\oint \frac{\eta_x}{\rho_x^3} ds + \boxed{\frac{2}{B^2 \rho_x^2} \oint \eta_x B \frac{dB}{dx} ds}}{\oint \frac{ds}{\rho_x^2}}$$

D=-1 =>

H. Abualrob, P. Brunelle, M-E. Couprie, O. Marcouillé, A. Nadji, L. Nadolski, R. Nagaoka, SOLEIL emittance reduction using a Robinson wiggler, IPAC12:, New Oerlans, Louisiana, 2012

- partition number reduction with a pair of coupling cavities driven in TM210 mode and set in π betatron phase difference in a mirror symmetrical optics

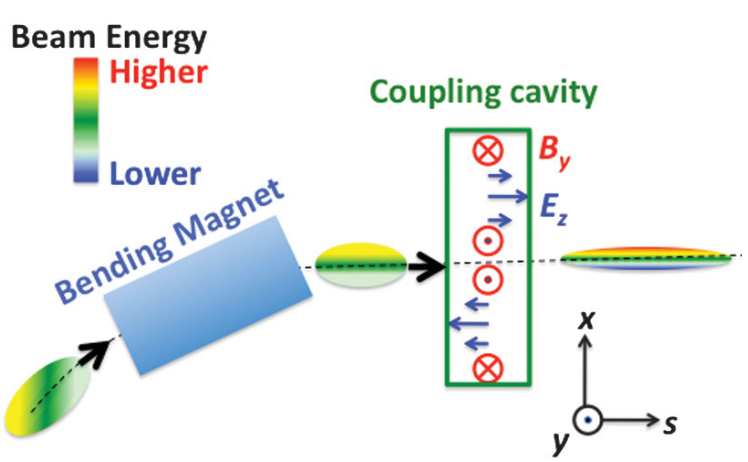

$\theta_c = 2 \pi V \eta_x / \alpha U_o$

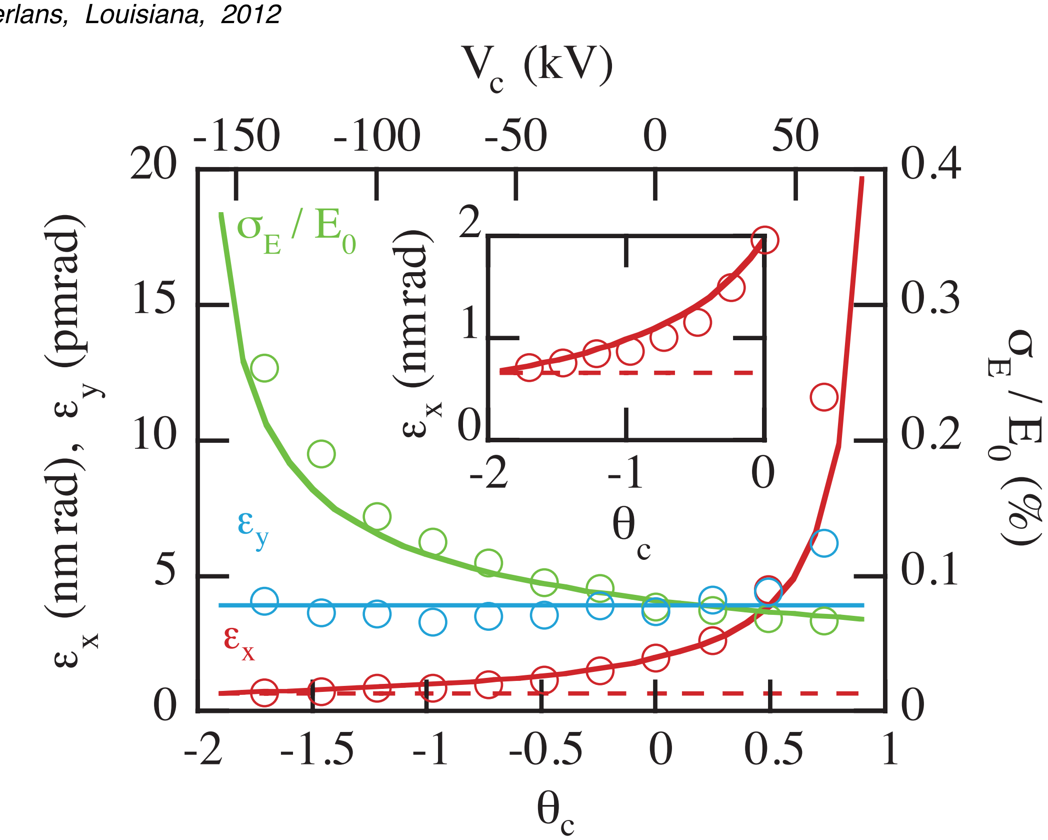

Y. Shimosaki, H. tanaka, Control of damping parititon numbers in a Ring Accelerator with rf Electromagnetic Fields, PRL 110, 154802 (2013) 154802

Emittance reduction via partition number

- partition number reduction by combined magnet scheme, Robinon wiggler

$$\varepsilon_x = \frac{C_q \gamma^2 \langle H \rangle_{dipole}}{J_x \rho_x} \qquad J_x = 1 - D \qquad \varepsilon_x = \varepsilon_{x,0} \frac{1}{1-D} \qquad \left(\frac{\sigma_E}{E_0}\right)^2 = \frac{2}{2+D}\left(\frac{\sigma_{E,0}}{E_0}\right)^2$$

D=-1 => $\varepsilon_x/2$ and energy spread x$\sqrt{2}$

B*dB/dx ≠0 and $\eta_x \neq 0$

SOLEIL case, horizontal emittance : 3.7 nmrad⇒1.85 nmrad

$$D = \frac{\oint \frac{\eta_x}{\rho_x^3} ds + \boxed{\frac{2}{B^2 \rho_x^2} \oint \eta_x B \frac{dB}{dx} ds}}{\oint \frac{ds}{\rho_x^2}}$$

η_x= dispersion function

ρ_x = radius of curvature due to B

D=-1 =>

H. Abualrob, P. Brunelle, M-E. Couprie, O. Marcouillé, A. Nadji, L. Nadolski, R. Nagaoka, SOLEIL emittance reduction using a Robinson wiggler, IPAC12:, New Oerlans, Louisiana, 2012

- partition number reduction with a pair of coupling cavities driven in TM210 mode and set in π betatron phase difference in a mirror symmetrical optics

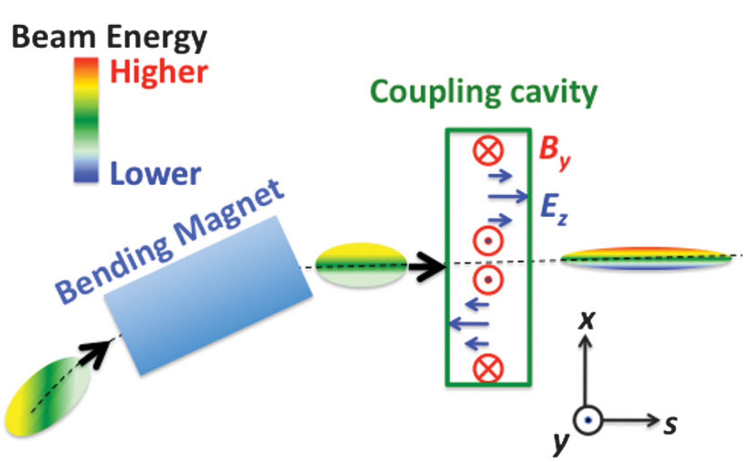

$\theta_c = 2 \pi V \eta_x / \alpha U_o$

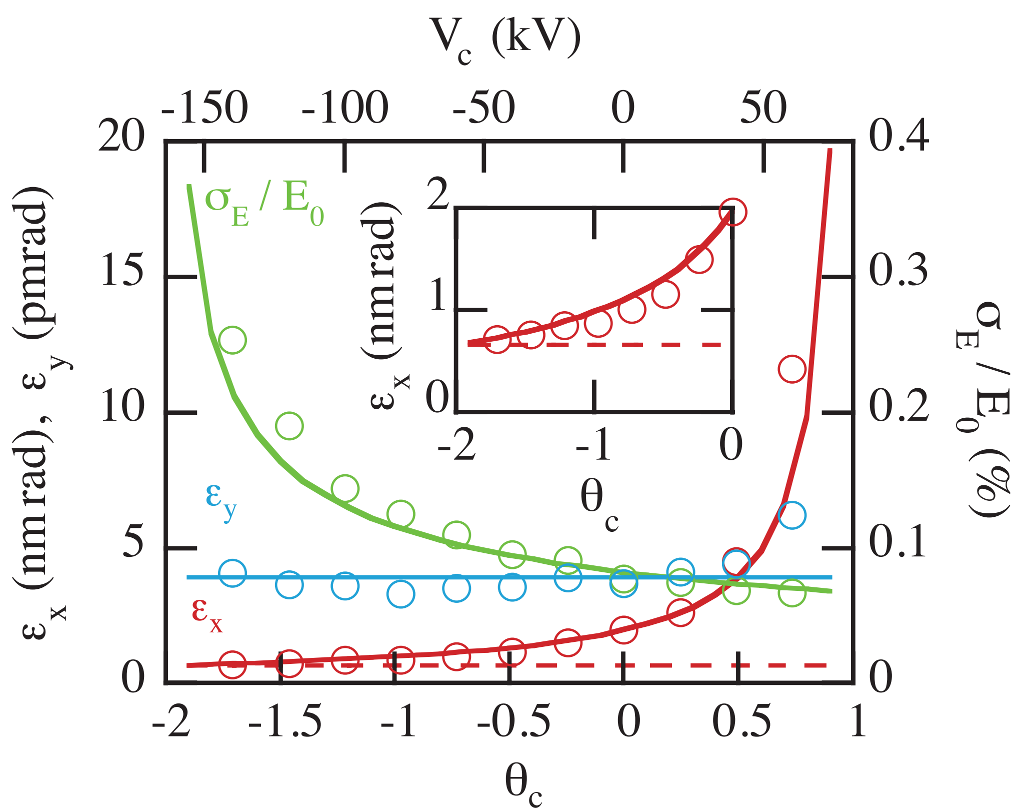

Y. Shimosaki, H. tanaka, Control of damping parititon numbers in a Ring Accelerator with rf Electromagnetic Fields, PRL 110, 154802 (2013) 154802

Emittance reduction via partition number

- partition number reduction by combined magnet scheme, Robinon wiggler

$$\varepsilon_x = \frac{C_q \gamma^2 \langle H \rangle_{dipole}}{J_x \rho_x} \qquad J_x = 1 - D \qquad \varepsilon_x = \varepsilon_{x,0} \frac{1}{1-D} \qquad \left(\frac{\sigma_E}{E_0}\right)^2 = \frac{2}{2+D}\left(\frac{\sigma_{E,0}}{E_0}\right)^2$$

D=-1 => $\varepsilon_x/2$ and energy spread x$\sqrt{2}$

B*dB/dx ≠0 and $\eta_x \neq 0$

SOLEIL case, horizontal emittance : 3.7 nmrad⇒1.85 nmrad

$$D = \frac{\oint \frac{\eta_x}{\rho_x^3} ds + \frac{2}{B^2 \rho_x^2} \oint \eta_x B \frac{dB}{dx} ds}{\oint \frac{ds}{\rho_x^2}}$$

η_x= dispersion function

ρ_x = radius of curvature due to B

D=-1 => $\frac{\hat{B}^2_{w,z}}{2g} \approx 89\ \mathrm{T^2/m}$

H. Abualrob, P. Brunelle, M-E. Couprie, O. Marcouillé, A. Nadji, L. Nadolski, R. Nagaoka, SOLEIL emittance reduction using a Robinson wiggler, IPAC12:, New Oerlans, Louisiana, 2012

- partition number reduction with a pair of coupling cavities driven in TM210 mode and set in π betatron phase difference in a mirror symmetrical optics

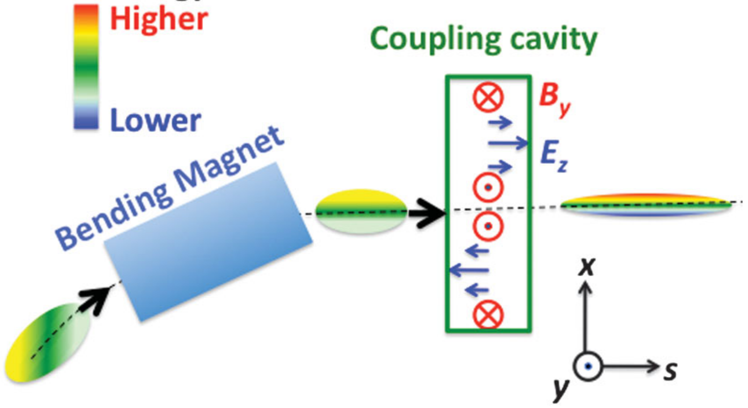

$\theta_c = 2\pi V \eta_x / \alpha U_o$

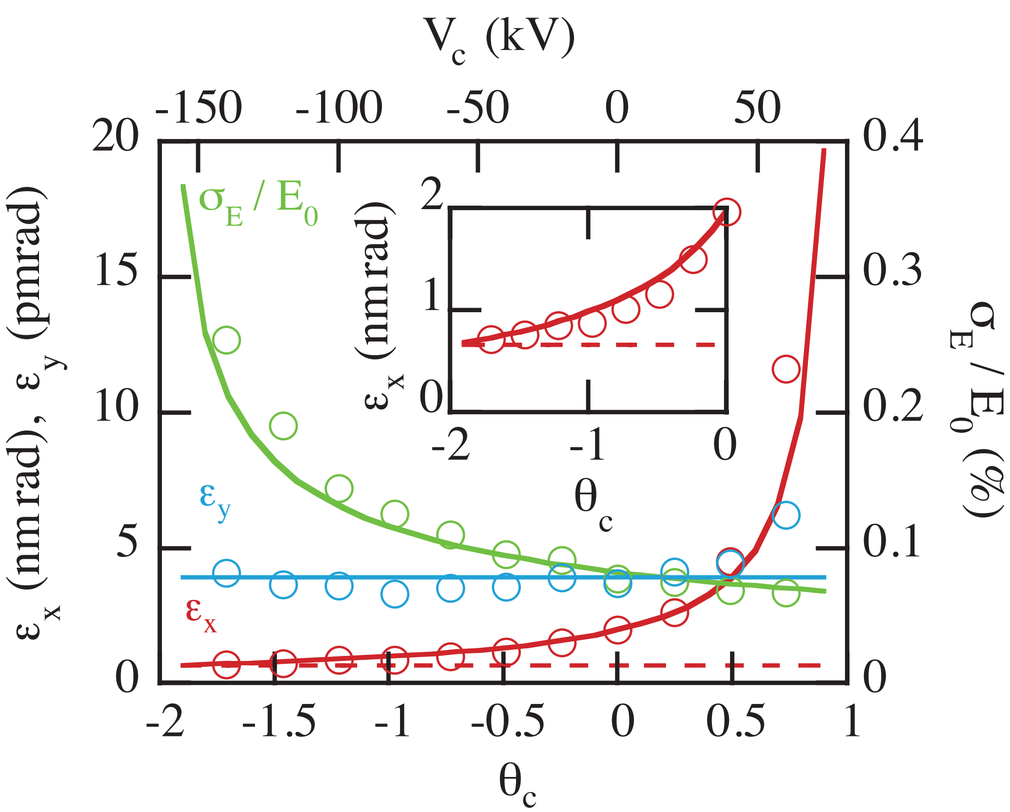

Y. Shimosaki, H. tanaka, Control of damping parititon numbers in a Ring Accelerator with rf Electromagnetic Fields, PRL 110, 154802 (2013) 154802

Somes examples

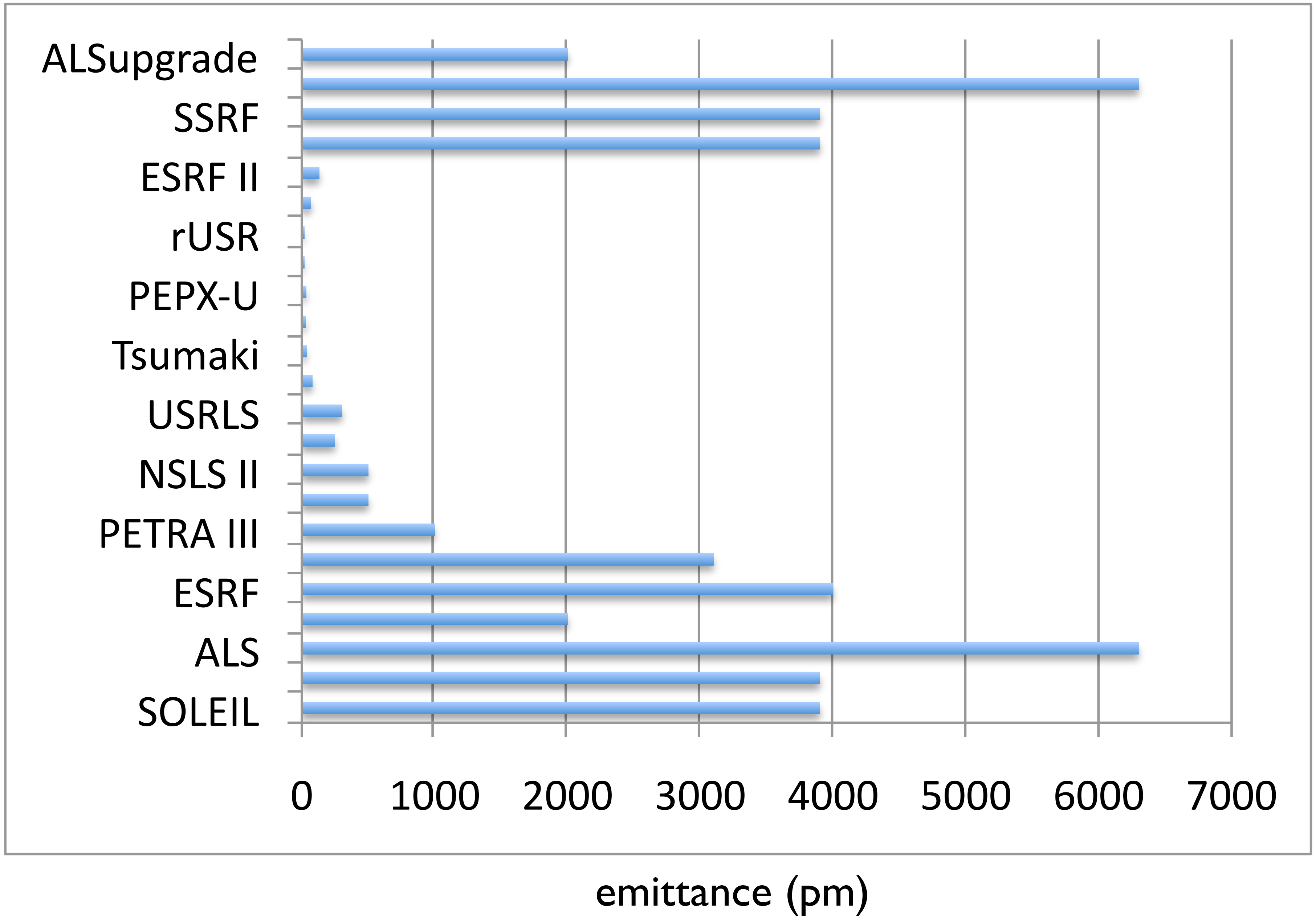

Brightness increase

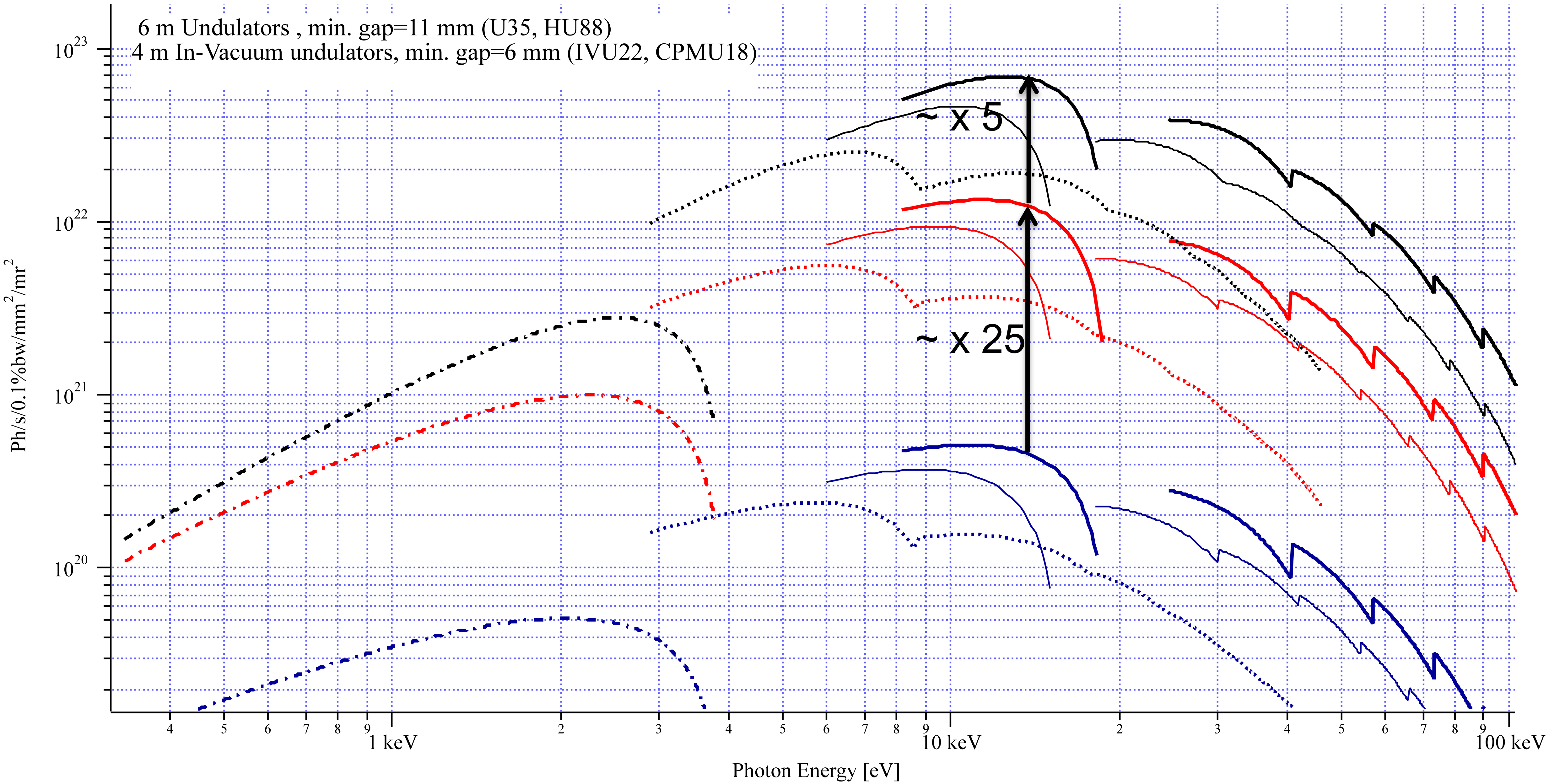

Hor. Emittance [nm]	4	0.15	0.01
Vert. Emittance [pm]	3	2	2
Energy spread [%]	0.1	0.09	0.09
Betax[m]/Betaz [m]	37/3	6/2	6/2

P. Raimondi USR Accelerator R&D Workshop, Huairou (Beijing), China, October 30, 2012

Brightness increase

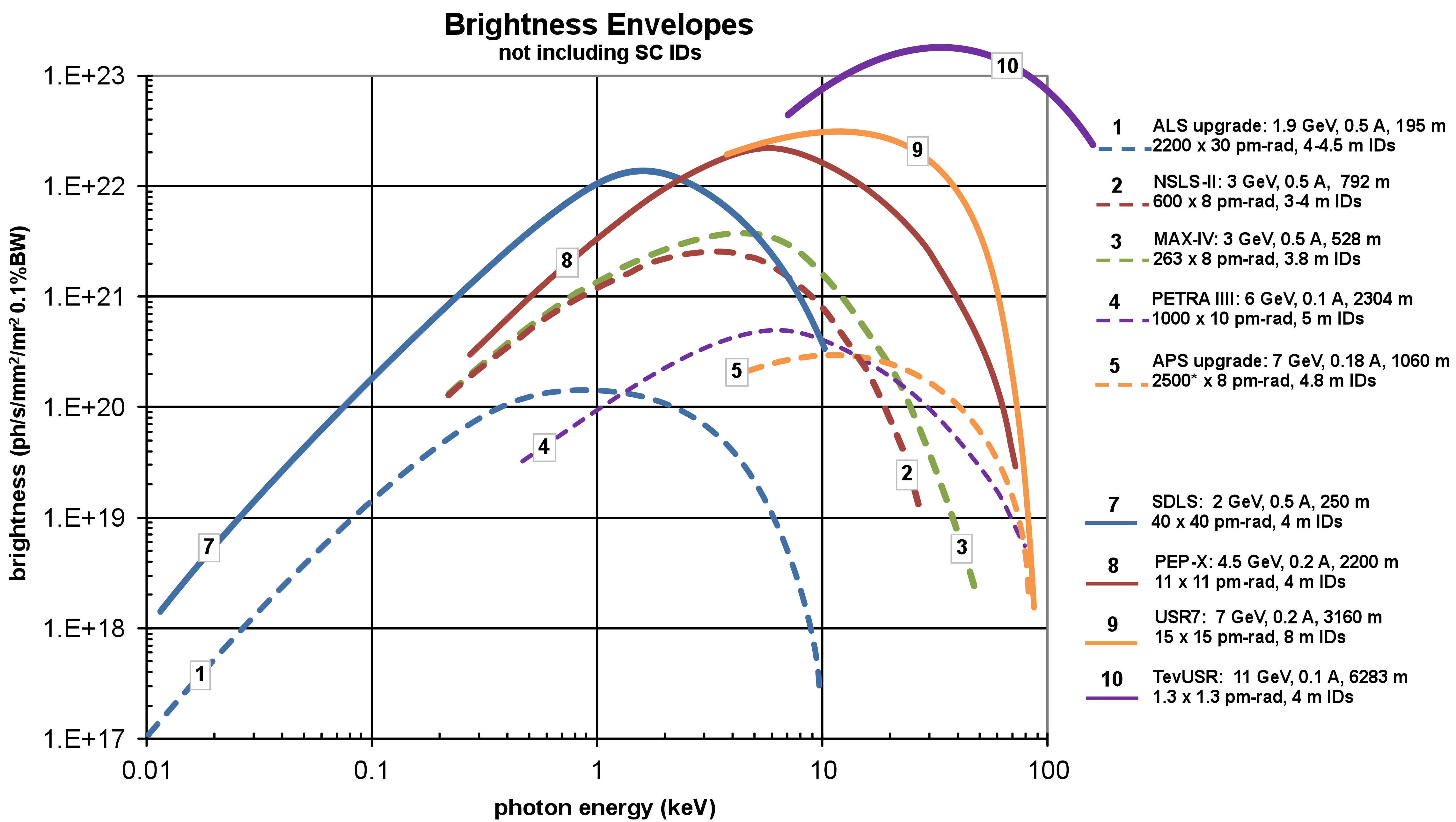

Probably for the next 40-50 years

Short pulses

- reduction of the momentum compression factor
- high RF voltage / modulated RF voltage or phase

$\sigma_l = \alpha c \sigma_\gamma / \Omega_s$

Dedicated user shifts at ANKA, SOLEIL, BESSY....

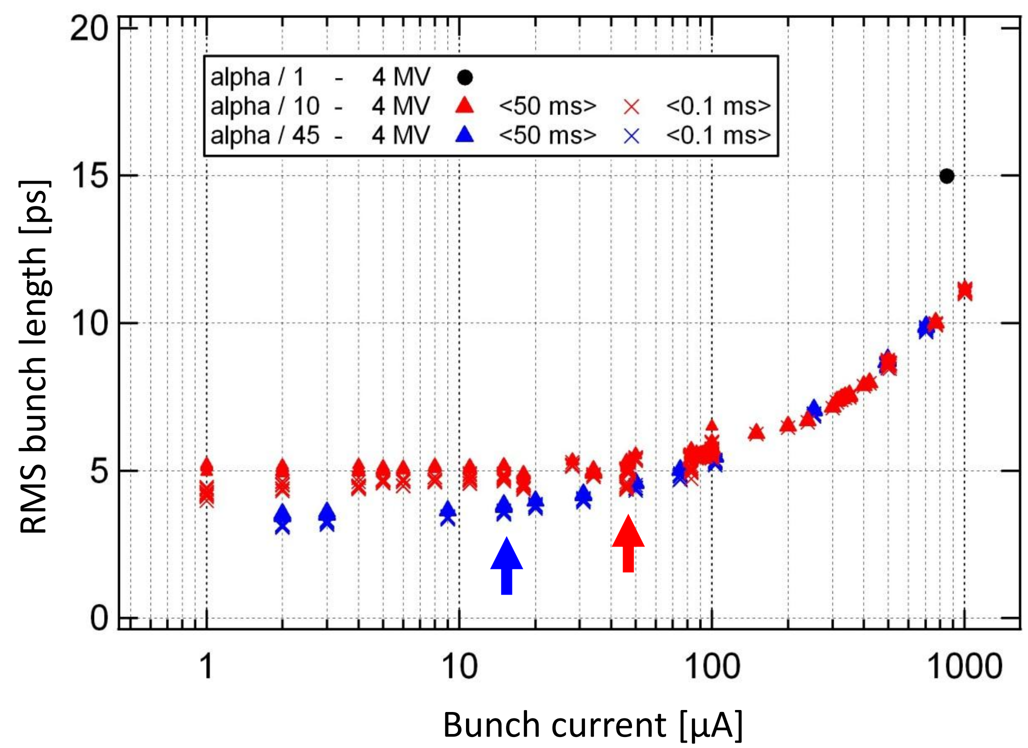

- flipping of the transerse phase space to longitudinal and vis-versa (CRAB cavities) : 1 ps vertical kick

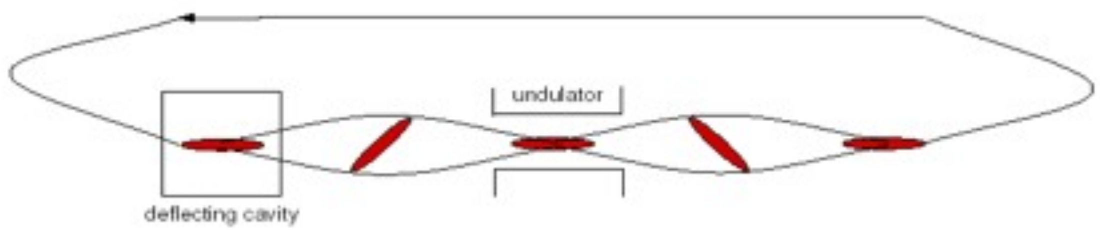

- slicing : 100 fs, reduced intensity

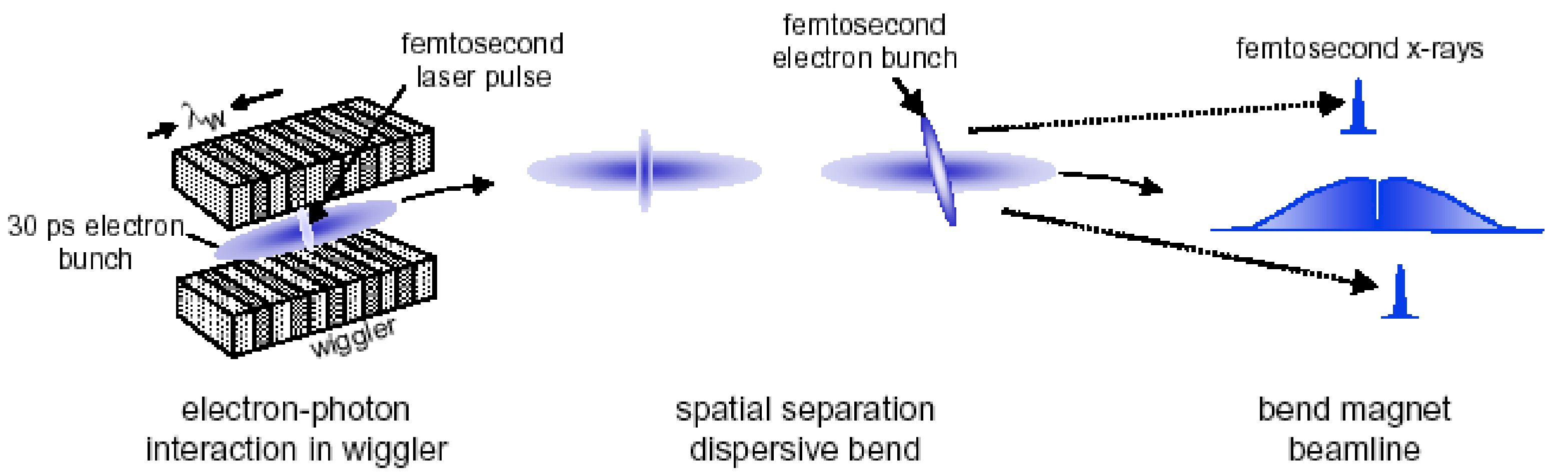

A. Zholents et al. PRL 76,1996, 916

III-Storage rings based light sources

Short pulses

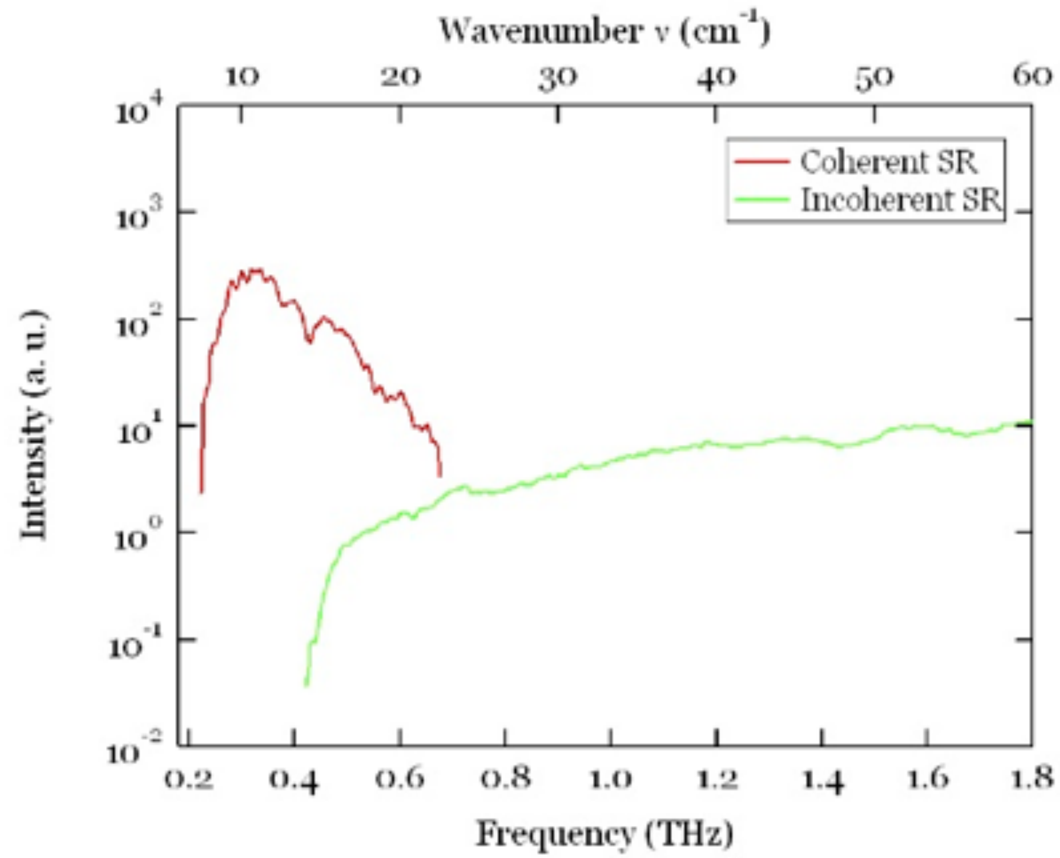

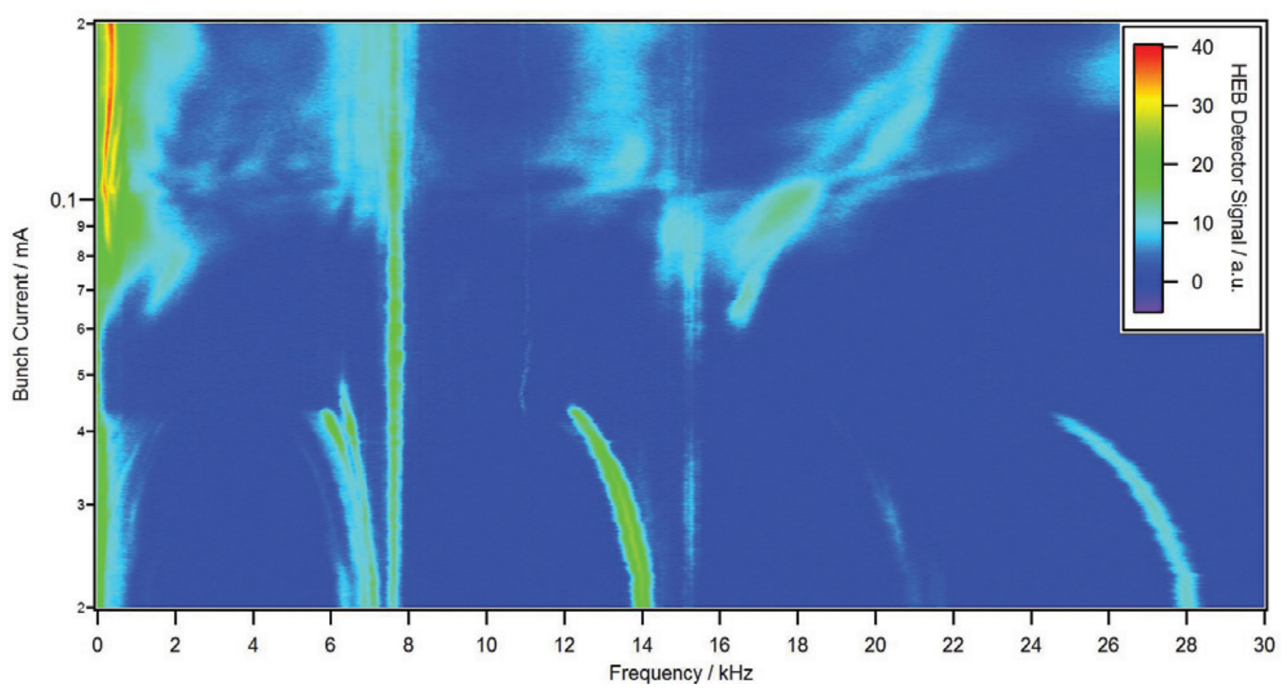

Figure 5: Spectrogram of the turn-by-turn THz signal measured with the HEB detector system at ANKA as a function of the single bunch current [24].

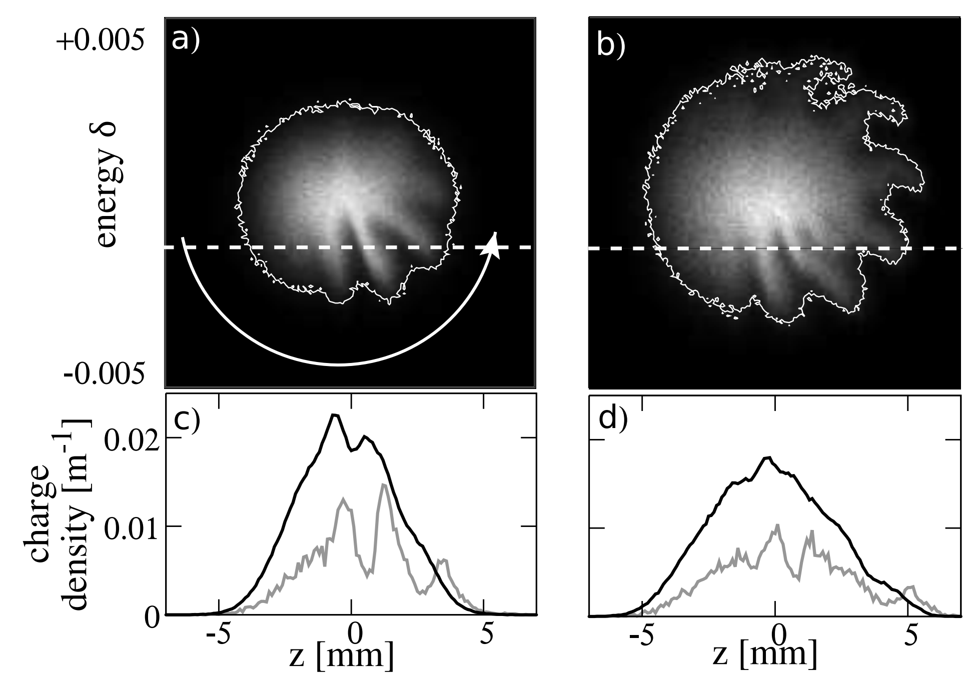

C. Evain et al. EPL 98, 4006 (2012)

A. S. Muller, IPAC 2013, Shanghai, China, 2013

Different simultaneous short pulses operation

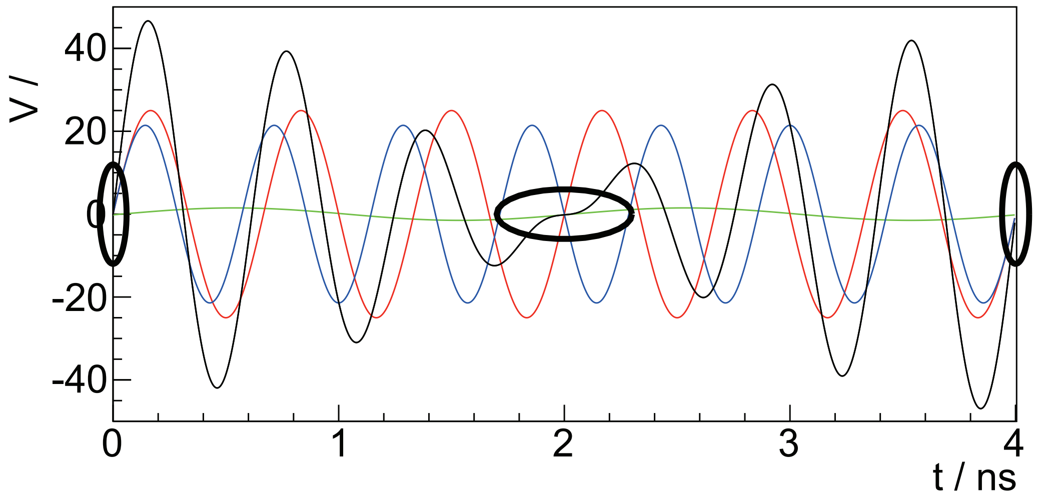

Figure 1: Accelerating voltage versus time. Voltages of the fundamental RF cavity (green), the 1.5 GHz cavity system (red), the 1.75 GHz cavity system (blue) and the sum (black) are drawn. The ellipses indicate the locations of the short bunch ($t = 0$ and $t = 4$ ns) and the long bunch ($t = 2$ ns).

1.5 ps and 15 ps

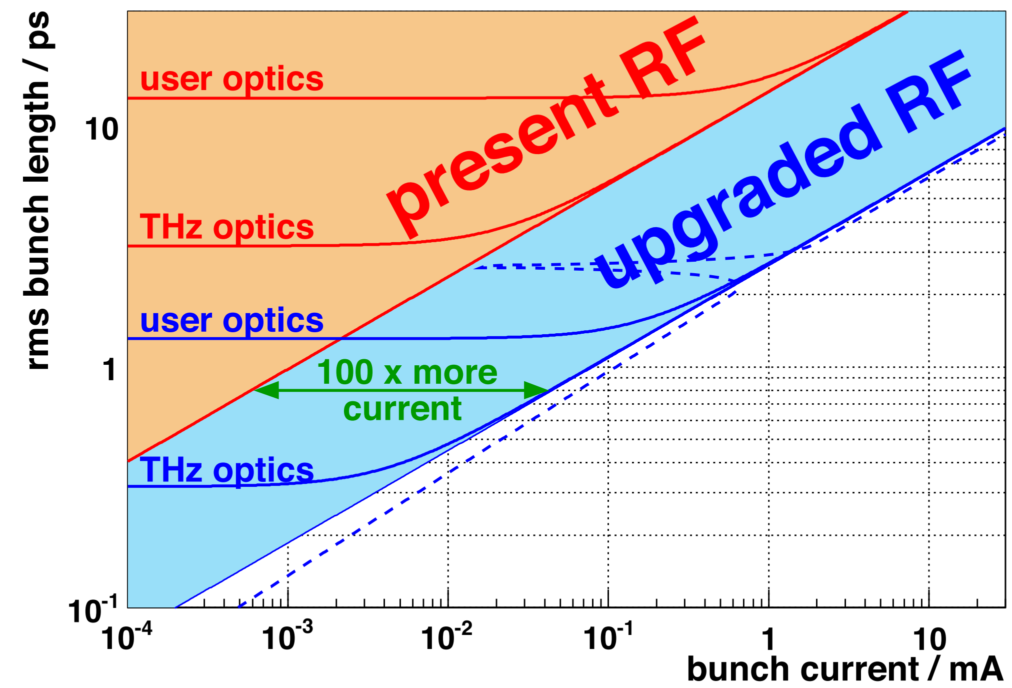

Figure 1: Schematic view of the bunch length-current relation. The bursting limit is given by the straight line. The present situation is given in red, the predicted BESSY^{VSR} upgrading in blue, and the bursting threshold is shifted by a factor of 100 to higher currents [15]. The dotted line indicates the predicted deviations from the simple exponential scaling relation.

G. Wustefeld et al., IPAC 2011, San Sebastian, Spain, p. 2936.
M. Ruprecht, IPAC 2013
A. Jankowiack, G. Wustefeld, Synch. rad. News 11 June 2013, 37-41

besides isolated bunch and multi-bunches filling pattern, «tailored bunch operation» by varying the orbit or the energy of one bunch with respect to the remaining ones.

ERLs

ERL advantages :

- freedom to use the optimum beta function
- ability to provide ultra low emittance
- possible implementation of long undulators
- easy longitudinal bunch manipulation => short pulses

Table 1
Present advanced photon source beam parameters compared to ERL X-ray source parameters in high coherence and high flux modes [4].

Quantity	APS	ERL high coherence	ERL high flux
Beam energy (GeV)	7	7	7
Average current (mA)	100	25	100
Repetition rate (MHz)	6.5–352	1300	1300
Bunch charge (nC)	<59	0.019	0.077
Horizontal emittance (geometric pm), [normalized (μm)]	3100 [42]	6 [0.08]	20 [0.27]
Vertical emittance (geometric pm), [normalized (μm)]	25–50 [0.35–0.70]	6 [0.08]	20 [0.27]
rms bunch length (ps)	>20	2	1.7
rms energy spread (%)	0.1	0.015	0.014
Photon brightness (10^{20}p/(s mm^2 mrad^2 0.1%BW))	0.3	200	60

Photon brightness at 10 keV reported.

S. benson et al. NIM A 637 (2011) 1-11

ERL challenges :

- injector (ultra-low emittance), photocathode and drive laser
- emittance preservation
- beam stability and collective effects (space charge, wakefields, ion trapping, IBS...)
- beam loss, halo
- cryogenics

At present : ERL test facilities driver for IR-FELs

towards ERL X-ray source

probably for the next 50 years

XFEL on ERLs

Optics of high reflectivity in normal incidence : C, BeO, SiC, Al_2O_3

Ex : Al_2O_3 case in normal incidence in (0 0 0 30) plane, 30K, 14,36 eV

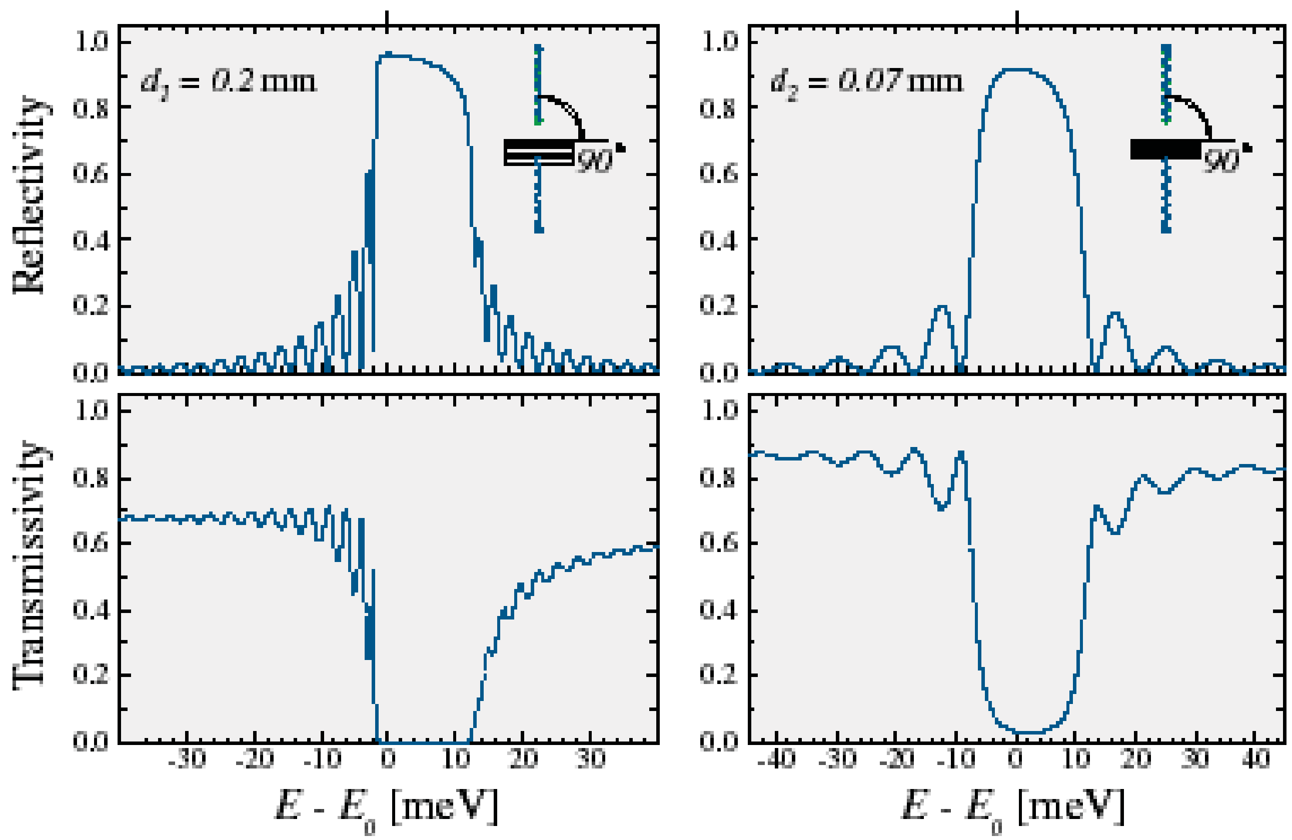

R=0.96, 4% transmission for extraction
R=0.99 for diamond

Cavity configuration

2 Al_2O_3 mirror cavity in normal incidence

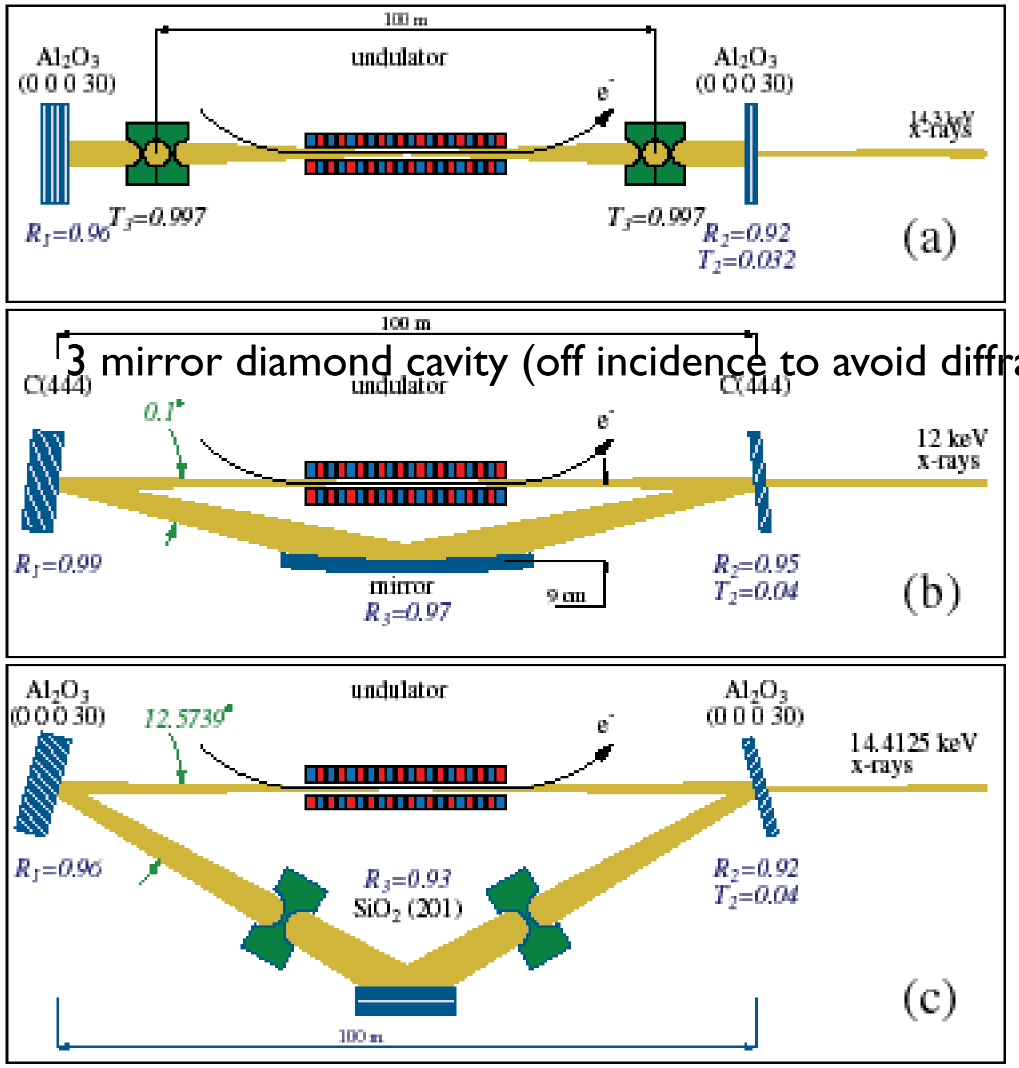

-CRL : parabolic compound refractive lenses:
2 parabolic mirrors (Be, T=0.997) + 1 eelipsoidal mirror in grazing incidence

***Kim** et al., Phys. Rev. Lett. 100 (2008) 244802*

First FELs

First demo : on linear accelerator, MARK III, Stanford, infra-red

D.A. G. Deacon et al, First Operation of a FEL. PRL 38, 16, 1977, 892

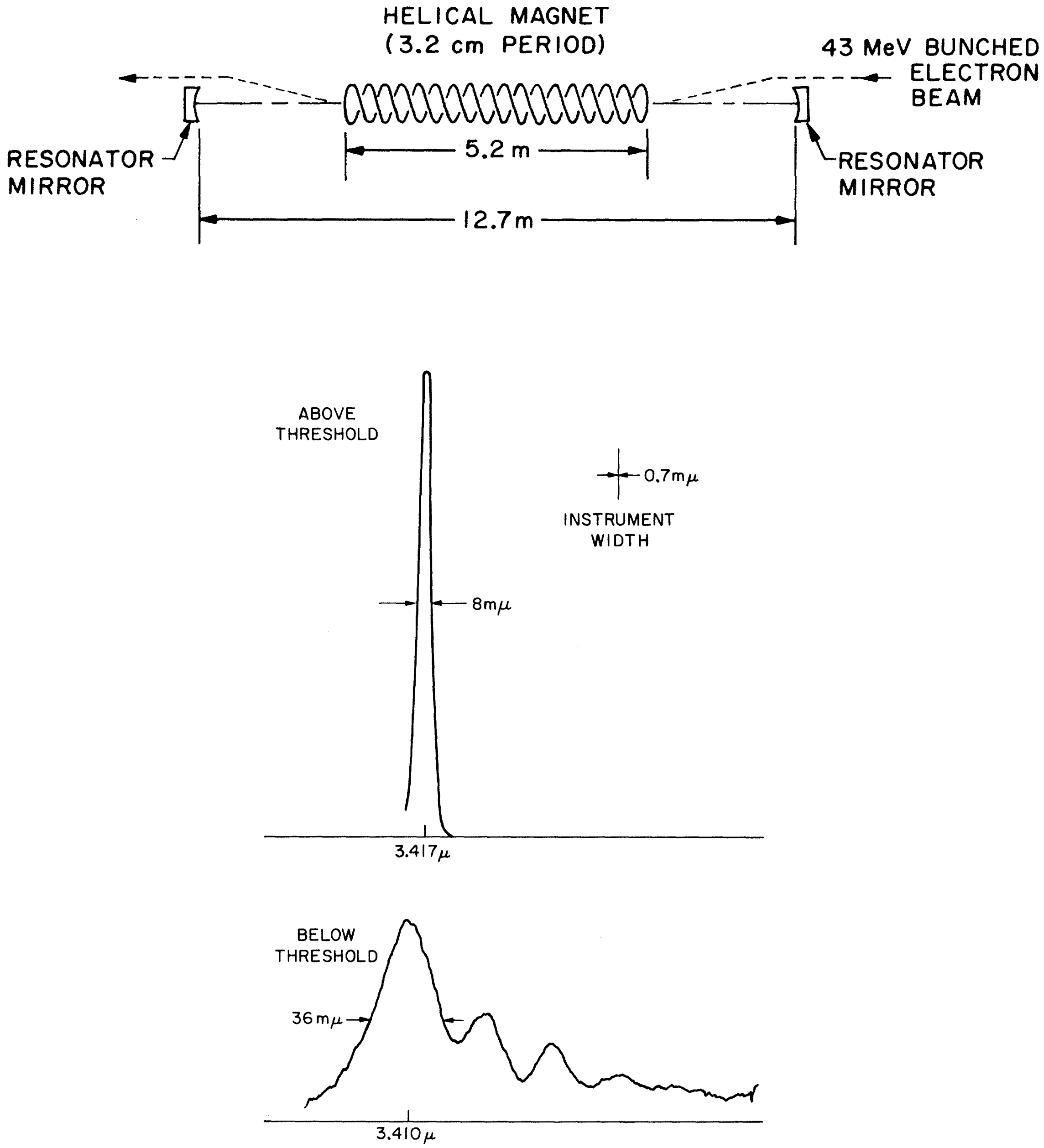

FIG. 2. Emission spectrum of the laser oscillator above threshold (top) and of the spontaneous radiation emitted by the electron beam (bottom).

Second FEL : on storage ring, ACO, Orsay, visible, 1983

M. Billardon et al., Phys. Rev. Lett. 51, 1652,(1983)

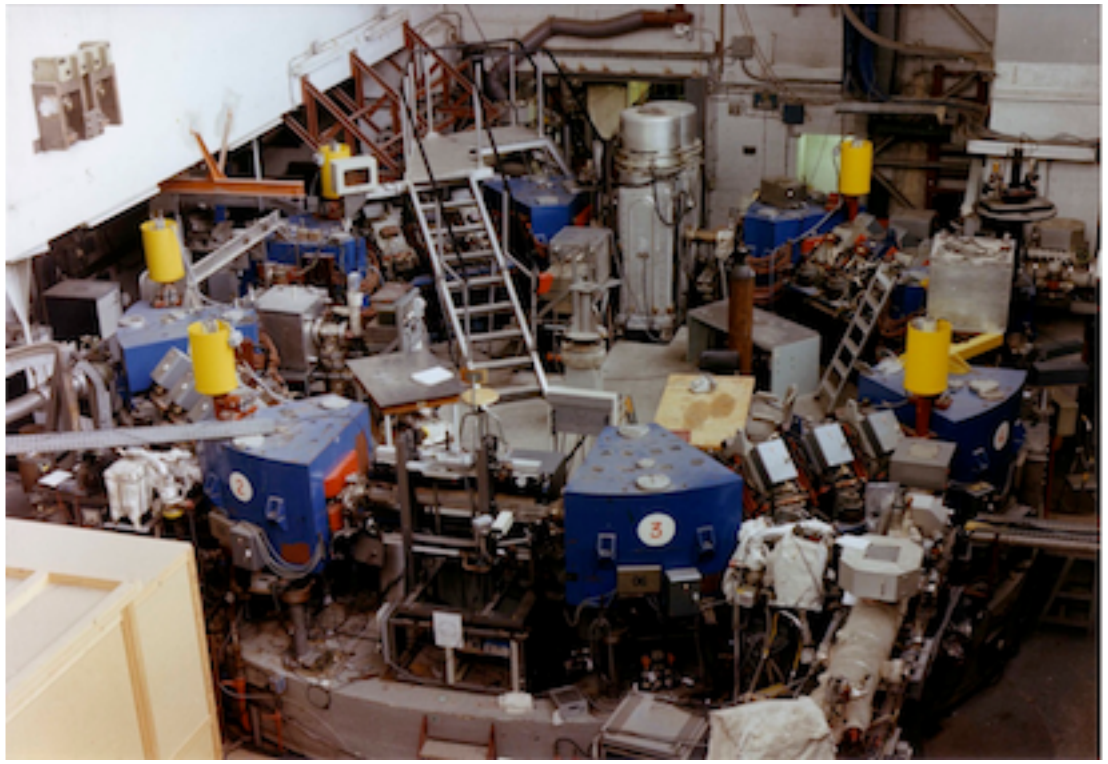

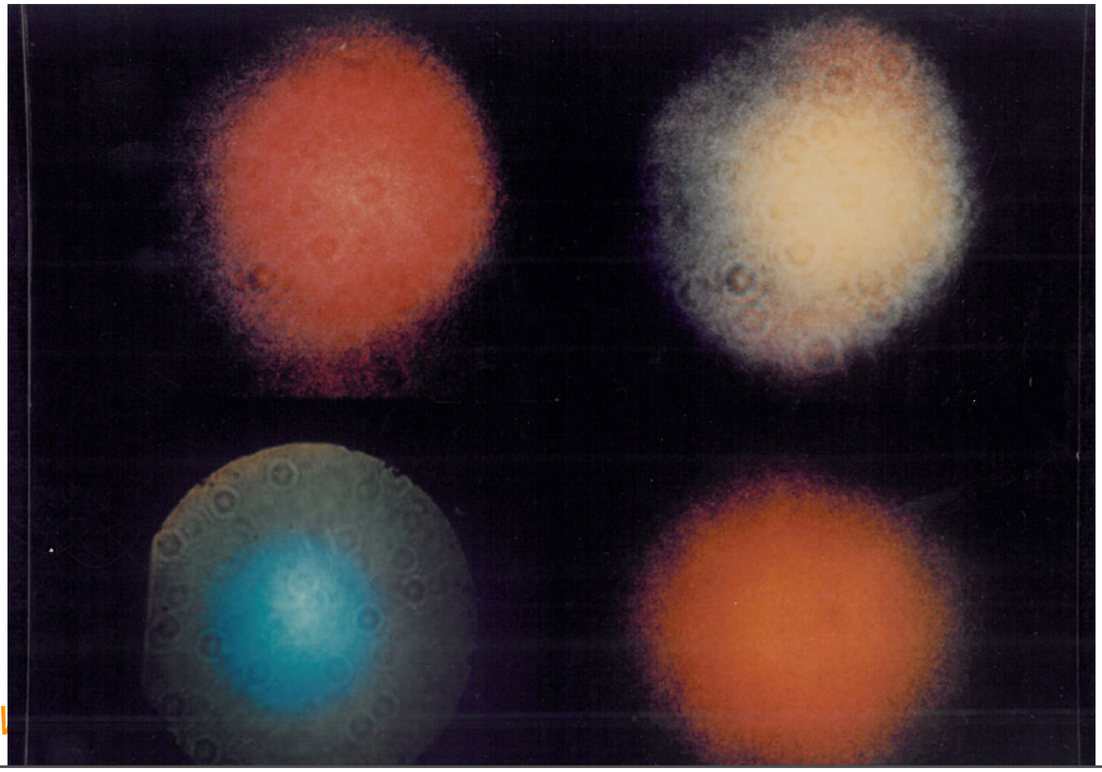

Overview of short wavelength FEL : present

operating FEL *VUV- soft X ray* *hard X ray*

Overview of short wavelength FEL : future

project operating FEL *VUV- soft X ray* *hard X ray*

IV-(Linac-based) FELs & ERLs

X-ray FELs : LCLS (USA, 1.5-15 Å, 2 mJ)

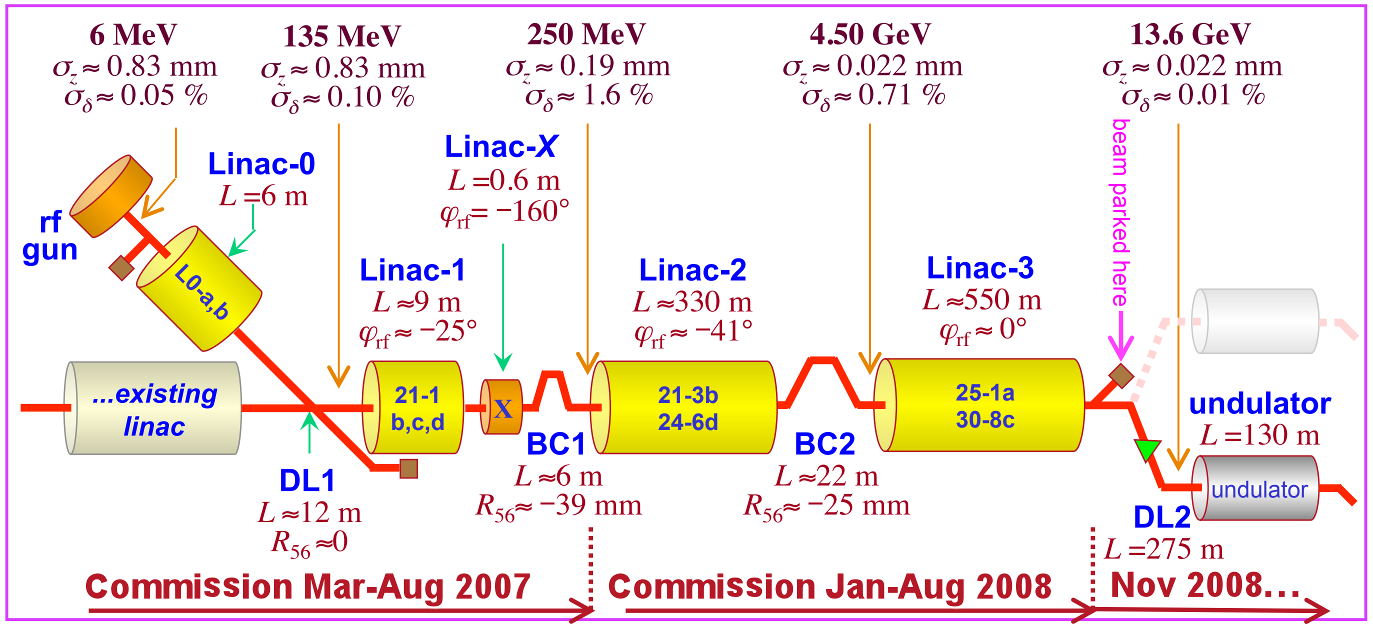

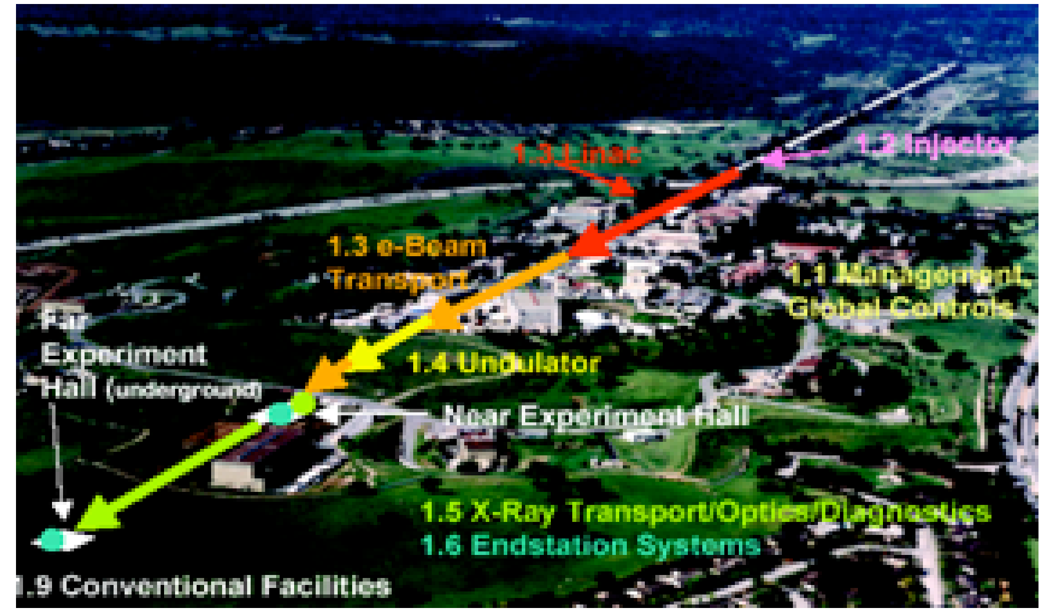

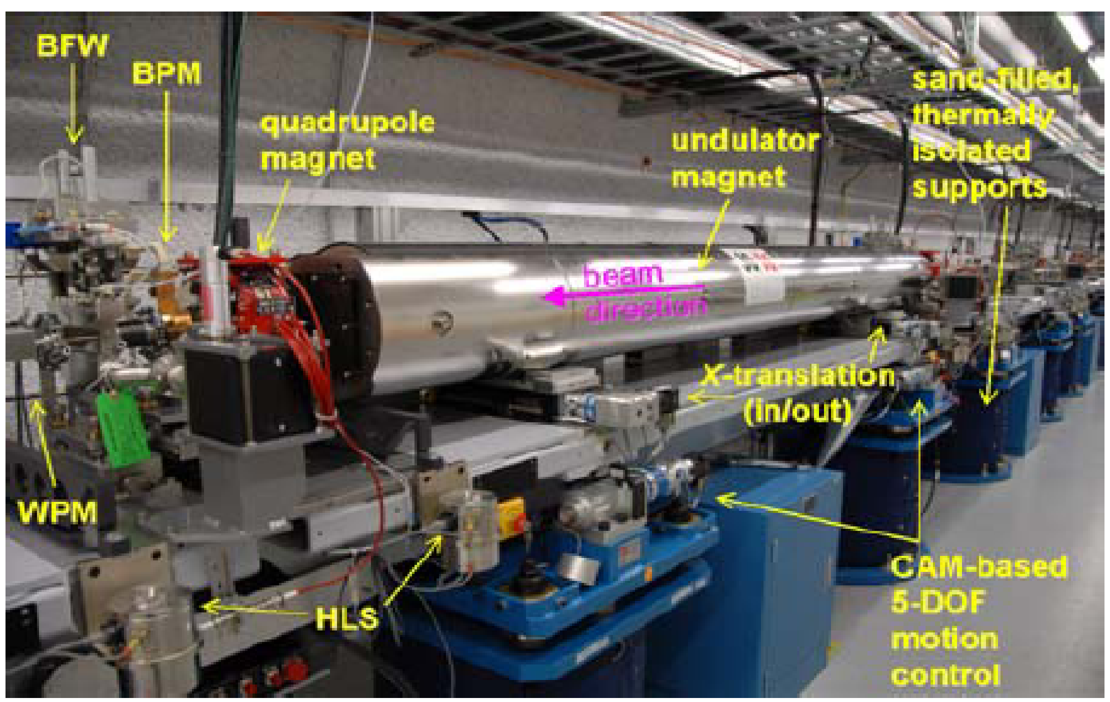

P. Emma et al., Nature Photonics, 2010,(PUBLISHED ONLINE: 1AUGUST 2010 | DOI: 10.1038/NPHOTON.2010.176)

http://www-ssrl.slac.stanford.edu/lcls/

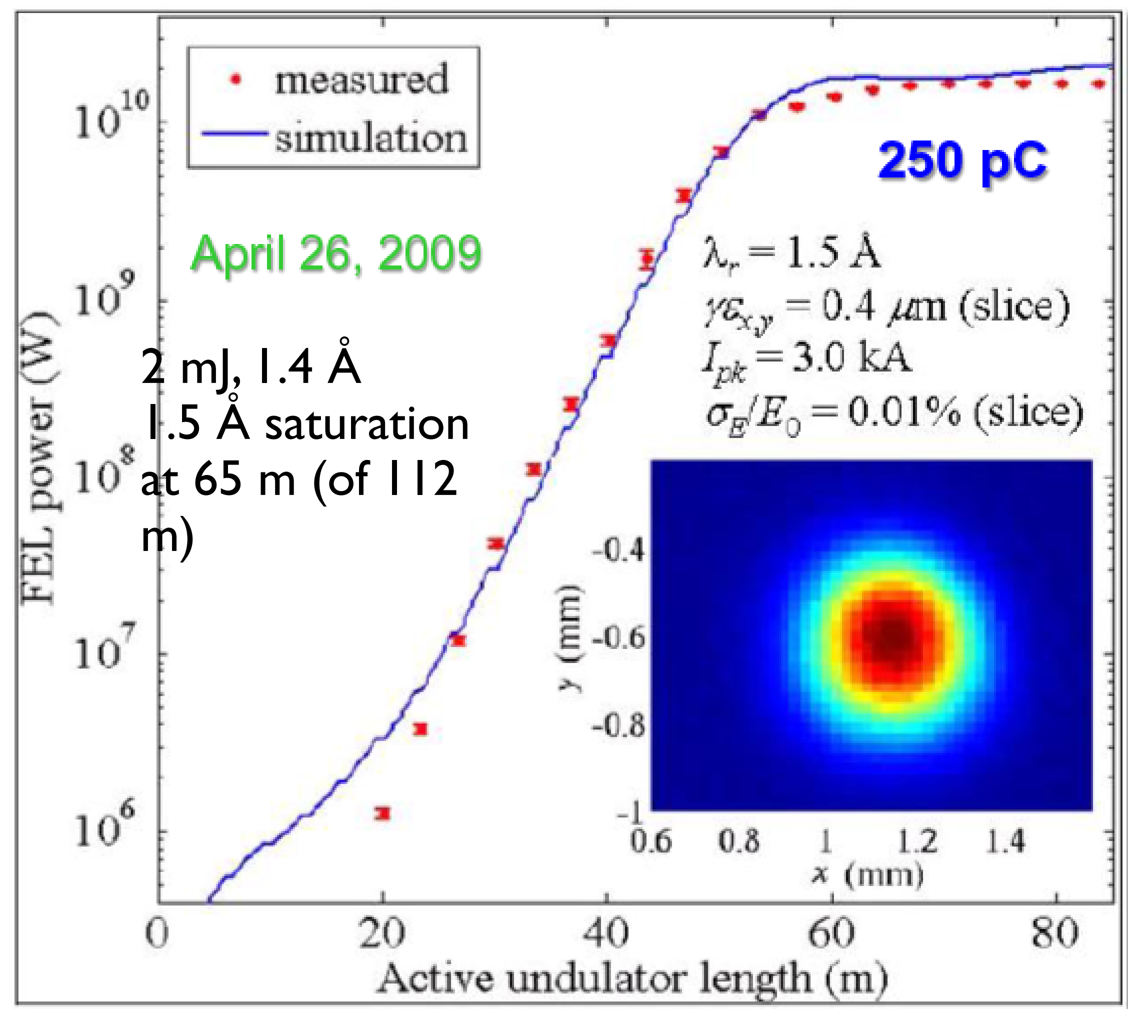

32 years after the first FEL, 50 years after the first laser

X-ray FELs : LCLS

LCLS Operational Performance :

280 eV – 10 keV, > 70 GW, 6 mJ, 96.7 % (94.8) electron (photon) avalaibility.

Courtesy T. Raubenheimer

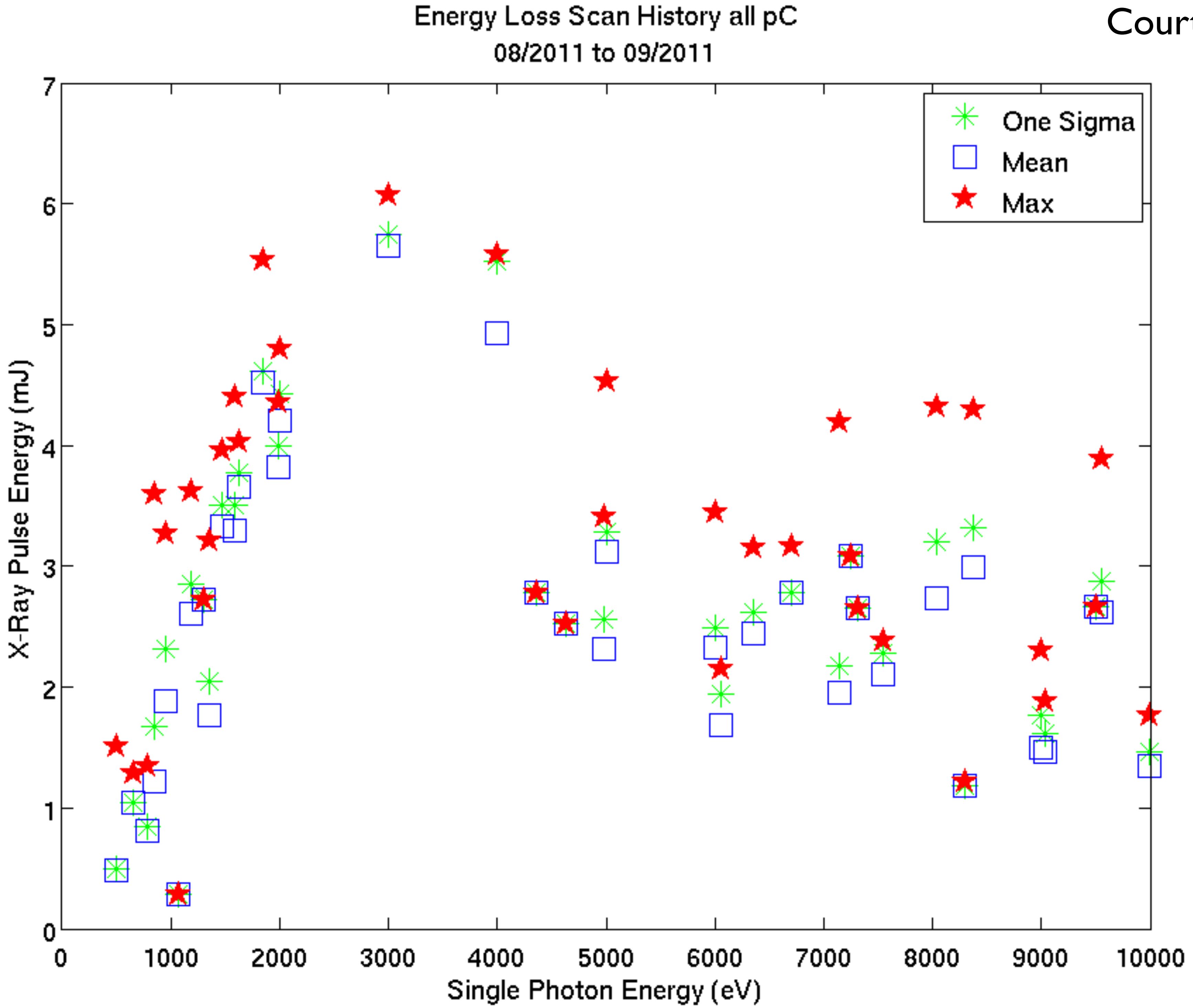

X-ray FELs : LCLS II (250 pC, 120 Hz) 250 eV- 13 keV

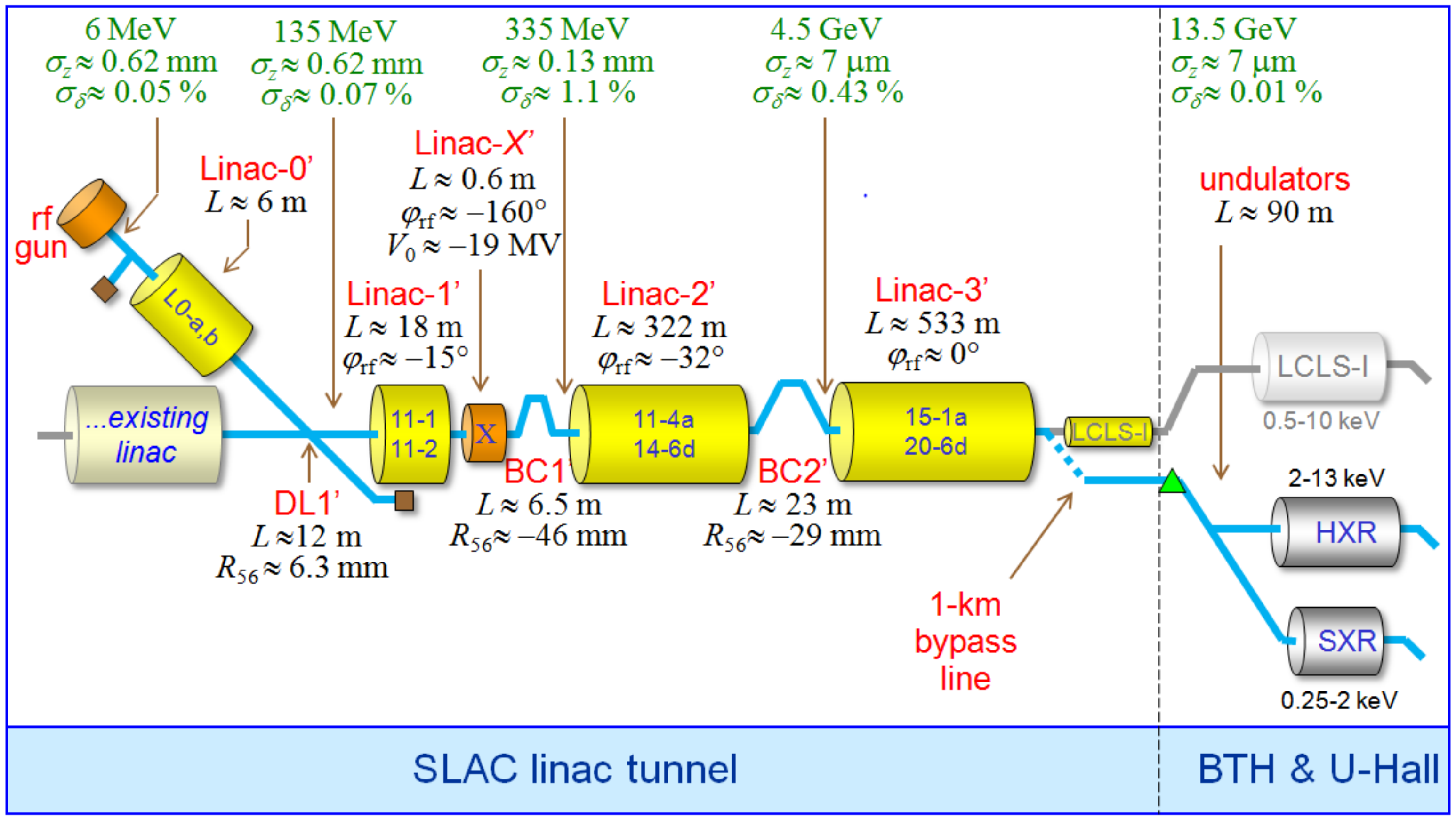

Courtesy T. Raubenheimer

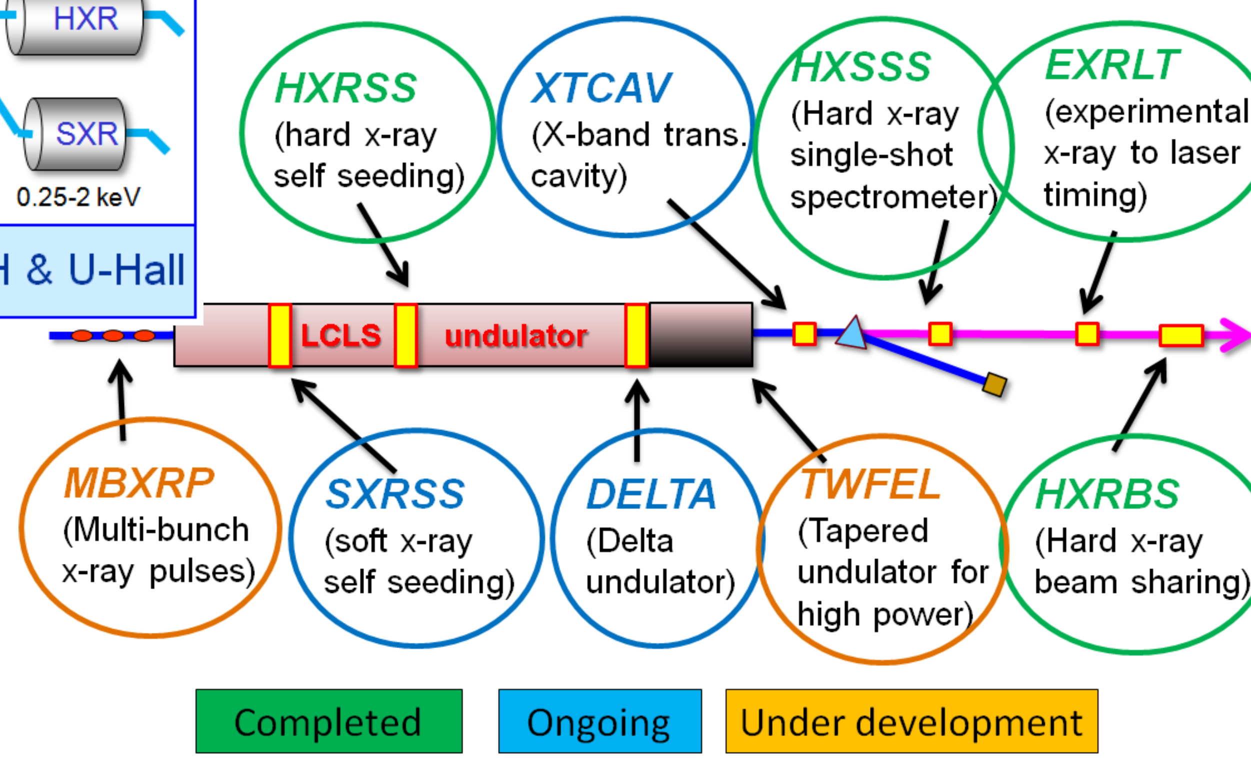

- Polarisation control (DELTA undulator)
- TW level by tapering
- self seeding in soft X-ray

IV-(Linac-based) FELs & ERLs

Hard X ray FEL : SACLA (SPring-8 Angstrom Compact LAser)

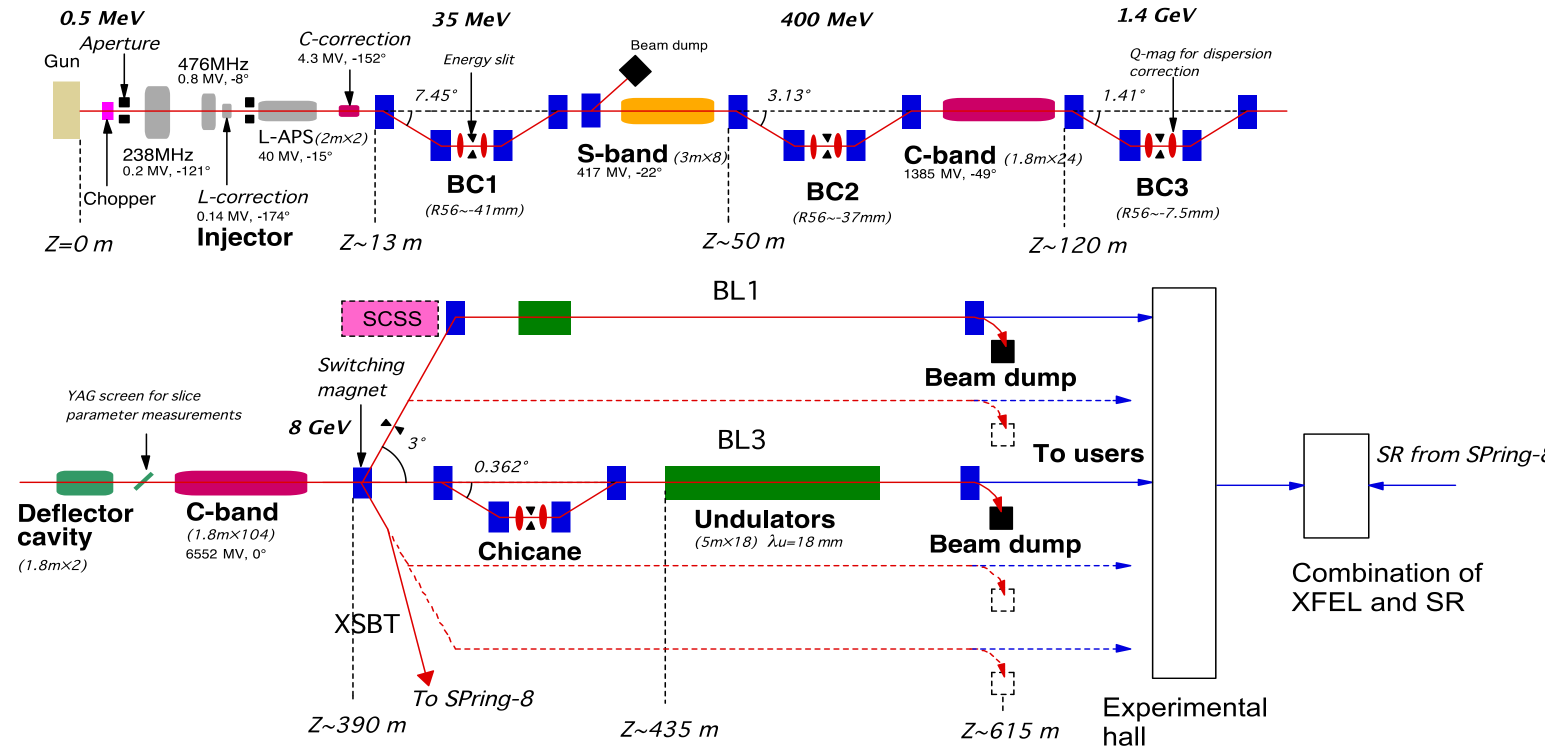

Courtesy T. Hara

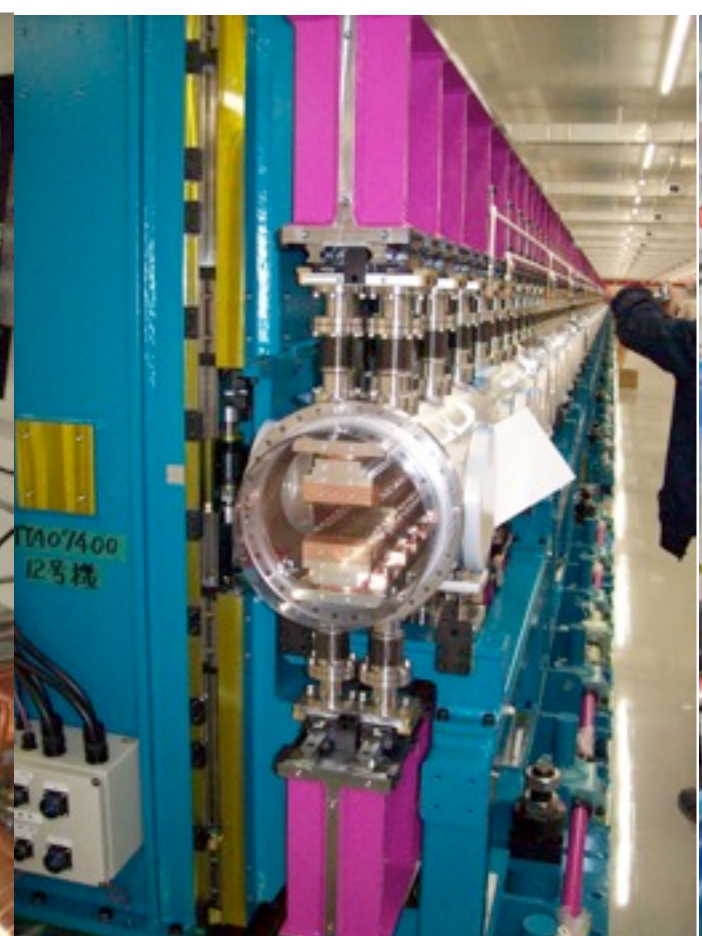

Possibility to use the LINAC for injecting SPring-8 in ERL=> SR of high energy

2011 : Lasing SACLA on 7 June 7- 2011 : 0.12 nm

http://www-xfel.spring8.or.jp/index.htm

Hard X ray FEL : SACLA (SPring-8 Angstrom Compact LAser)

Gain curve of 10 keV

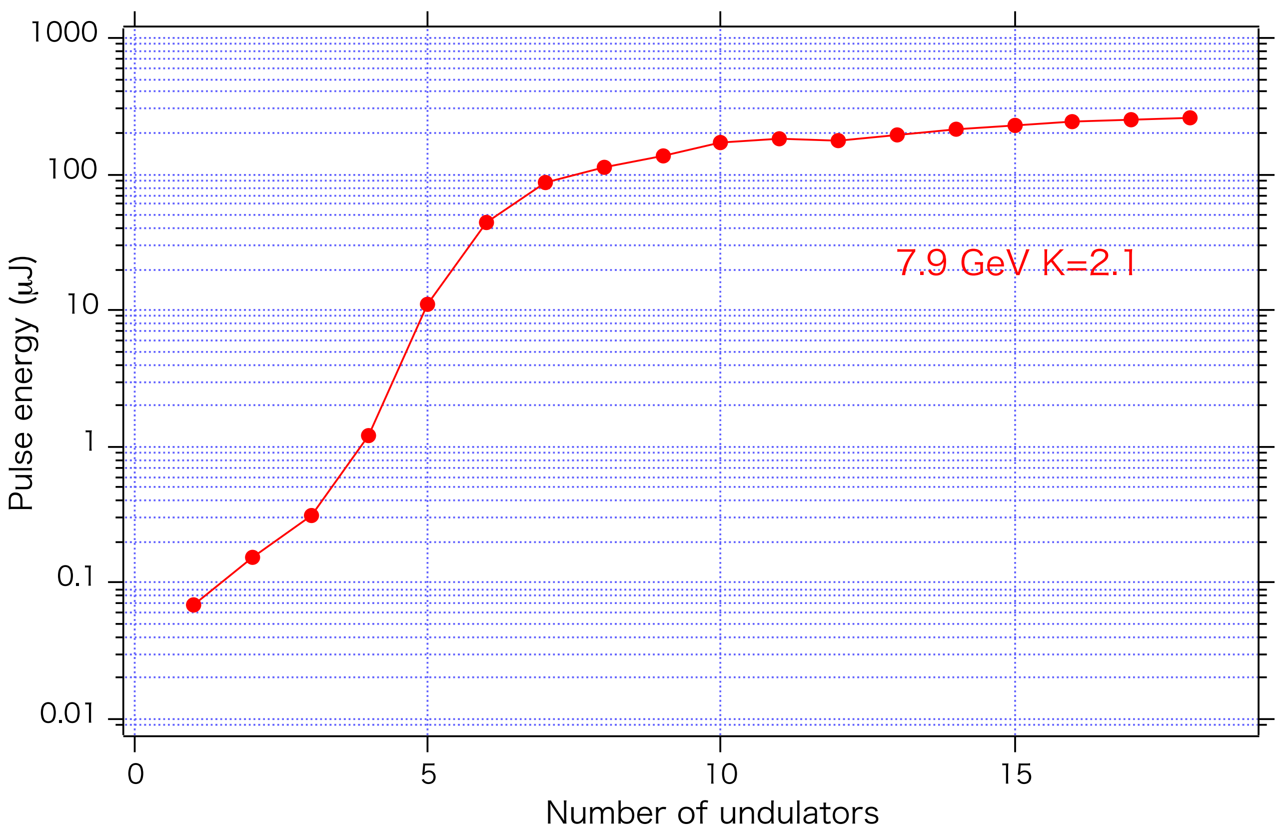

H.Tanaka, M.Yabashi et al., Nature Photonics 6, 2012, 540-544

Photon energy range

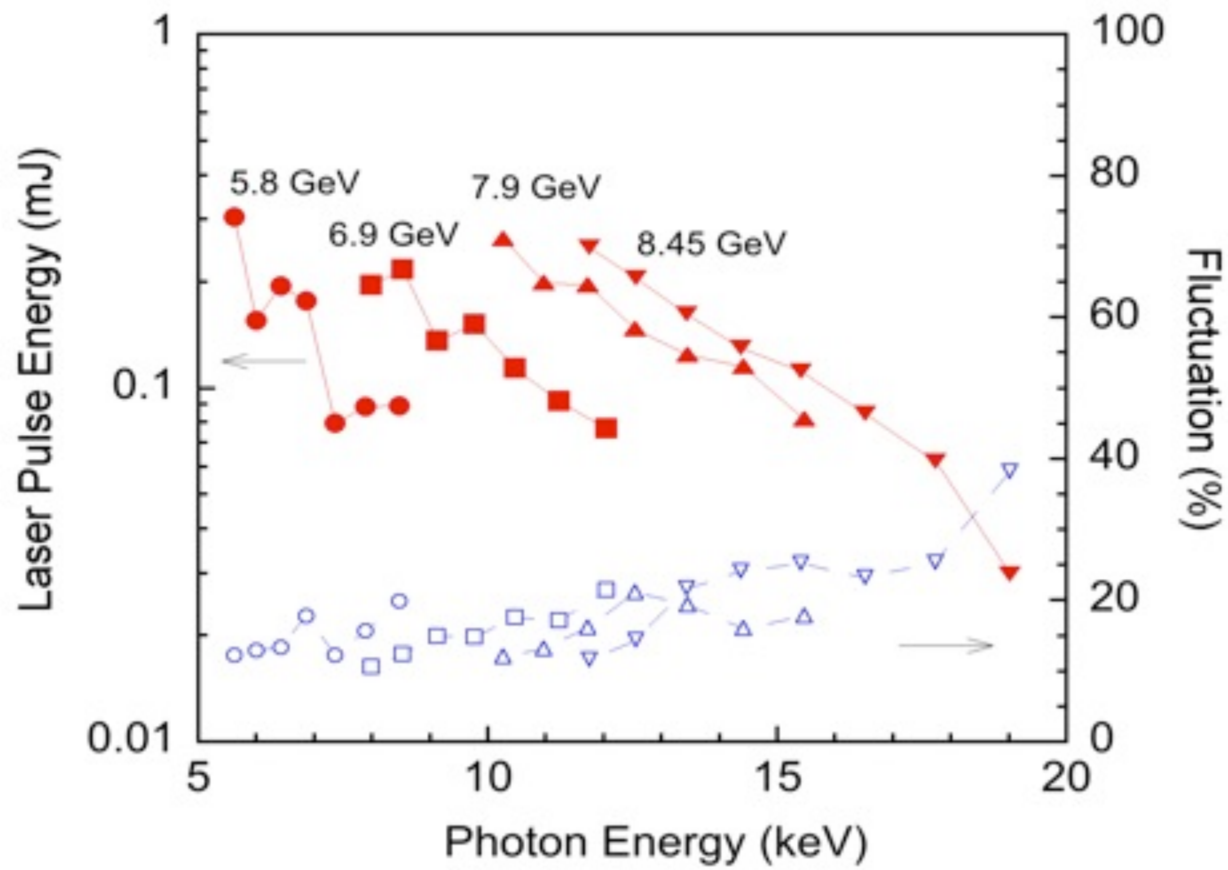

Stability of FEL pulse energy
(10 keV, 7.9 GeV, K=2.1)

Courtesy T. Hara

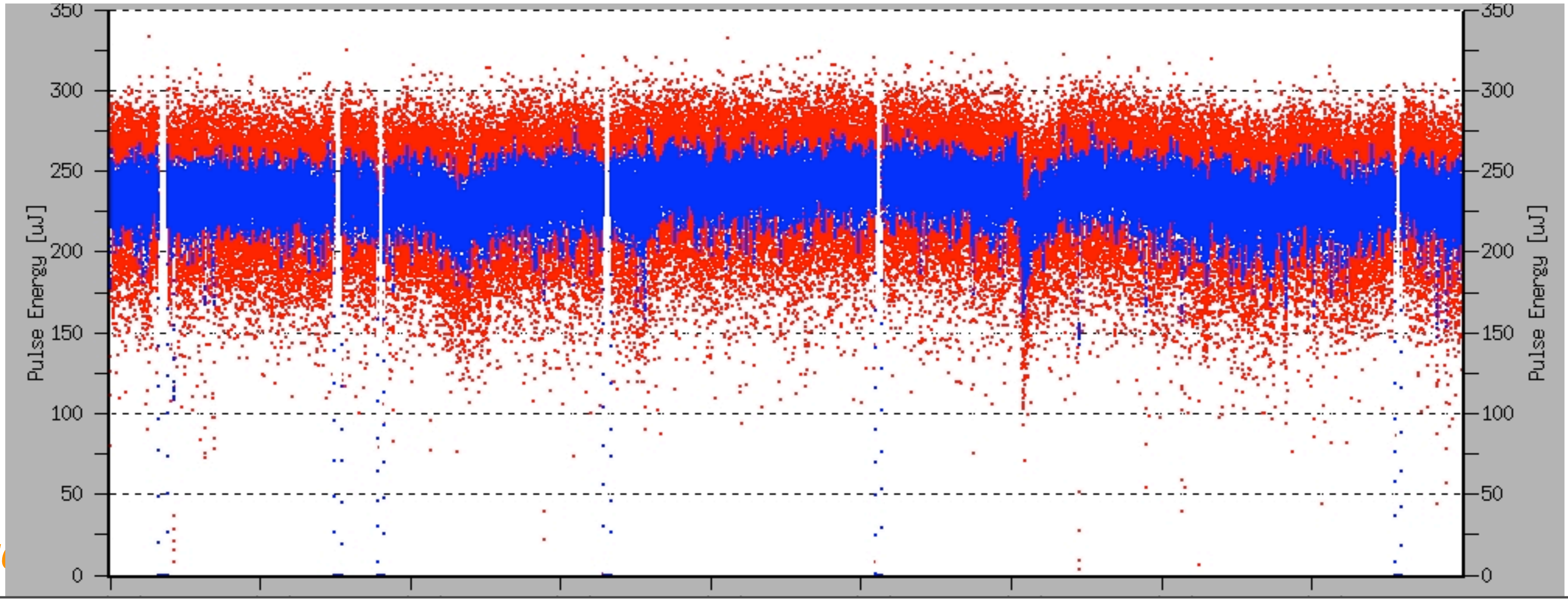

IV-(Linac-based) FELs & ERLs

Hard X ray FELs under construction/project

- European XFEL (17 GeV)

SC Linac, 2 km, 23 MV/m, 1 nC , 1.4 π mm.mrad, uncorrelated σ_γ = 2.5 MeV rms, 10 Hz,

Parameter	Unit	SASE 1	SASE 2		SASE 3		
Electron energy	GeV	17.5	17.5	17.5	17.5	17.5	10.0**
Wavelength	nm	0.1	0.1	0.4	0.4	1.6	6.4
Photon energy	keV	12.4	12.4	3.1	3.1	0.8	0.2
Peak power	GW	20	20	80	80	130	135
Average power*	W	65	65	260	260	420	580
Photon beam size (FWHM)	µm	70	85	55	60	70	95
Photon beam divergence (FWHM)	µrad	1	0.84	3.4	3.4	11.4	27
Coherence time	fs	0.2	0.22	0.38	0.34	0.88	1.9
Spectral bandwidth	%	0.08	0.08	0.18	0.2	0.3	0.73
Pulse duration	fs	100	100	100	100	100	100
Photons per pulse	#	10^{12}	10^{12}	1.6×10^{13}	1.6×10^{13}	1.0×10^{14}	4.3×10^{14}
Average flux	#/s	3.3×10^{16}	3.3×10^{16}	5.2×10^{17}	5.2×10^{17}	3.4×10^{18}	1.4×10^{19}
Peak brilliance	B	5.0×10^{33}	5.0×10^{33}	2.2×10^{33}	2.0×10^{33}	5.0×10^{32}	0.6×10^{32}
Average brilliance*	B	1.6×10^{25}	1.6×10^{25}	7.1×10^{24}	6.4×10^{24}	1.6×10^{24}	2.0×10^{23}

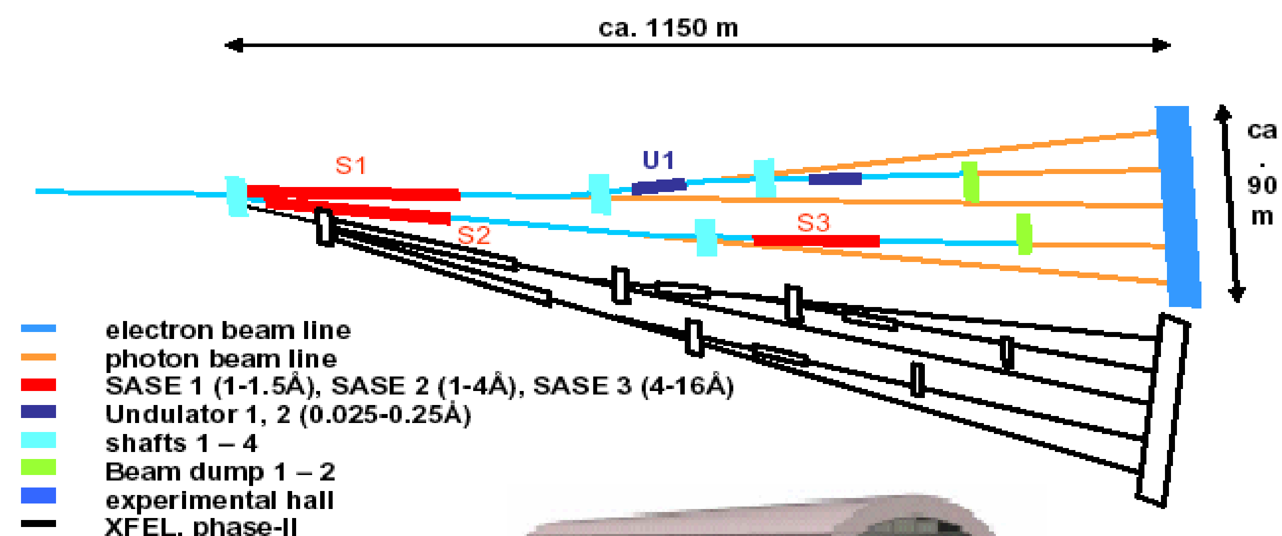

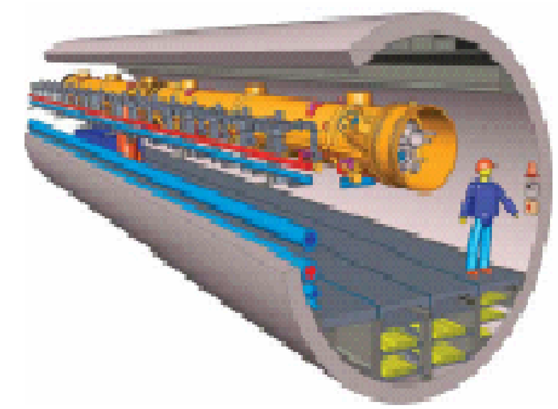

http://xfel.desy.de/

- Swiss FEL

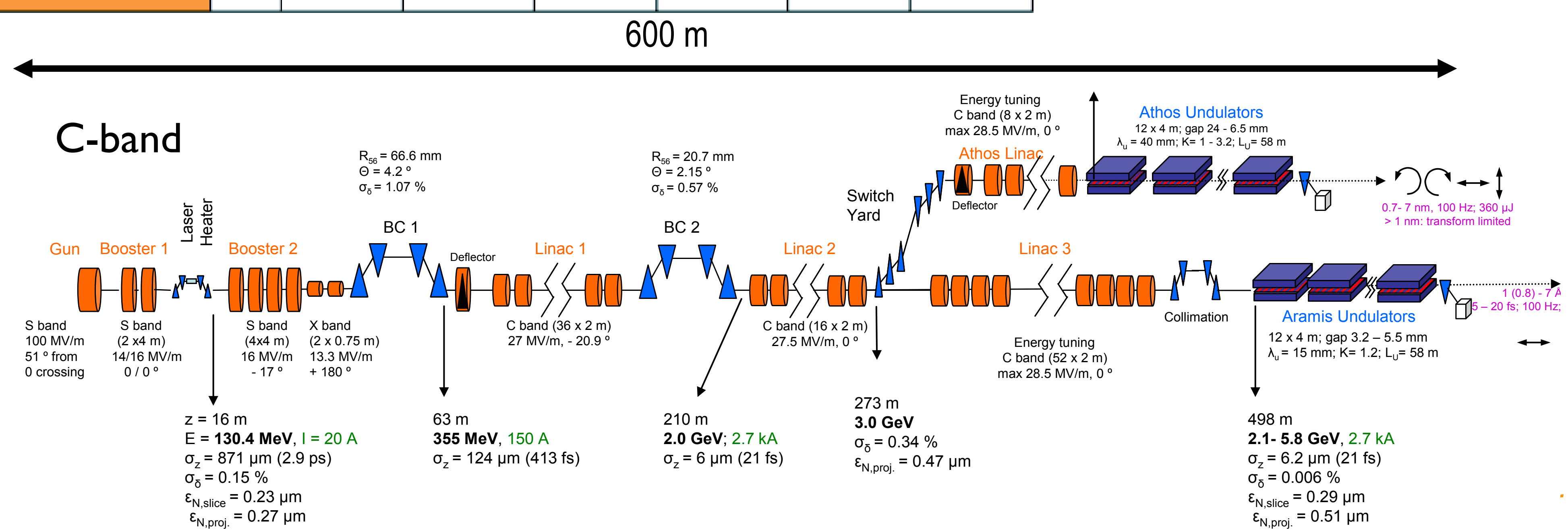

- Korean FEL
- Shanghai FEL
- MaRIE

future, CERN, June 11-13, 2013

Soft X ray FELs : FLASH, SCSS test. Acc.

FLASH : 30 nm (2005) 6 nm (2007), 4.5 nm (2010), FLASH-II under construction

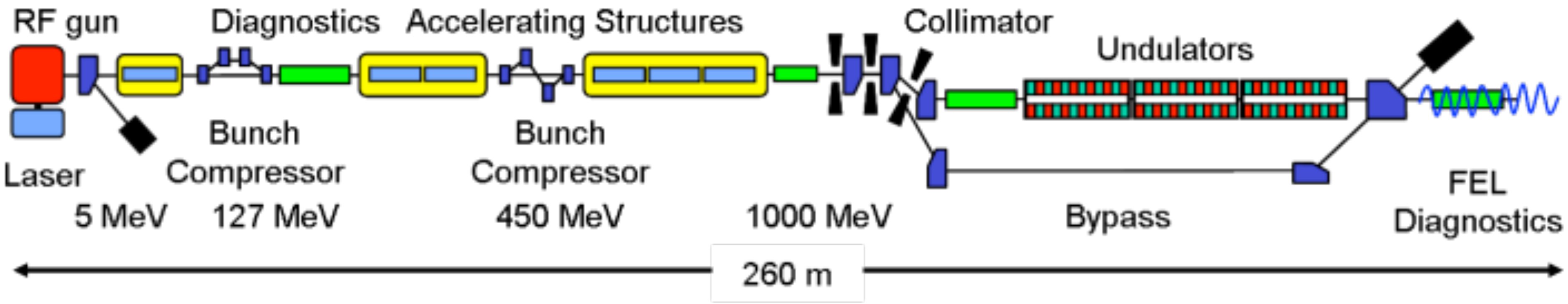

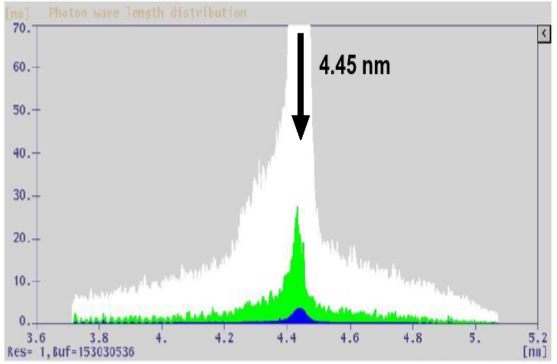

SCSS Test Accelerator : 60-40 nm, to be moved to SACLA (3 nm, 1.3 GeV)

T. Shintake et al., Nat. Phot. 2, 555-559 (2008) *T. Shintake et al. Proceedings EPAC 2006.*

38,3 μJ

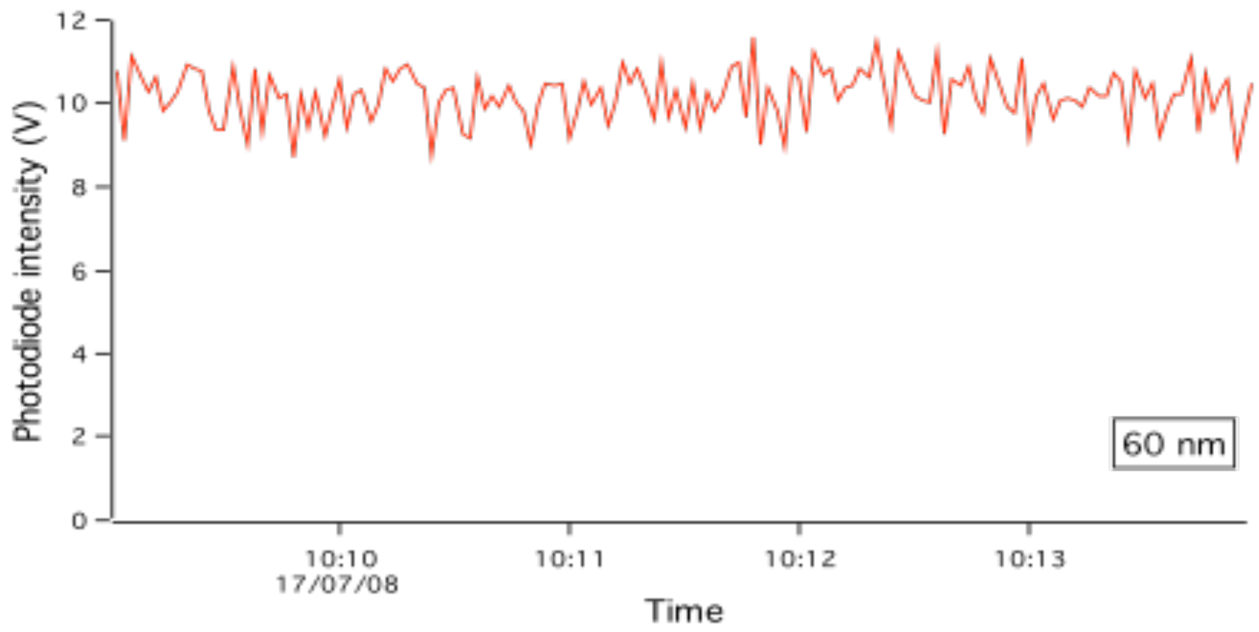

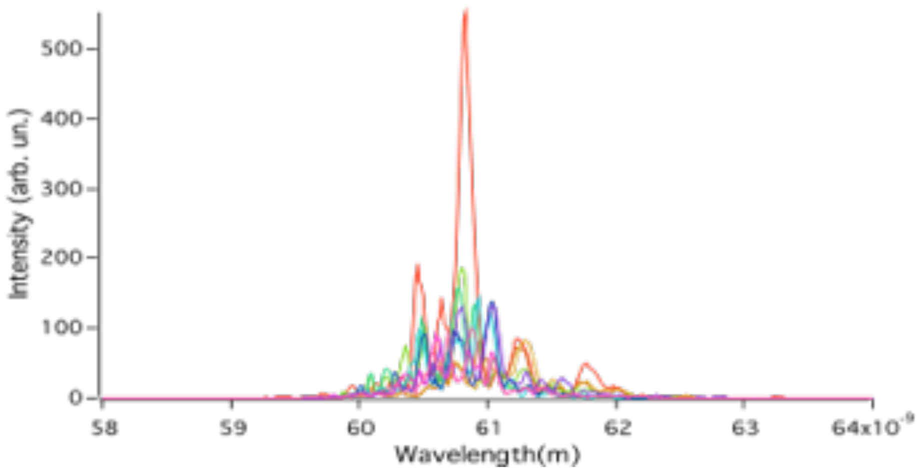

Soft X ray FELs : FERMI@ELLETRA

- 0.3 – GW's range, sub-ps to 10 fs , variable polarization

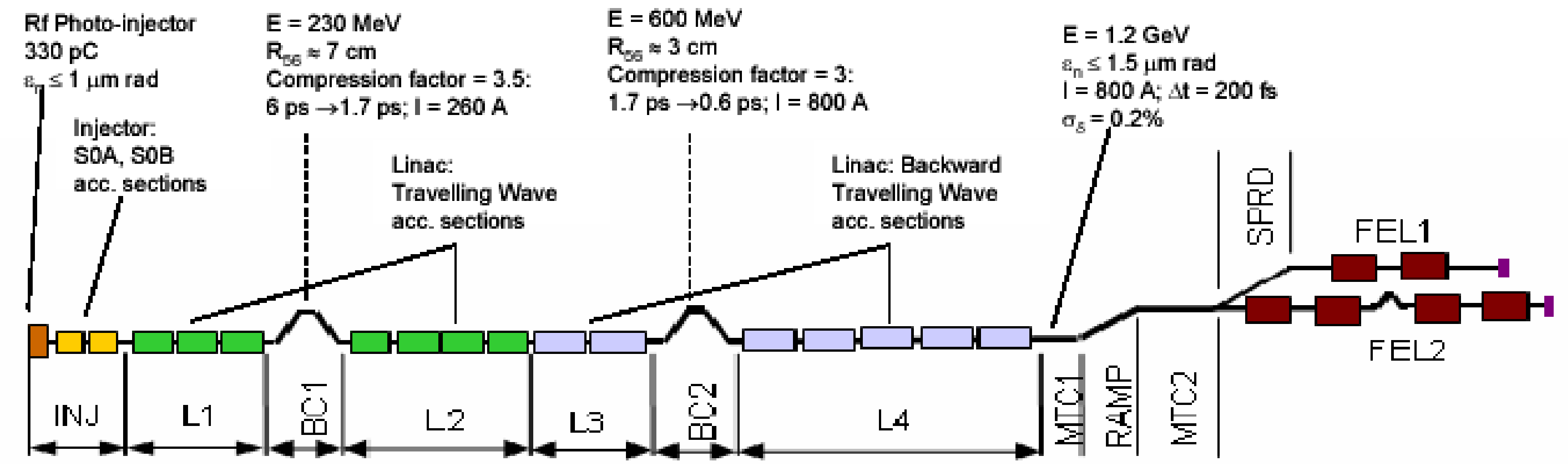

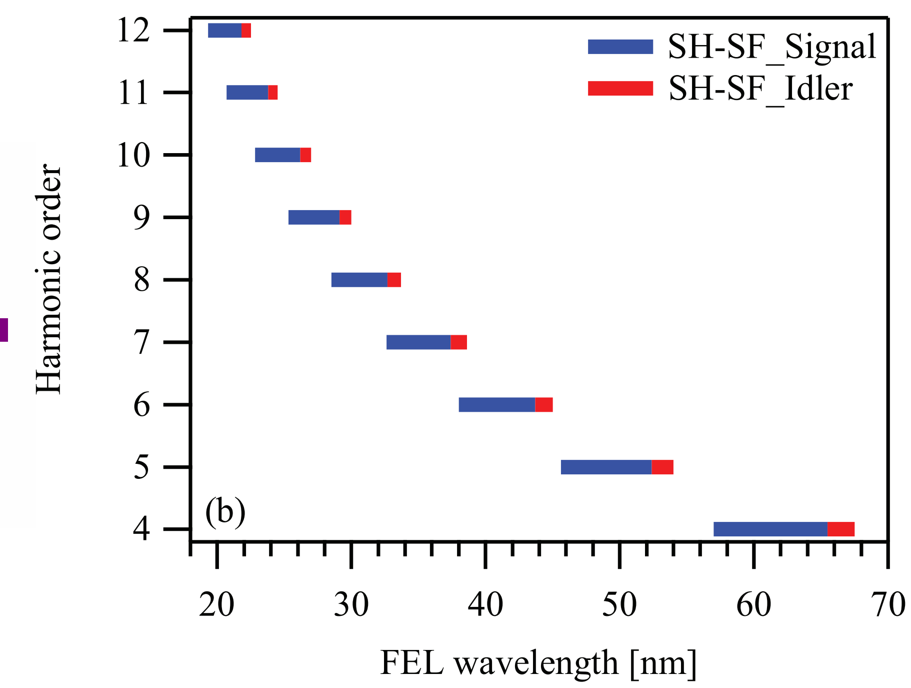

FEL1 : Single stage cascaded FEL, full specs. achieved, dedicated to user experiments

Continuously tuneable in the 20-65 nm range (up to 100 nm possible with specific machine setup)

Bandwidth (best 0.06% @ 32 nm), 30-100 uJ / pulse (depending on wavelength setting – up to a factor 2-3 more relaxing the spectral purity requirements)

FEL2: Double stage, fresh bunch, cascade FEL, in commissioning

March 2013, commissioning @1.23GeV, 8.16 (25 µJ), 6.53, 5.44 nm, coherent spectra visible down to 4.35nm (≈200nJ), June 2013, commissioning @1.5 GeV …

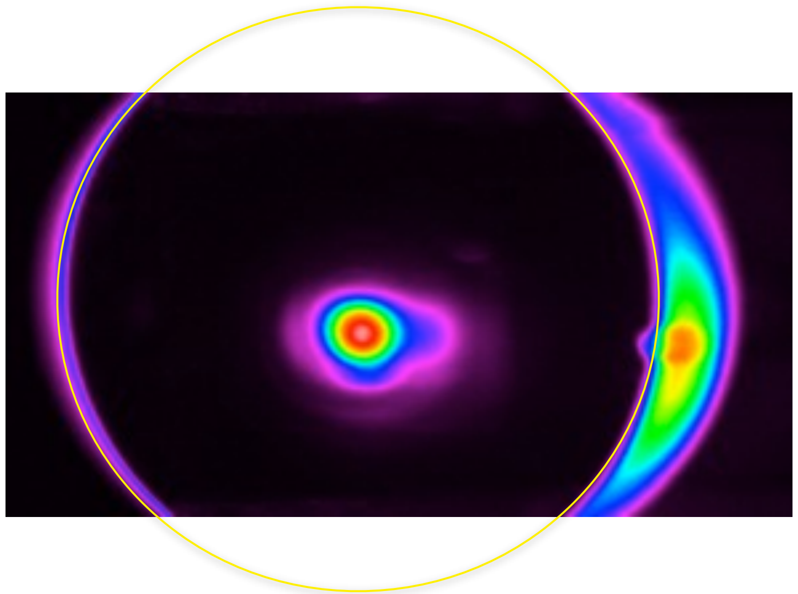

E. Allaria et al. New J. Phys. . 145, 112009, 2012
Allaria E et al 2012 Highly coherent and stable pulses from the FERMI seeded free-electron laser in the extreme ultraviolet Nature Photon. 6 699–704

SASE : spikes in longitudinal and spectral distributions

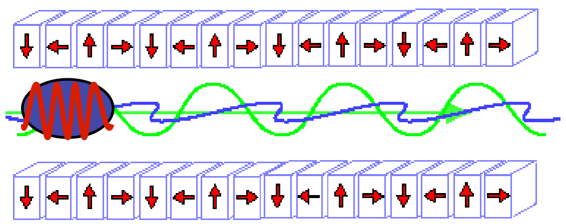

R. Bonifacio et al, Opt. Comm. 50, 1984,
C. Pelligrini et al, NIMA475, 2001, 1
K. J. Kim et al, PRL57, 1986, 1871
A.M. Kondratenko et al, Sou Phys. Dokl. 24 (12), 1979, 989

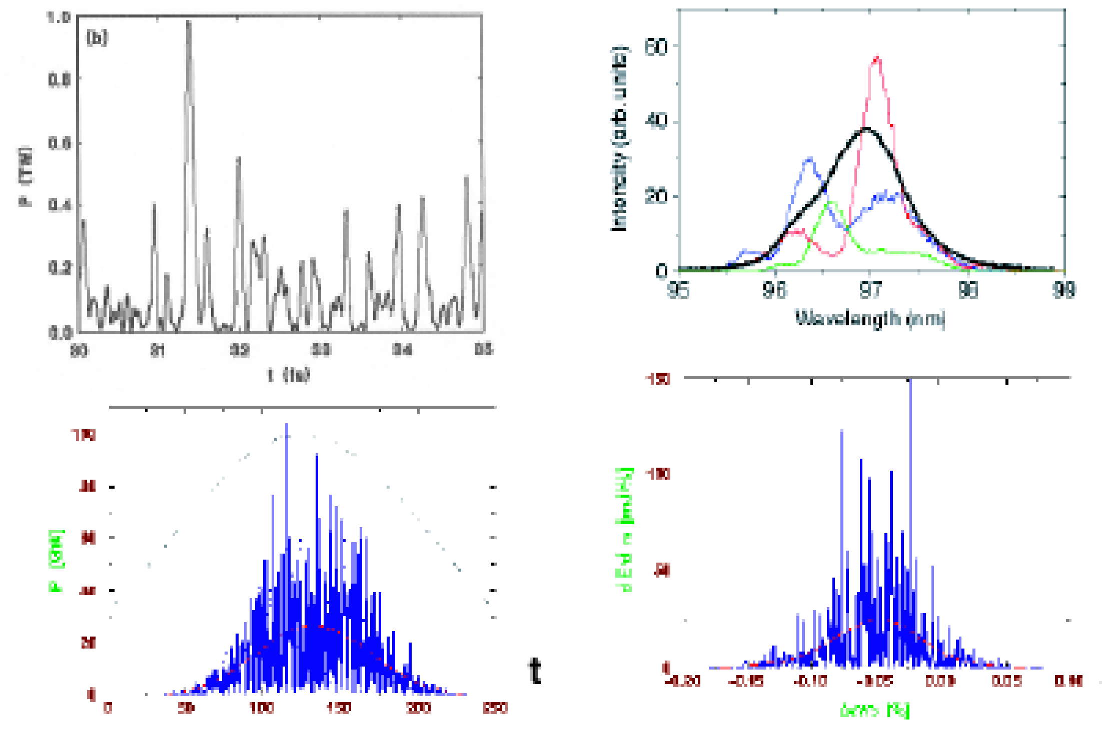

$$\rho = \frac{1}{4\pi\gamma}\left[\frac{2\pi^2}{\sigma_t}(JJ\lambda_o K)^2 \frac{I}{I_A}\right]^{1/3} \qquad L_g = \frac{\lambda_o}{4\sqrt{3}\pi\rho}$$

limited temporal coherence («spikes»), pulse to pulse jitter

Single spike operation

S. Reiche et al., NIMA 593 (2008) 45-48

with energy chirp on the electron beam and undulator tapering

SIMULATED FEL PULSES

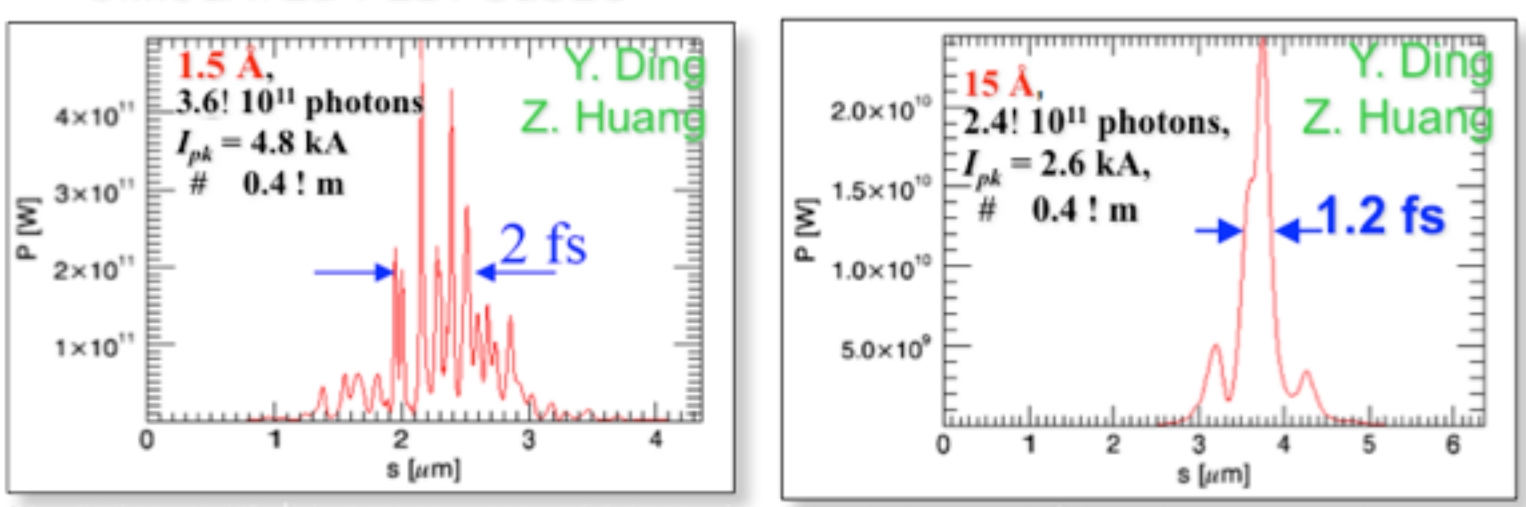

Simulation at 1.5 Å based on measured injector & linac beam & Elegant tracking, with CSR, at 20 pC.

Simulation at 15 Å based on measured injector & linac beam & Elegant tracking, with CSR, at 20 pC.

LCLS

20 ps, 14 GeV

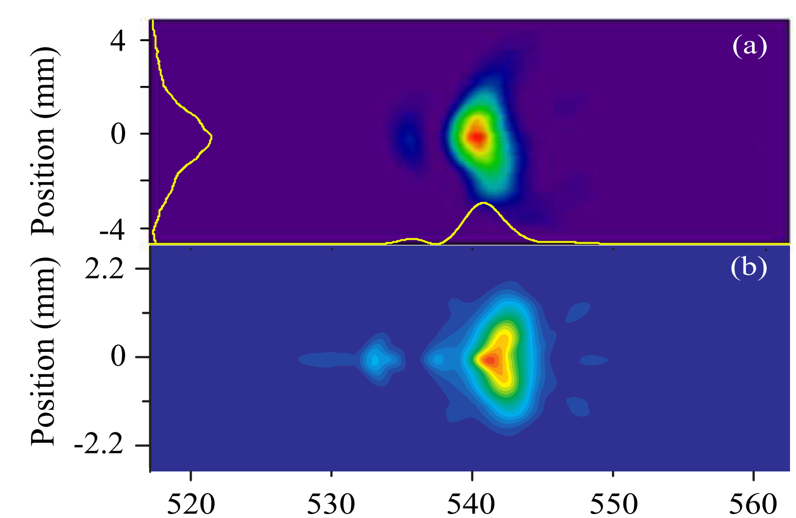

SPARC

L. Giannessi et al., Phys. Rev. Lett. 106, 144801 (2011)

Improvement of longitudinal coherence with seeding

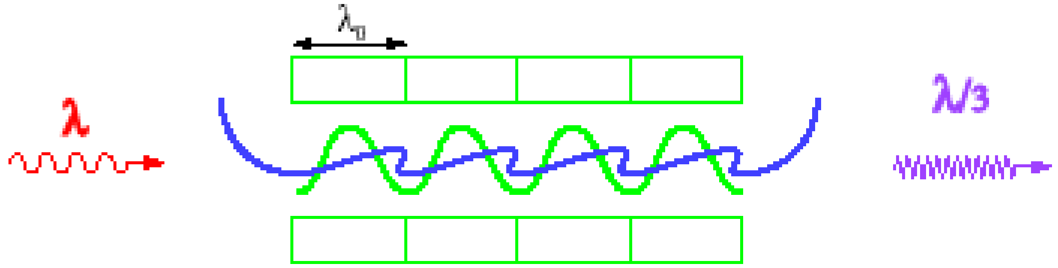

- temporal coherence given by the external seed laser
- improved stability (intensity, spectral fluctuations and jitter) => pump-probe experiments
- quicker saturation => cost and size reduction

L. H. Yu et al, PRL91 2003, 074801

T. Saftan APAC 2004, Gyeongu

L. H. Yu et al, Science 289, 2000, 932

ex case of seeding at BNL on linac

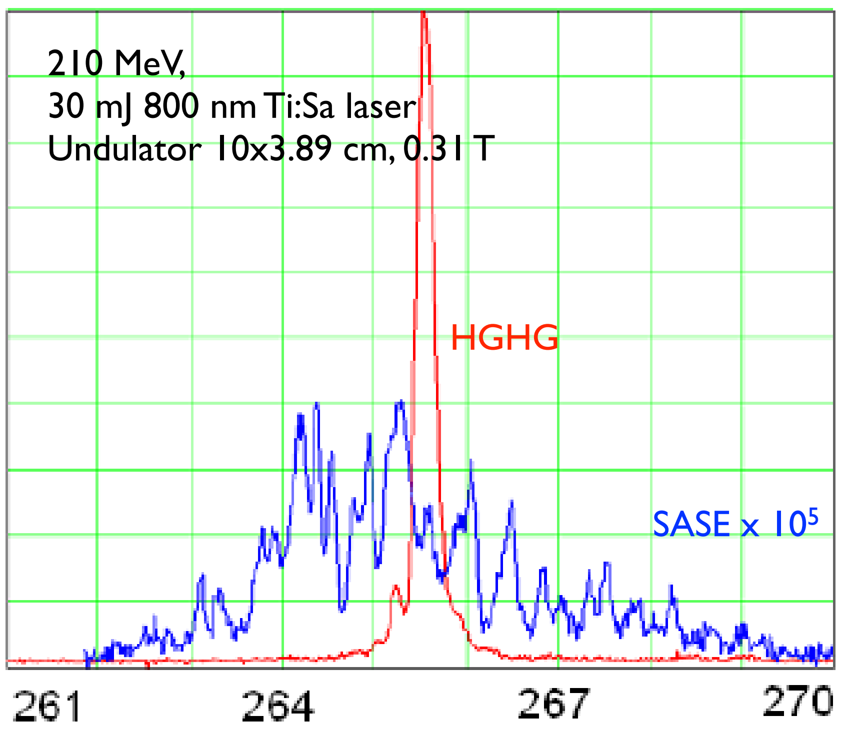

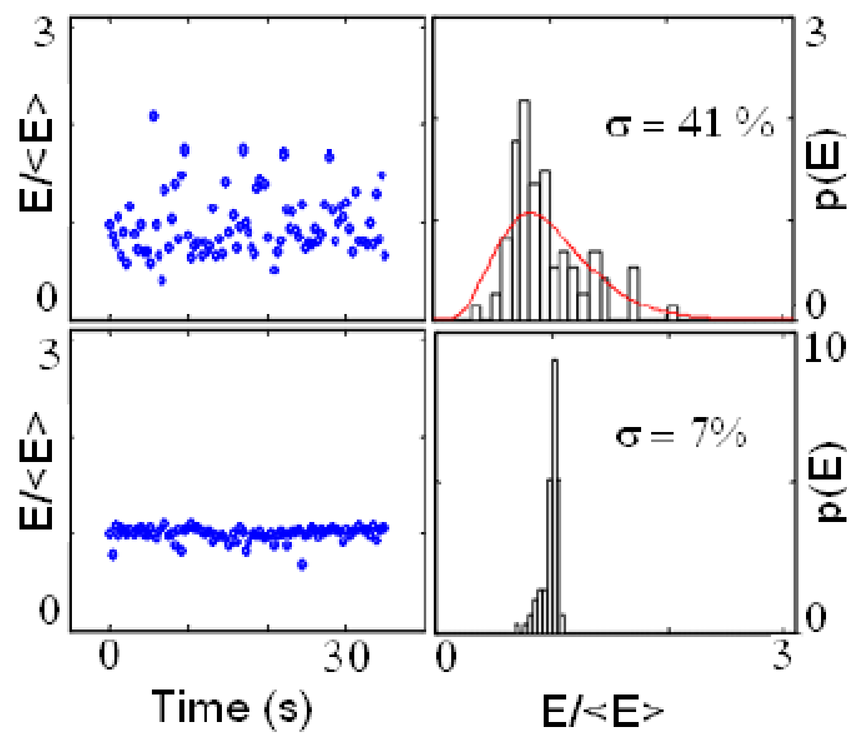

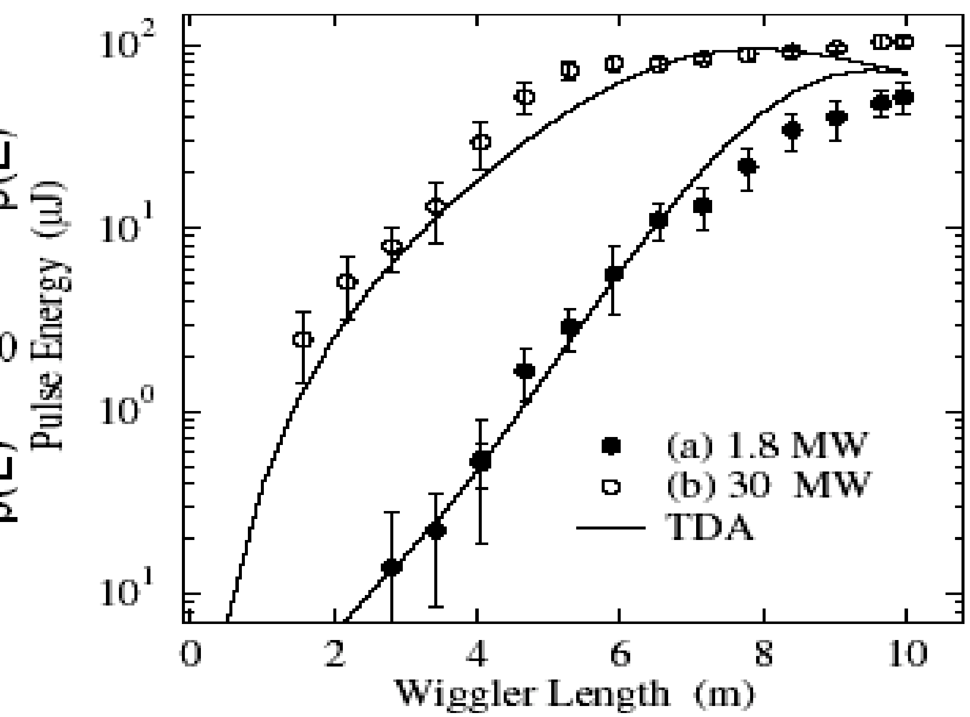

Short wavelength HHG direct seeding

SCSS Test Acc. SPARC, sFLASH

HHG seeding at 160 and 60 nm on SCSS Test Accelerator (coll. Franch-Jap), at 160 nm at SPARC, at 30 nm on SFLASH
Improvement of hit rate by EO sampling to 30 % (Tomizawa et al.)

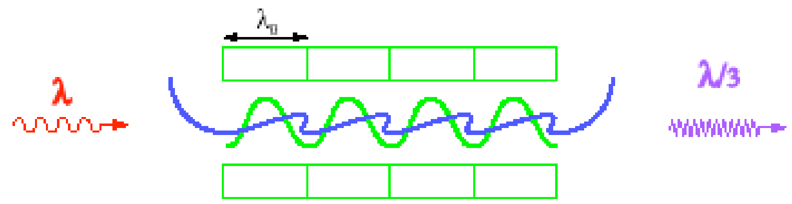

- improvement of temporal coherence,
- jitter reduction, quicker saturation,
- higher order harmonic level

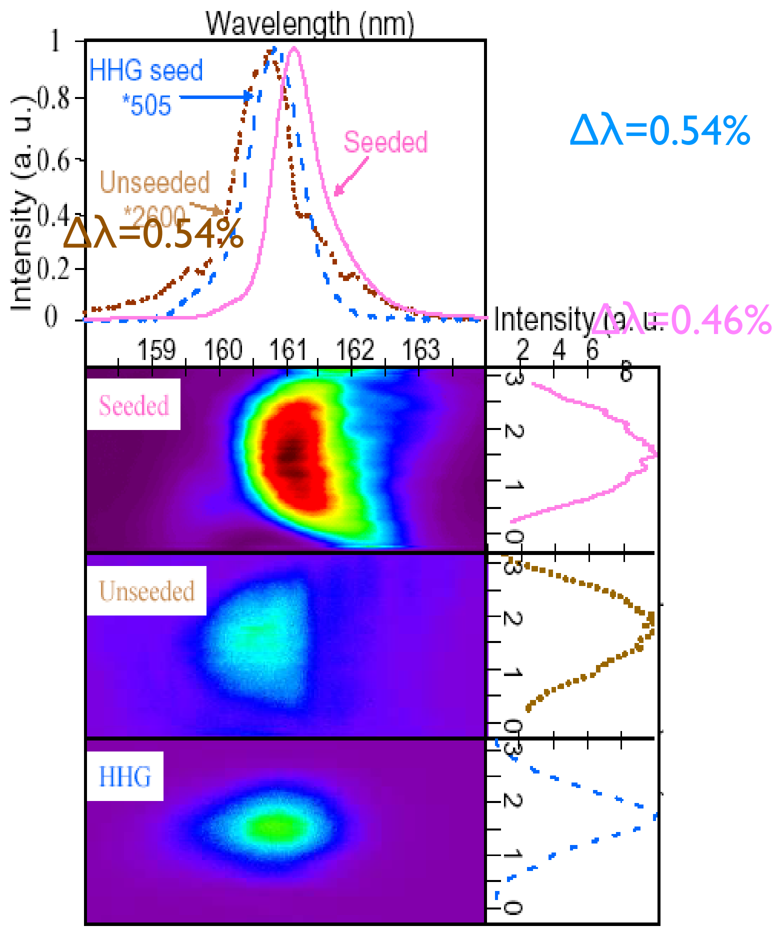

G. Lambert et al., Nature Physics Highlight, (2008) 296-30(

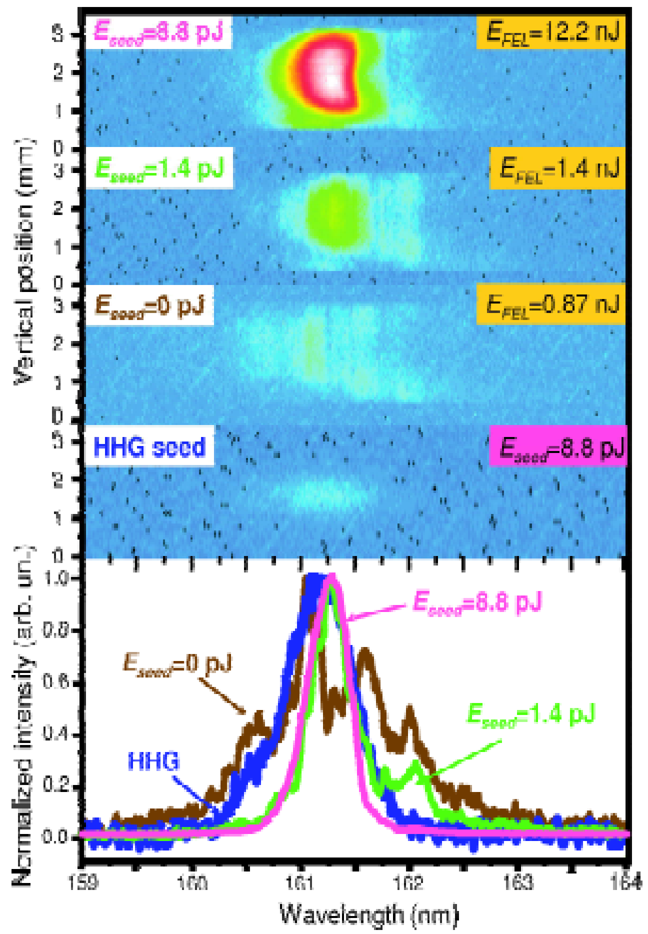

G. Lambert, et al. , EPL88-5-54002, 2009

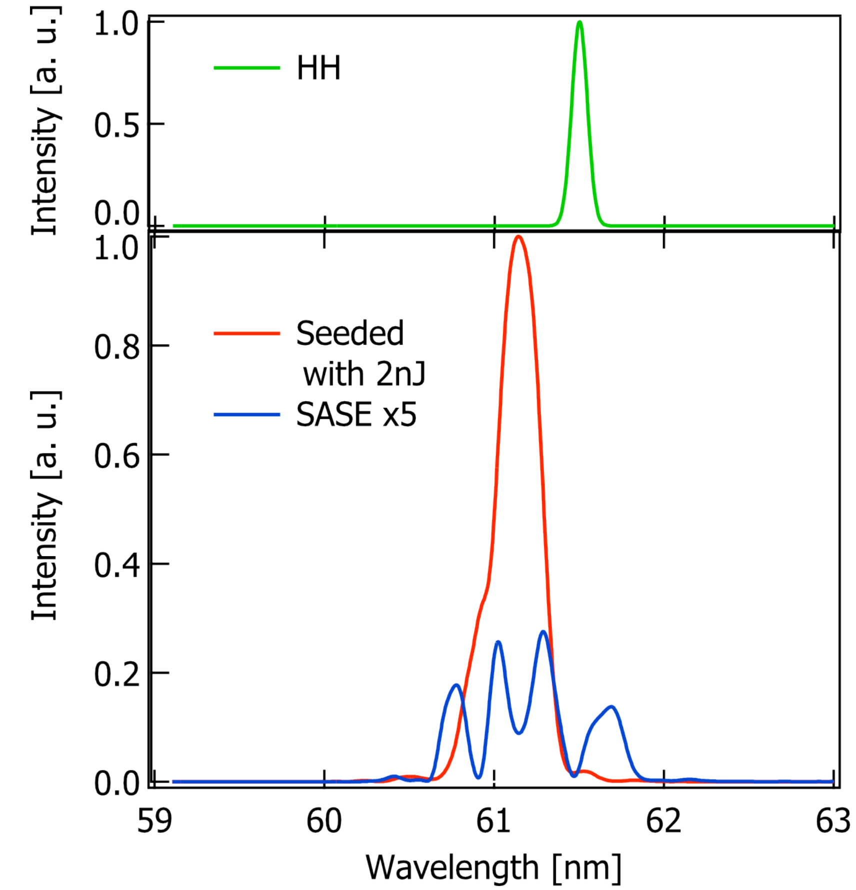

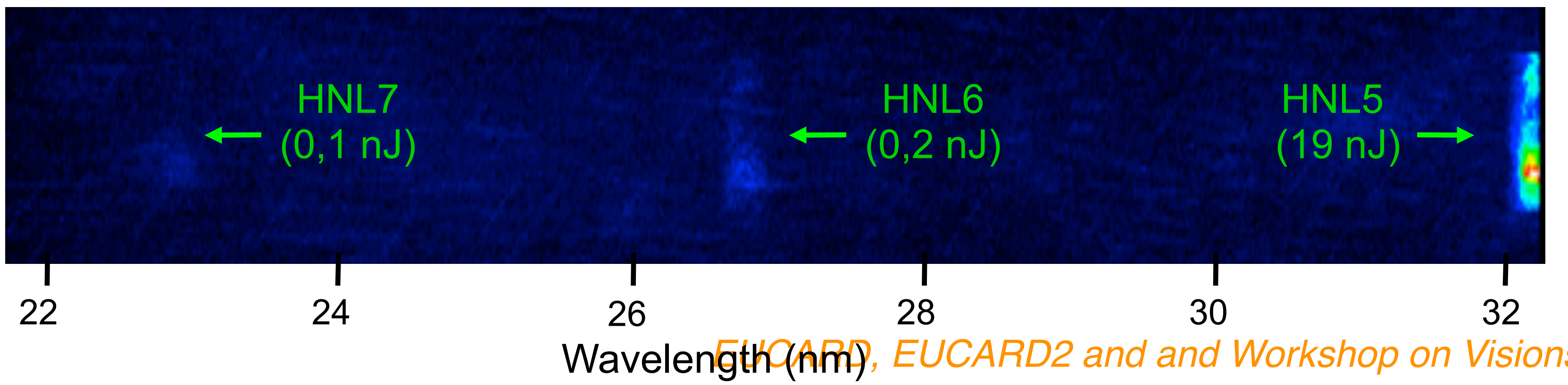

T. Tanikawa et al., EPL 106, 3 (2011) 34001

T. Togashi et al., Optics Express, 1, 2011, 317-324

Seeding and up-frequency conversion

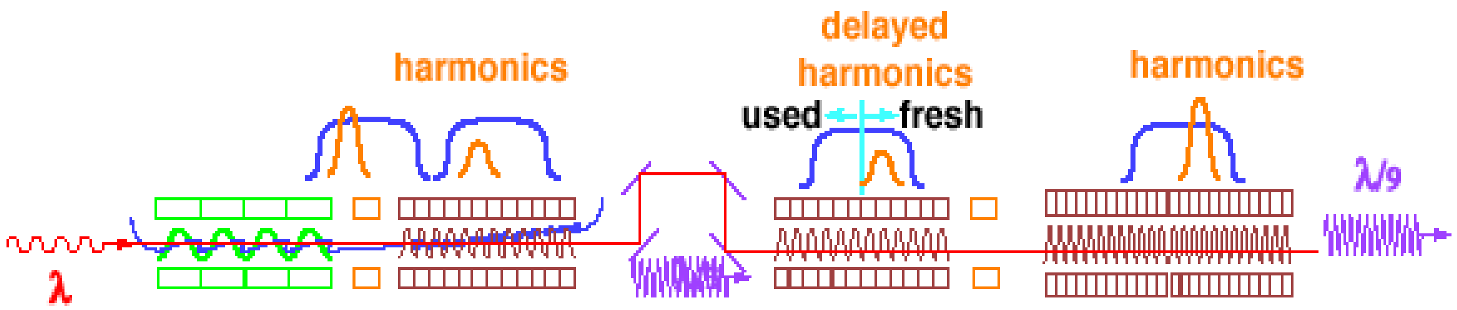

HGHG $\lambda_{u2} = \lambda_{u1}/q$, *L. H.Yu et al, NIM A 393 (1997) 96*

Fresh bunch HGHG : non heated part of the electron bunch used, *L. H.Yu et al, NIMA 483 (2002) 493*

Cascading HGHG : $\lambda_{u2} = \lambda_{u1}/q$, $\lambda_{u4} = \lambda_{u1}/p$

Harmonic cascade : $\lambda_{u2} = n\,\lambda_{u1}/q$,

L. Giannessi, P. Musumeci, New Journal Phys. 8, (2006), 294

H11 observed at SPARC

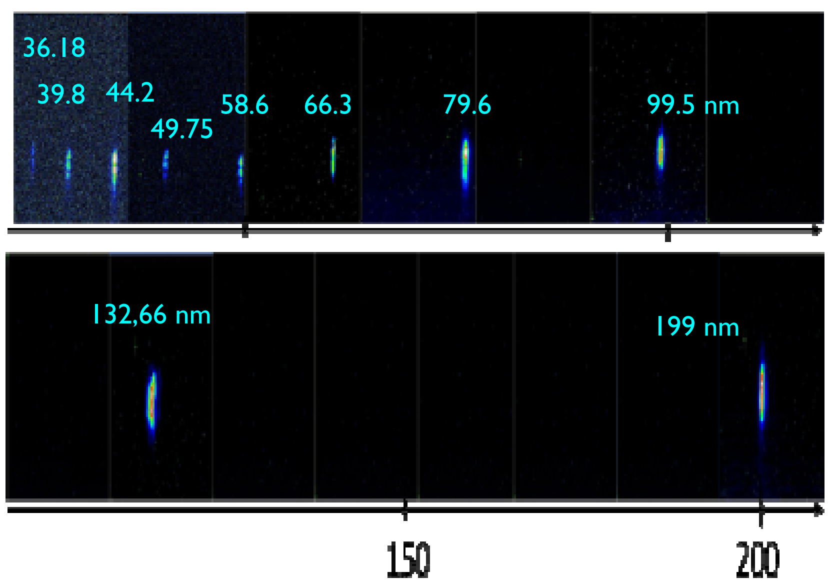

L. Giannessi et al., FEL experiment at SPARC : seeding with harmonics generated in gas, FEL 2010, Malmo, Sweden

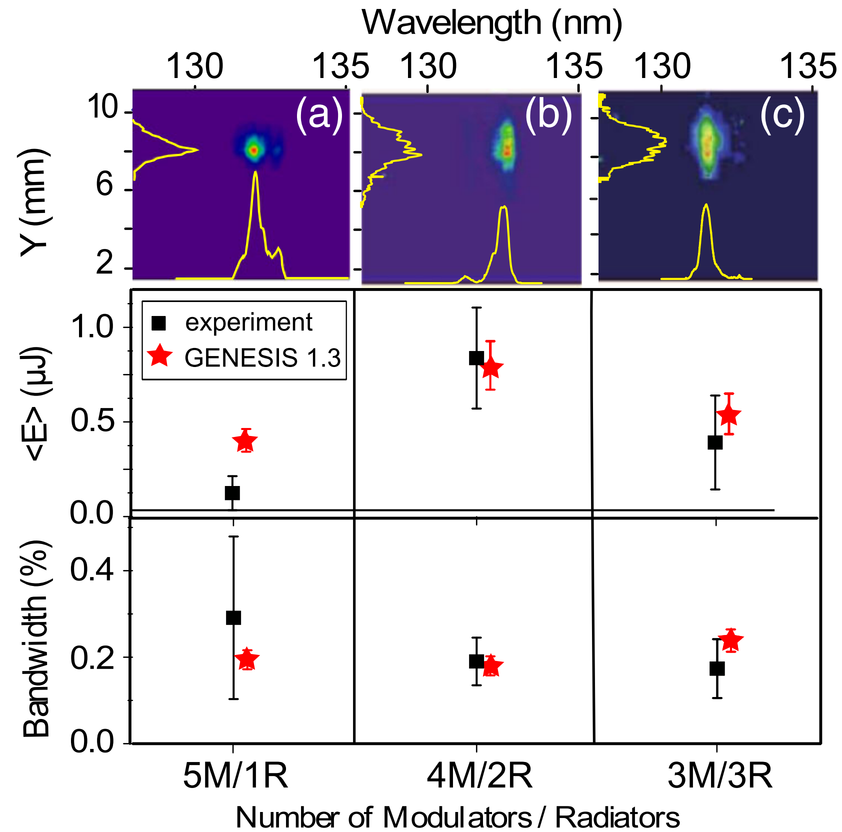

Ex cascade (modulator and radiator) @ SPARC

M. Labat, et al. , Phys. Rev. Lett. 107, 224801 (2011)

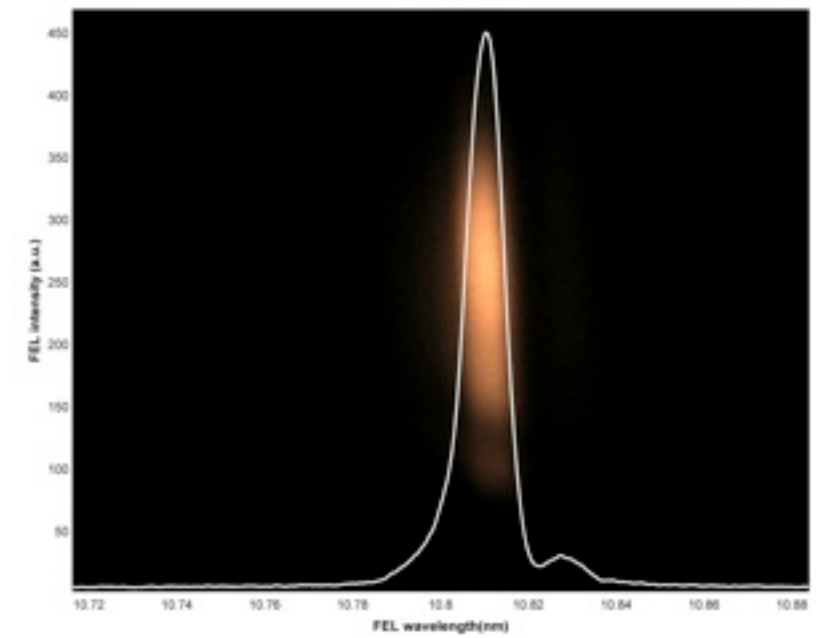

Ex FEL2 @ FERMI@ELETTRA with a 2-stage cascade, from 200 nm to 10.8 nm

Seeding stability

Seeding @ 160 nm (SCSS Test Accelerator)

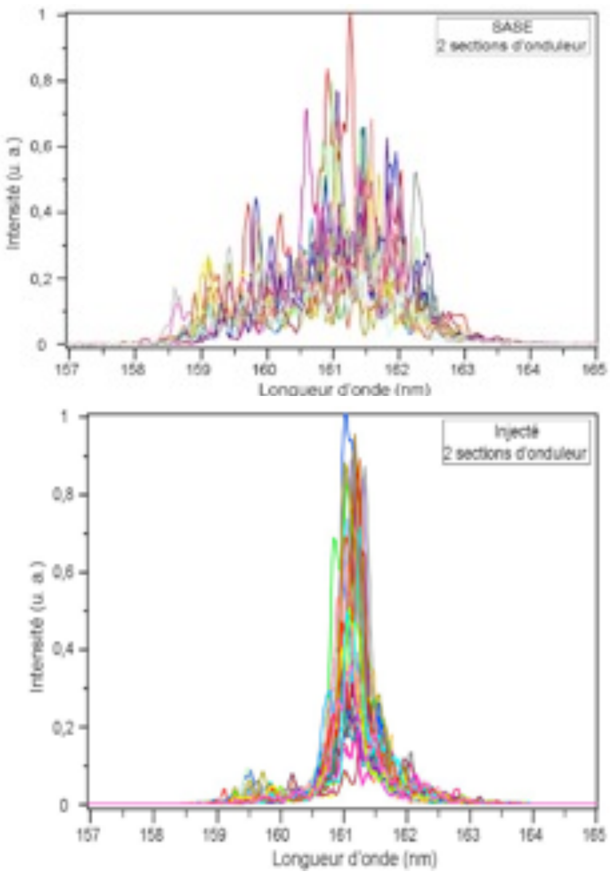

FERMI FEL1

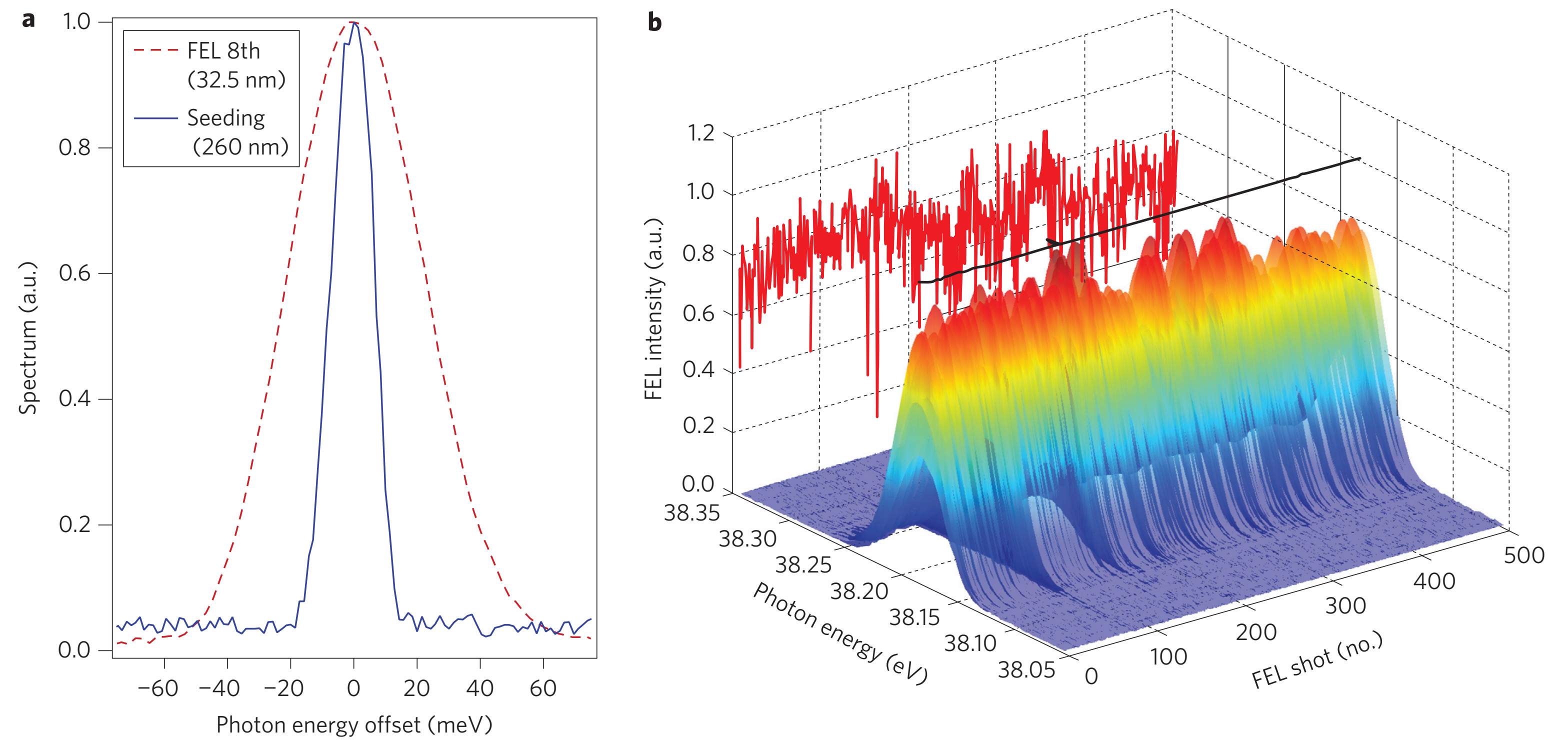

Figure 4 | Single-shot and multi-shot spectra at 32.5 nm. a, Measured FEL and seed laser spectrum (dashed red and continuous blue lines respectively). **b**, Acquisition of 500 consecutive FEL spectra.

Seeding @ 60 nm (SCSS Test Accelerator) synchronisation improvement by Electro-Optical Sampling (Tomizawa et al.)

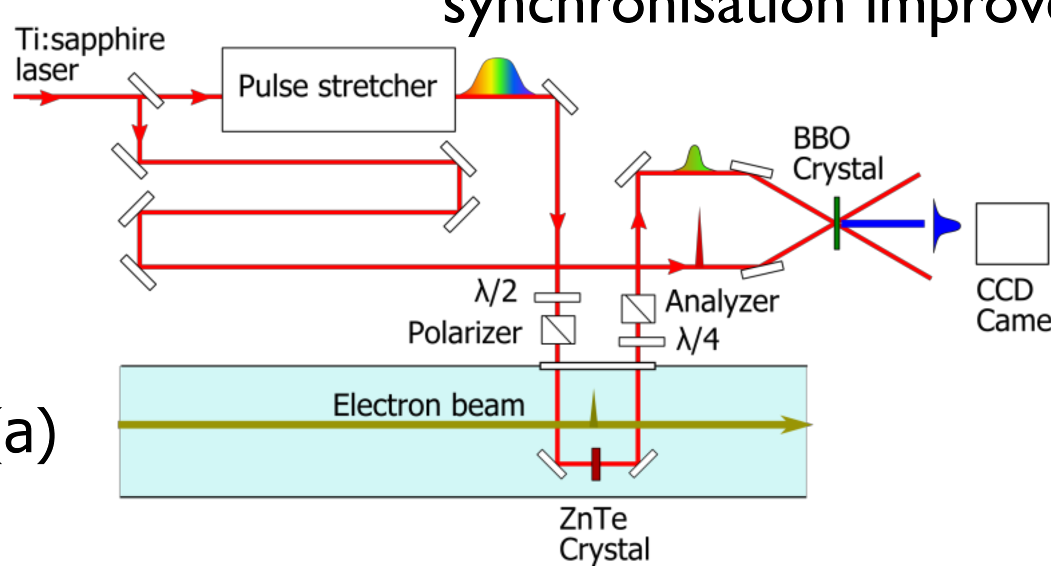

(a)

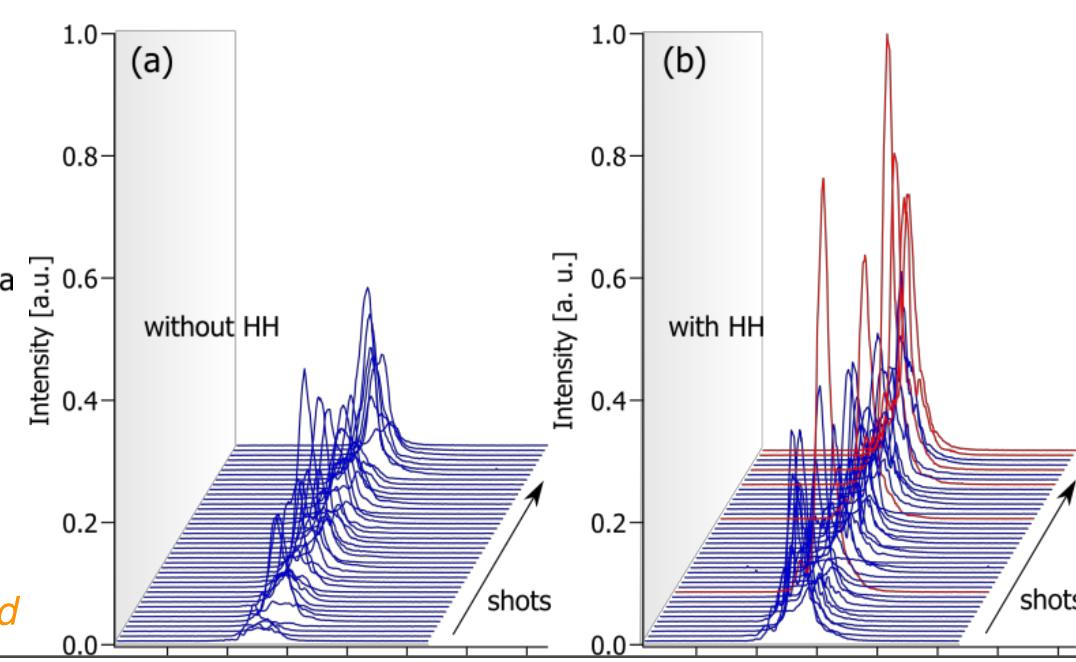

Tomizawa et al, Seeding workshop, Trieste, 2012 Dec.,

Self-seeding for soft and hard X ray domain

Feldhaus et al., Opt. Comm 140 (1997) 341
Geloni, Jounral. Modern Optics, 58, 16, 2011

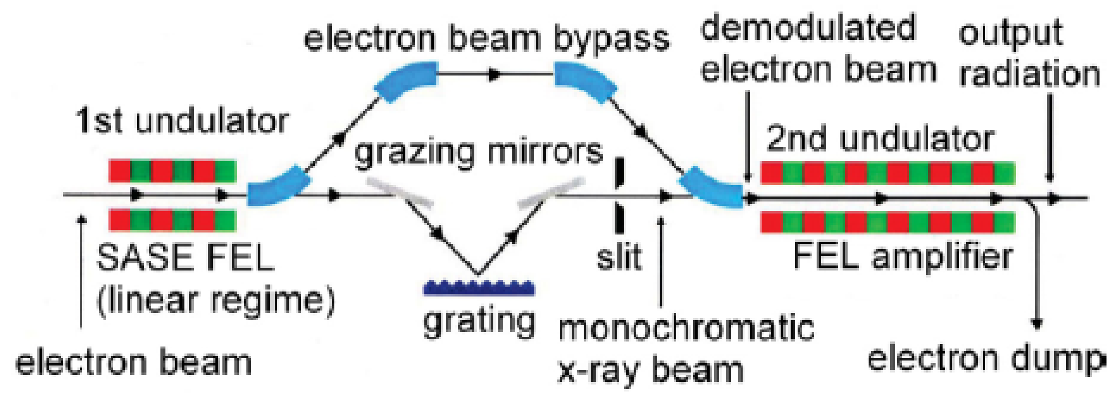

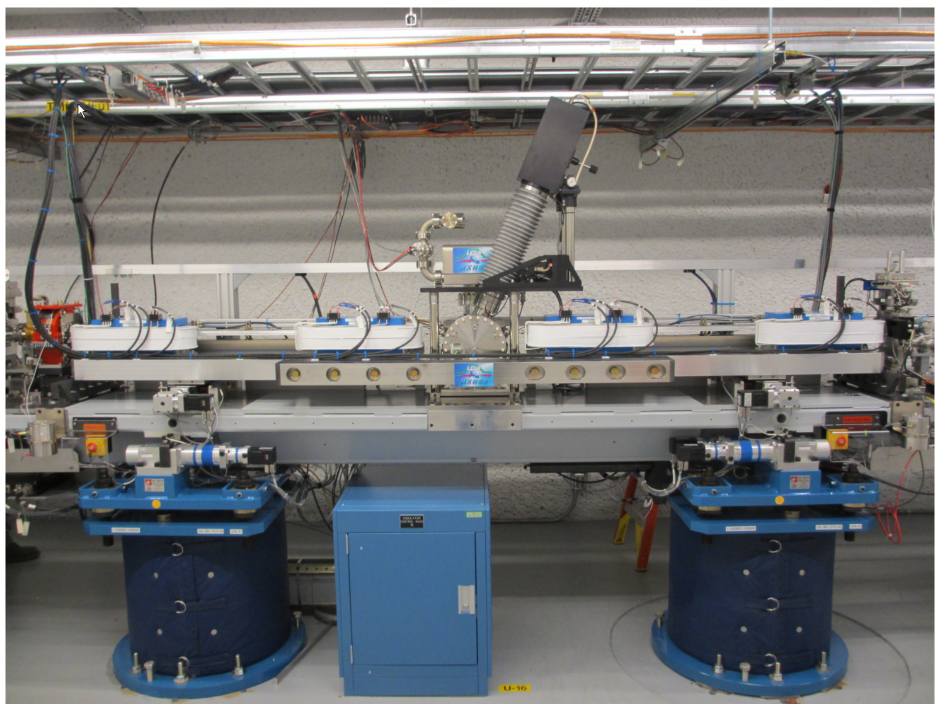

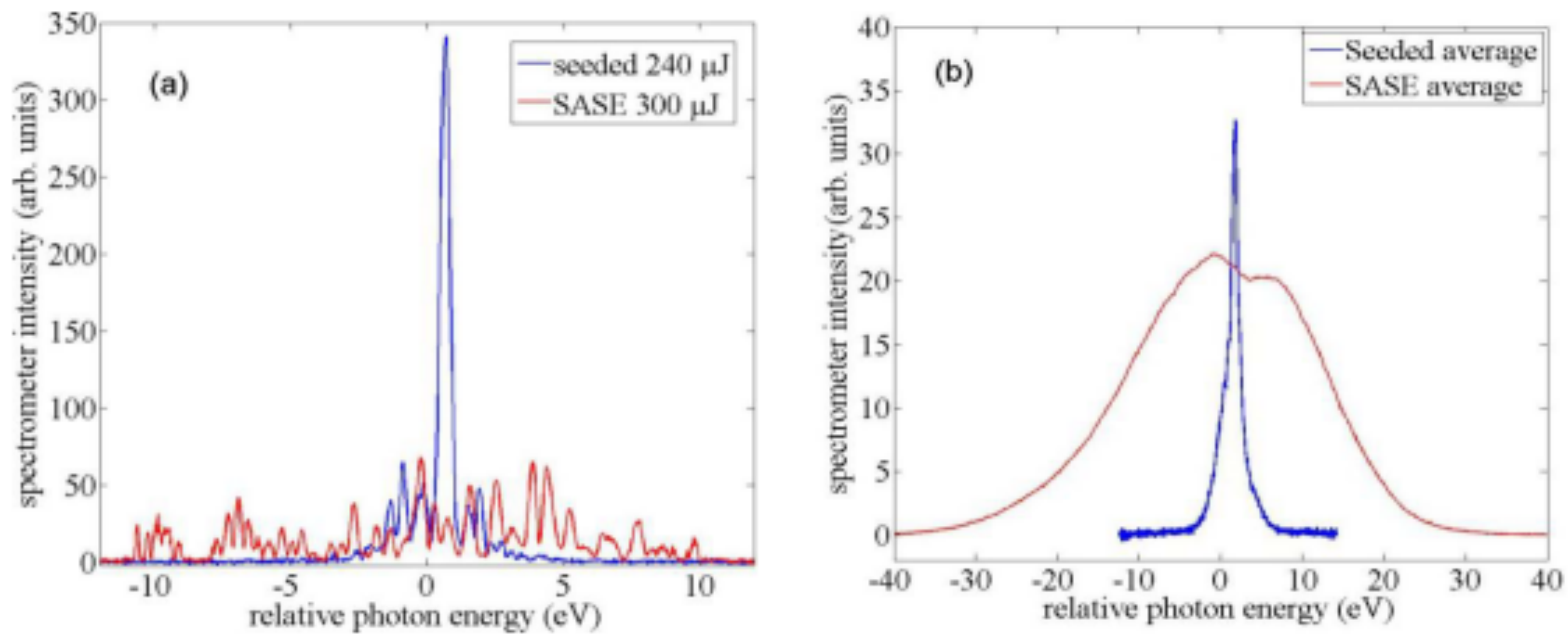

Figure 5. Single-shot (a) and averaged (b) x-ray spectrum in SASE mode (red) and self-seeded mode (blue). The FWHM single-shot seeded bandwidth is 0.4 eV, whereas the SASE FWHM bandwidth is approximately 20 eV. Vertical scales have the same arbitrary units in both plots (a) and (b). The chicane is turned off for the SASE measurements, but necessarily switched on for the self-seeded mode.

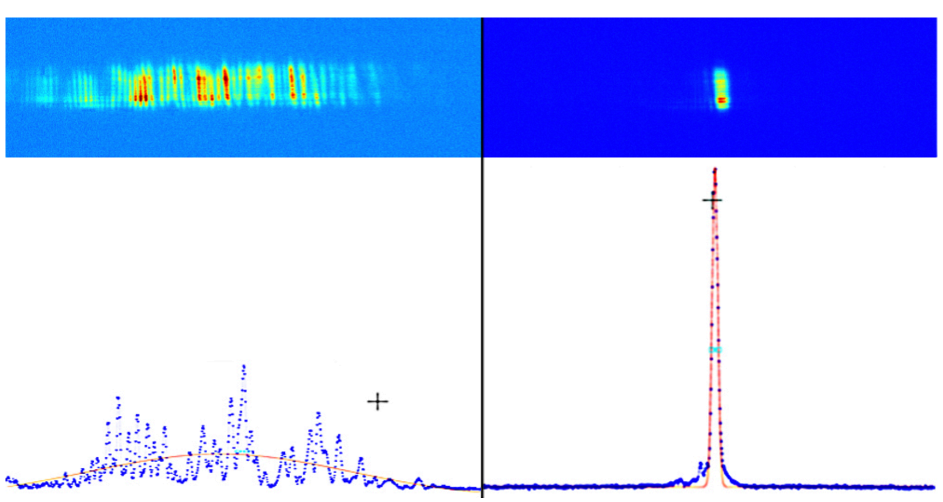

Demonstration of self-seeding in a hard-X-ray free-electron laser, J. Amann, W. Berg, V. Blank, F.-J. Decker, Y. Ding, P. Emma, Y. Feng, J. Frisch, D. Fritz, J. Hastings, Z. Huang, J. Krzywinski, R. Lindberg, H. Loos, A. Lutman, H.-D. Nuhn, D. Ratner, J. Rzepiela, D. Shu, Yu. Shvyd'ko, S. Spampinati, S. Stoupin, S. Terentyev, E. Trakhtenberg, D. Walz et al., Nature Photonics 6, 693–698 (2012)

Two laser- electron interactions : echo

- with phasing of the emettors on linac :

first proposition on Linac for LEL (Stanford)
experimental demo at Stanford and in Shanghai Test machine in the UV

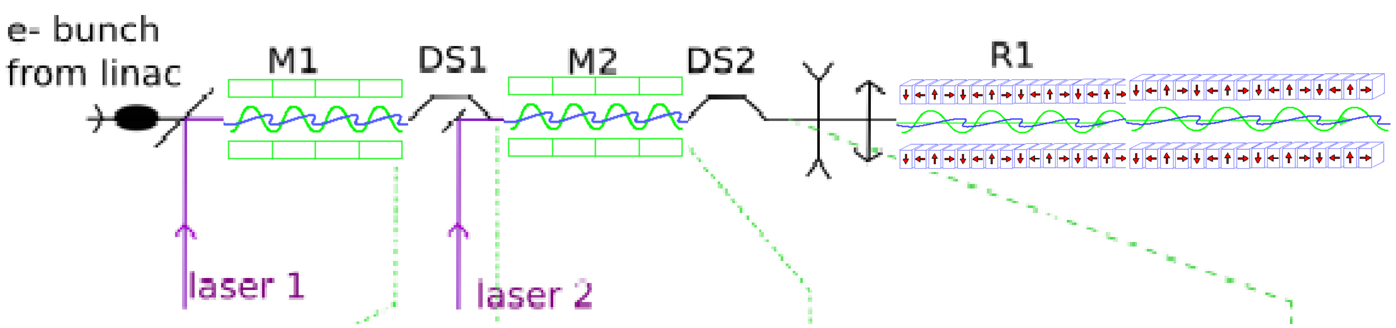

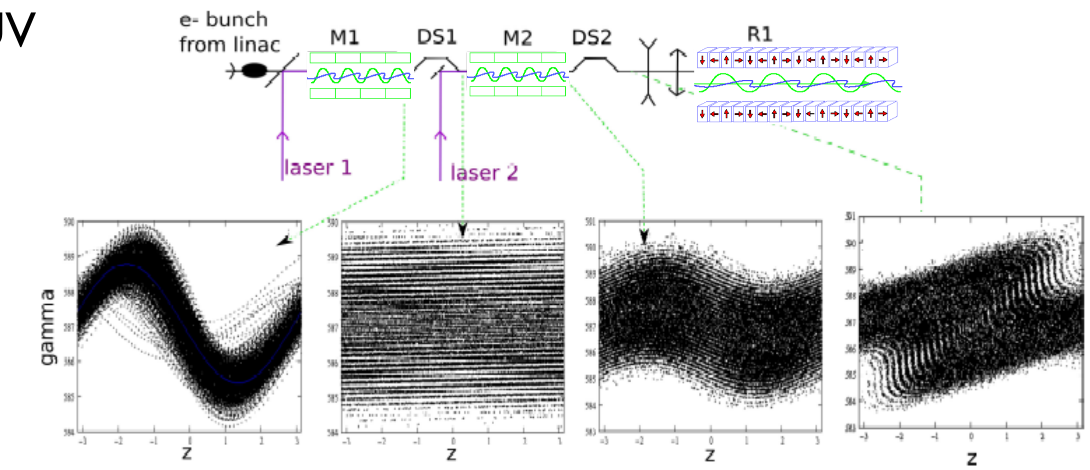

G. Stupakov., PRL 102, 074801 (2009)

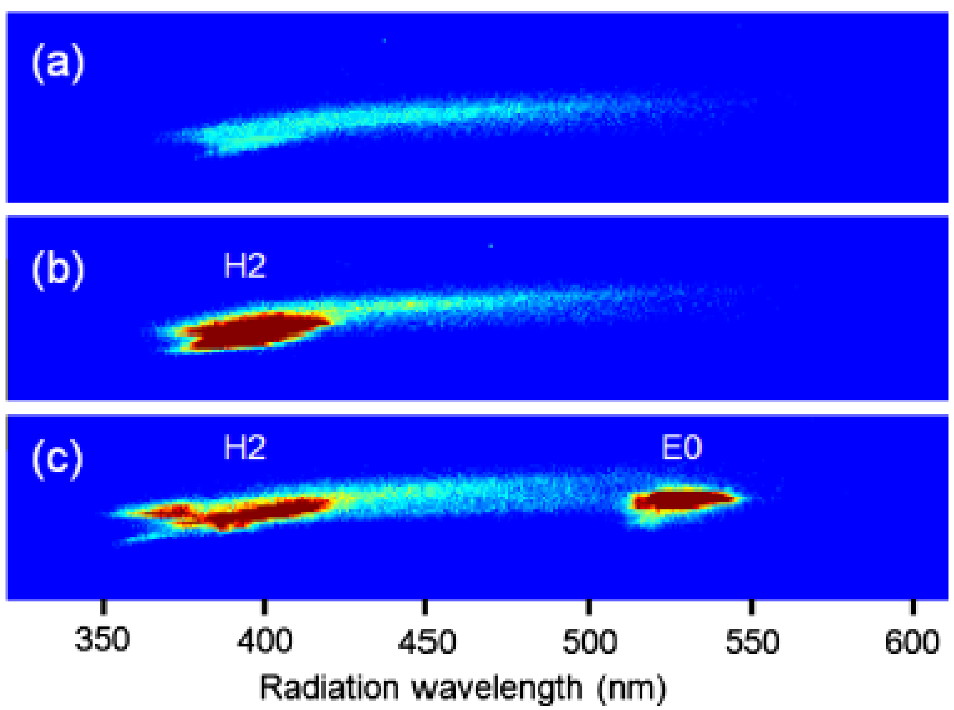

D. Xiang et al., PRL 105, 114801 (2010)

$$\frac{1}{\lambda_{echo}} = \frac{1}{\lambda_1} + \frac{1}{\lambda_2}$$

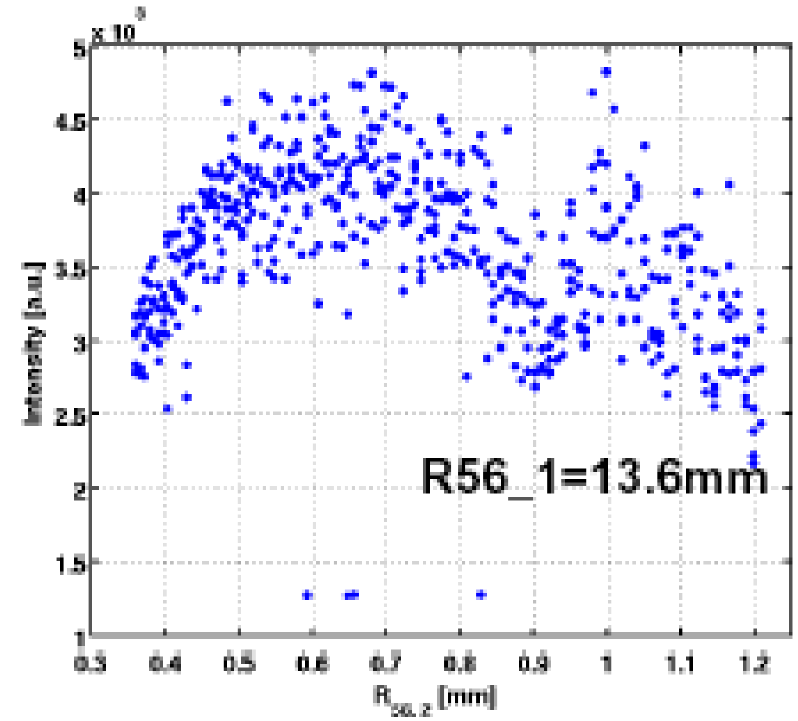

Zhao et al., Proceed FEL conf, Mamö (2010), Nature Photonics

Towards spikes reduction with iSASE

LCLS

Improve longitudinal coherence by increasing the longitudinal slippage (ISASE)

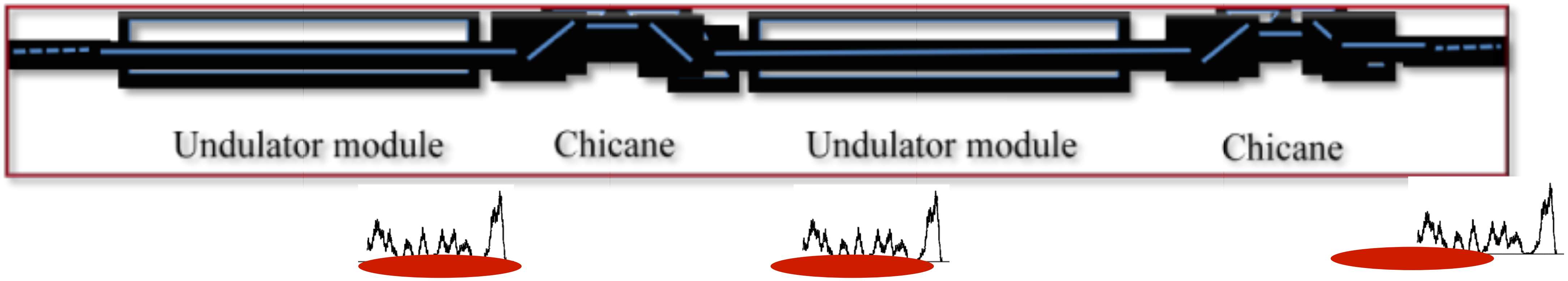

Single shot spectrum (13.8 GeV,150 pC)

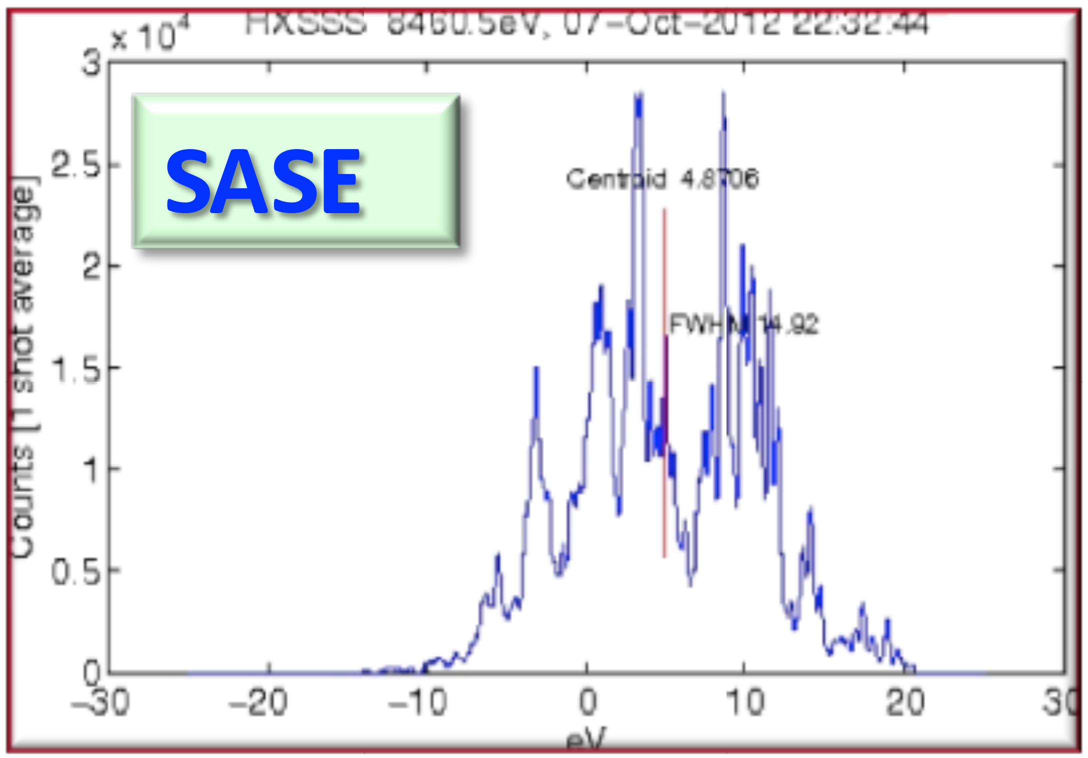

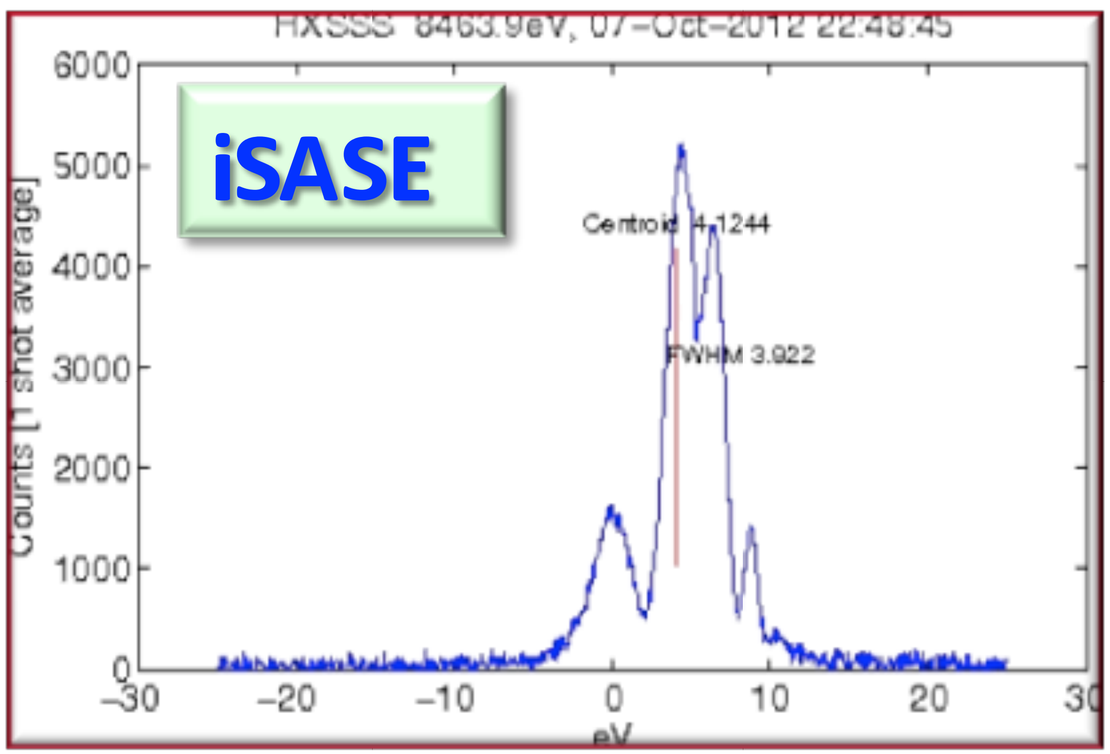

Courtesy T. Raubenheimer

J. Wu, A. Marinelli, C. Pelligrini. FEL 2012

Two-color FEL

Two colour operation of a Free Electron Laser and applications in the mid-infrared, R.Prazeres, F.Glotin, C.Insa, D.A.Jaroszynski, J.M.Ortega, Nuclear Instr. and Methods, A407, 464 (1998), Two colour operation of a Free Electron Laser and applications in the mid-infrared, R.Prazeres, F.. Glotin, C.Insa, D.A.Jaroszynski, J.M.Ortega, Eur. Phys. J. D3, 87 (1998)

LCLS with chicane delay

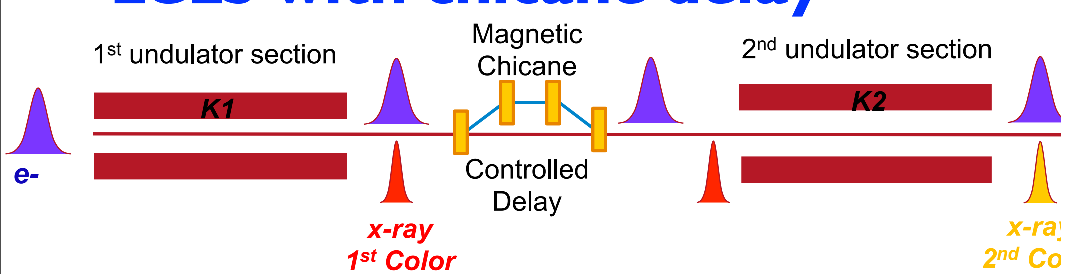

- double slotted emittance spoiler enabling to control the delay (fresh bunch)

- iSASE with delay (phase shifter), undulators slightly detuned to act as phase shifters. U1 5K1), U2 (K2), U1(K1), U2(K2)

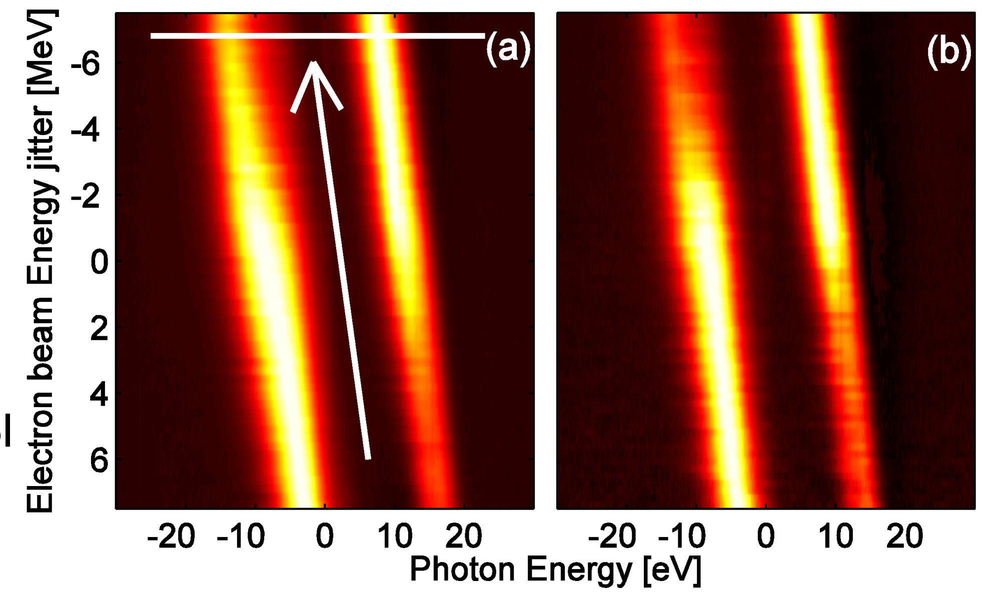

E_b = 5800 MeV and E_γ = 1.5 keV

A.A. Lutman et al., Experimental demonstration of fs two-color X-ray FELs, PRL 110, 134801 (2013)

Pulse splitting + chirp @ FERMI

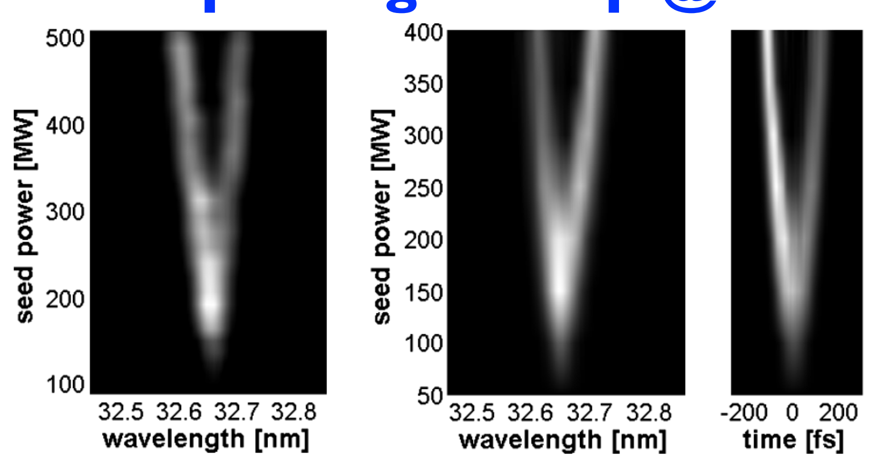

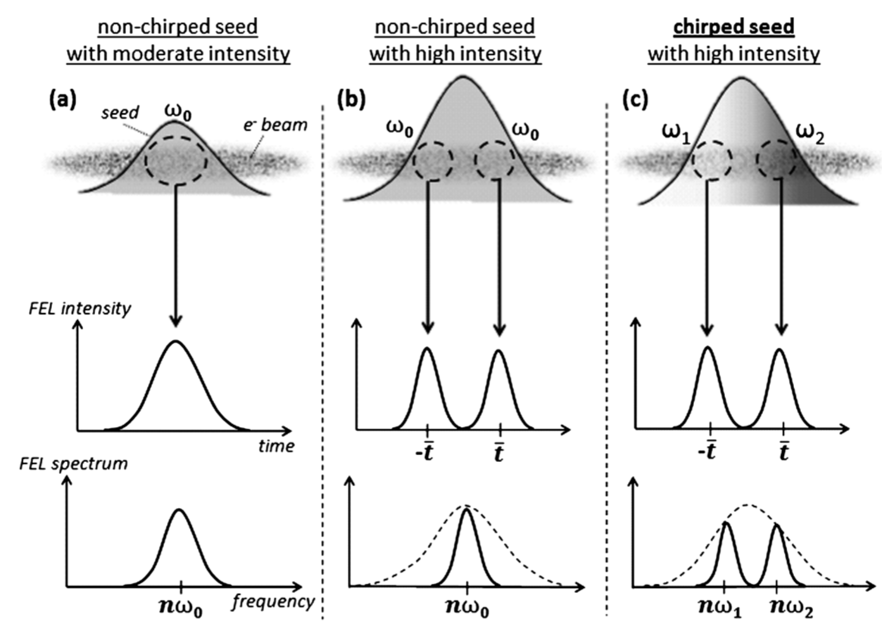

Pulse splitting in short wavelength free electron laser,
M. Labat, N. Joly, S. Bielawski, C. Swaj, C. Bruni, M. E. Couprie,
Phys. Rev. Lett. 103 (2009) 264801

G. De Ninno et al. PRL, 110, 064801 (2013)

X-ray direct splitting @LCLS

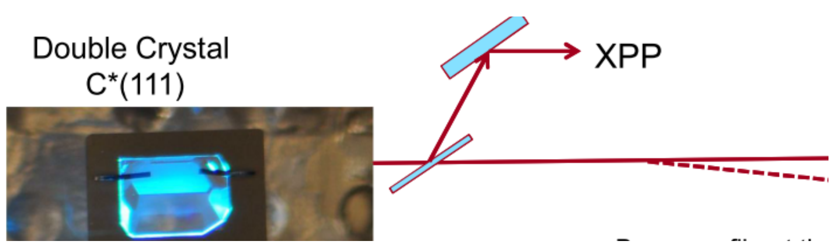

First C*(111) crystal is 100µm thick
- Highly transmissive for X-rays outside Bragg reflection bandwidth)

Ultra-short pulses

I. Martin, R. Bartolini, PRSTAB14, 030702 (2011)

Emittance spoiler

P. Emma. PRL 92 (7), 074801 (2004)

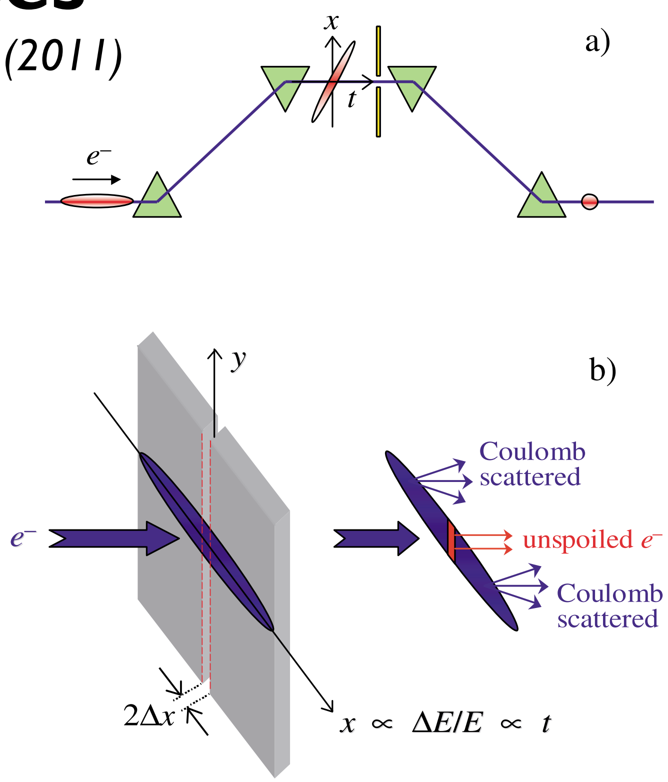

energy chirped electron beam :

-radiation from energy chirp beam used as a seed for a second stage

C. Schroeder et al., NIMA 483, 89 (2002)

- optical compression

C. Pelligrini, NIMA 445, 124 (2000)

electron energy/ trajectory modulation in a small part of the bunch with a few cycle laser

A.A. Zholents, PRSTAB 8, 040701 (2005); A.A. Zholents, G. Penn . PRSTAB 8, 050704 (2005), A. Zholents et al., New J. Physics 10, 025005 (2008)

selective amplification

Few cycle laser
1 mJ, 5 fs

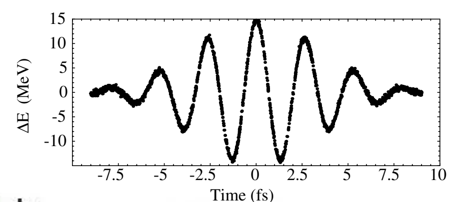

100 MW; 100 fs
X-ray

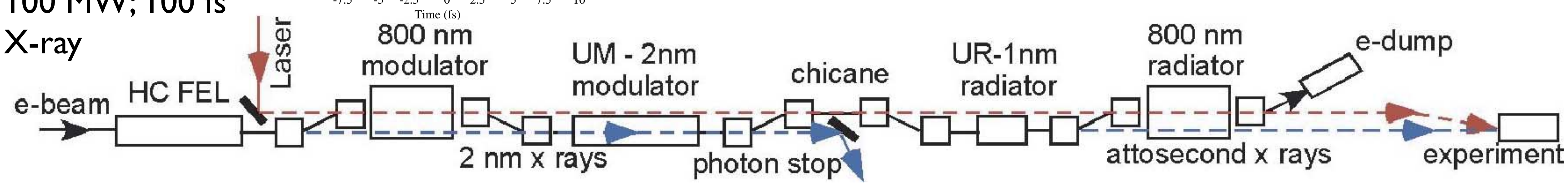

A.A. Zholents, W. Fawley . PRL 92 (22), 224801 (2004), E. Saldin et al. , Opit. Comm. 239, 161 (2004), E. Saldin et al., ¨PRSTAB9, 050702 (2006)

Towards higher power

Tapering : slightly adjust the undulator field to keep the resonance

$$\lambda = \frac{\lambda_0}{2n\gamma^2}\left(1+\frac{K^2}{2}\right) \qquad K = 0.94\,\lambda_0\,(\mathrm{cm})\,B_0\,(\mathrm{T})$$

N. M. Kroll, Phys. of Quantum Electron. 7, 113 (1980)
L. Giannessi et al. PRL 106, 144801 (2011)

Enhanced SASE (ESASE)

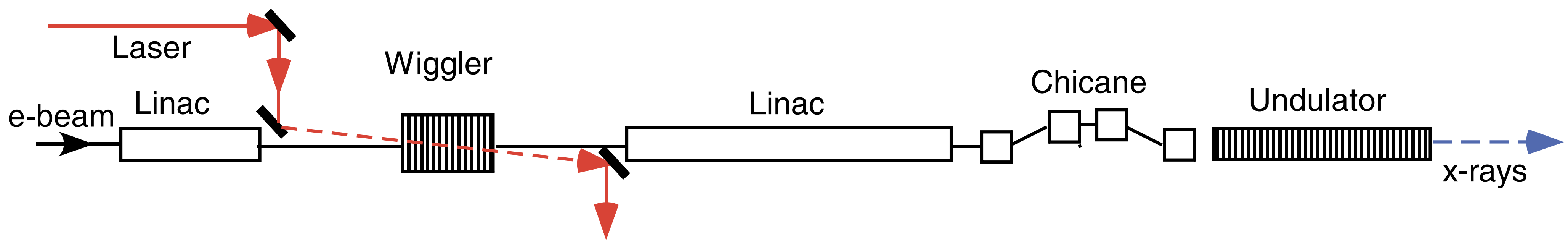

A.A. Zholents. PRSTAB 92 (8), 040701 (2005)

Transverse mode :Young slit experiments

FLASH

FERMI

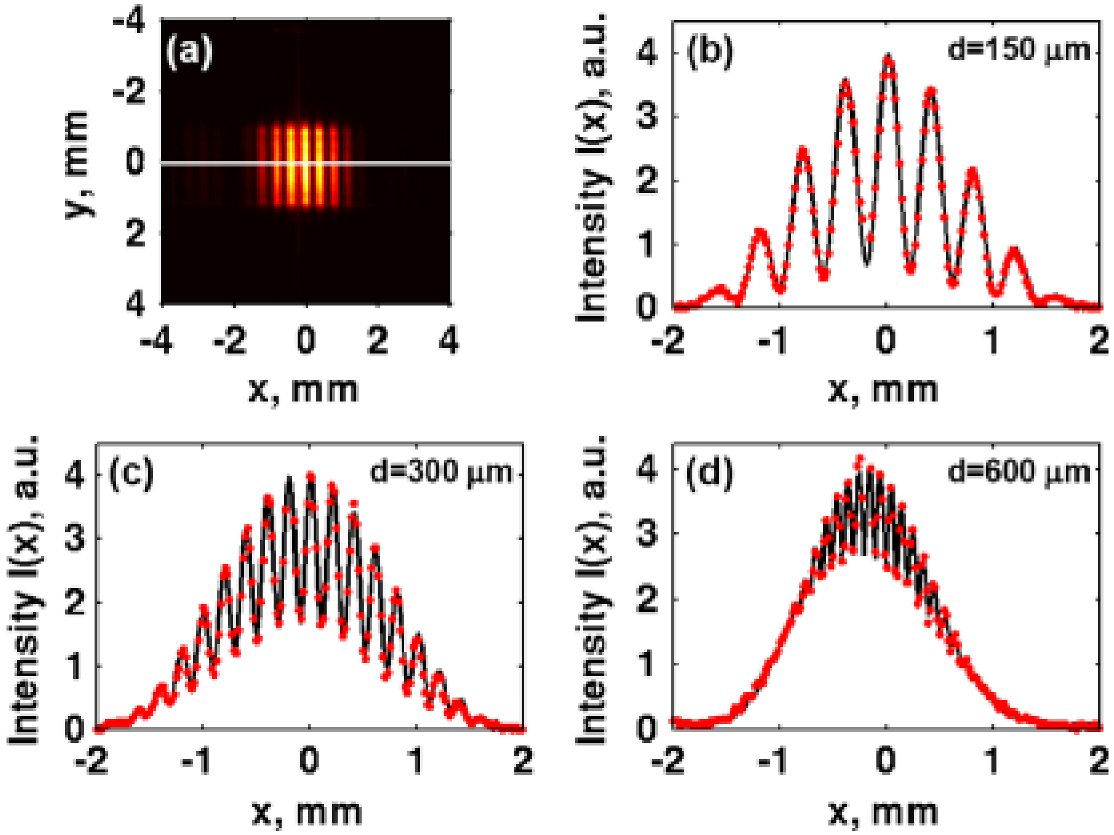

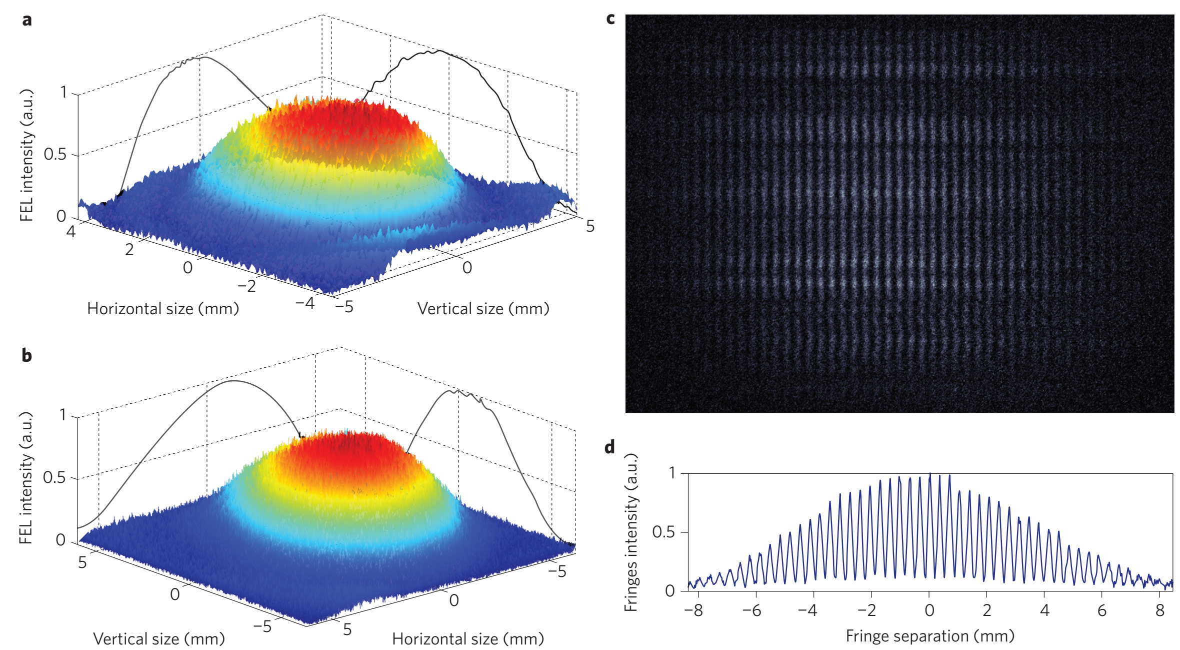

Figure 3 | Measured beam profiles and double slit diffraction pattern. a, FEL spot size measured on a YAG screen positioned 52.4 m downstream from the radiator exit. The main signal is well reproduced by a Gaussian profile and is characterized by a second moment of ~2 mm in both the vertical and horizontal directions. **b**, FEL spot size measured on a second YAG screen positioned 72.5 m downstream from the radiator exit. In this case the measured horizontal and vertical beam dimensions are 2.6 mm and 2.4 mm, respectively. **c**,**d**, Image and projection of the interference pattern recorded on the second YAG screen when the FEL beam propagates through two 20 μm slits, separated by 0.8 mm, placed ~8.5 m before the screen.

M. Kuhlmann et al, FEL06
P. Mercère et al, , Optics Letters, 28 (17), 1534-1536 (2003)
A. Singer et al. PRL 101, 254801 (2008)

Superconducting LINAC : Toward higher repetition rate

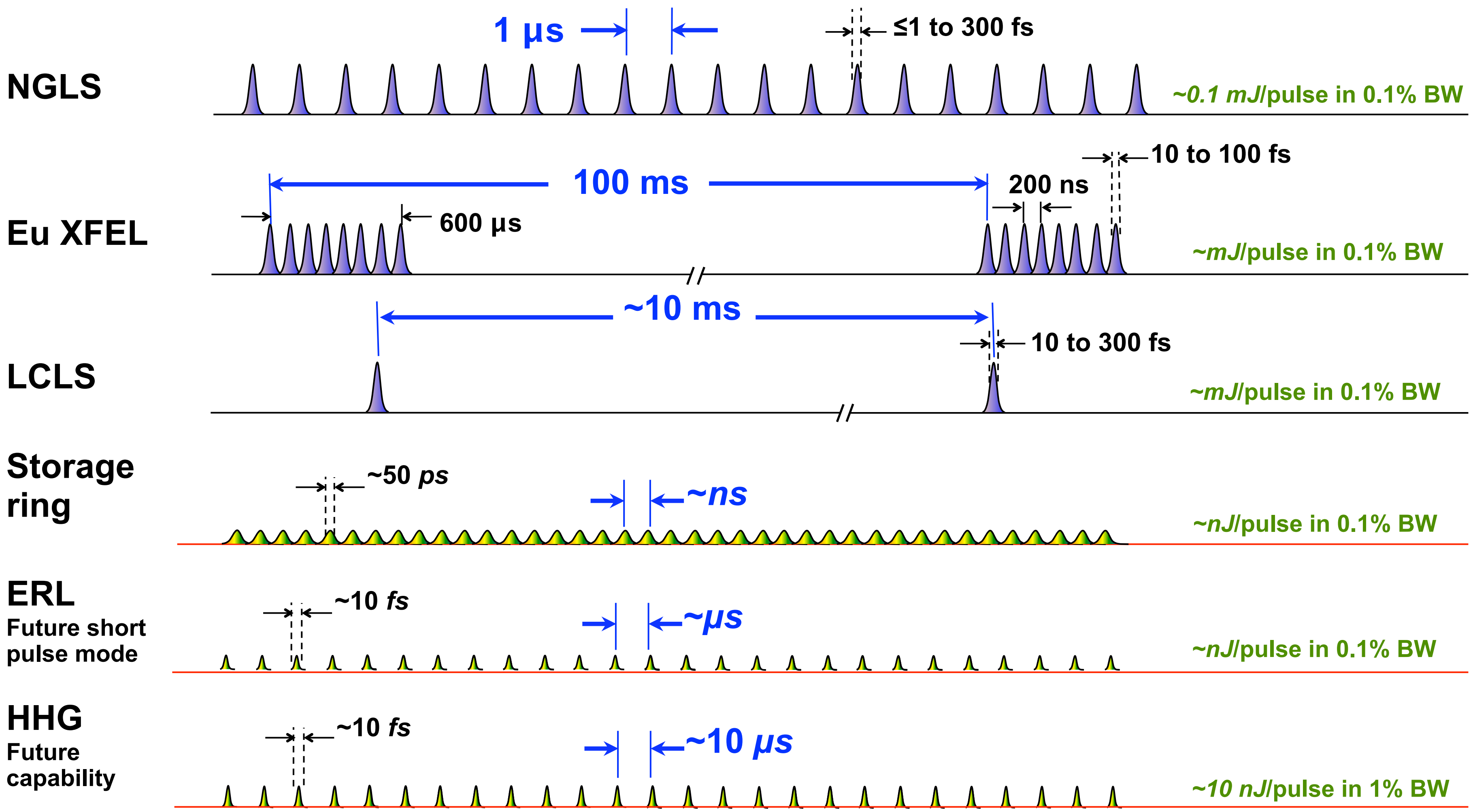

Courtesy J. Corlett

NGLS is a facility concept for soft X-ray science, providing X-ray lasers beams with:

- high temporal and spatial coherence
- high repetition rate
- high average power and brightness
- high peak power and brightness
- ultrafast pulses
- synchronization with experimental lasers
- multiple beamlines
- independent tunability for each beamline
- each FEL and beamline configured for specific science needs

High peak brightness high average brightness
≤ fs, evenly-spaced, ~time-bandwidth limited pulses

Superconducting LINAC : Toward higher multiple FEL lines

NGLS performance

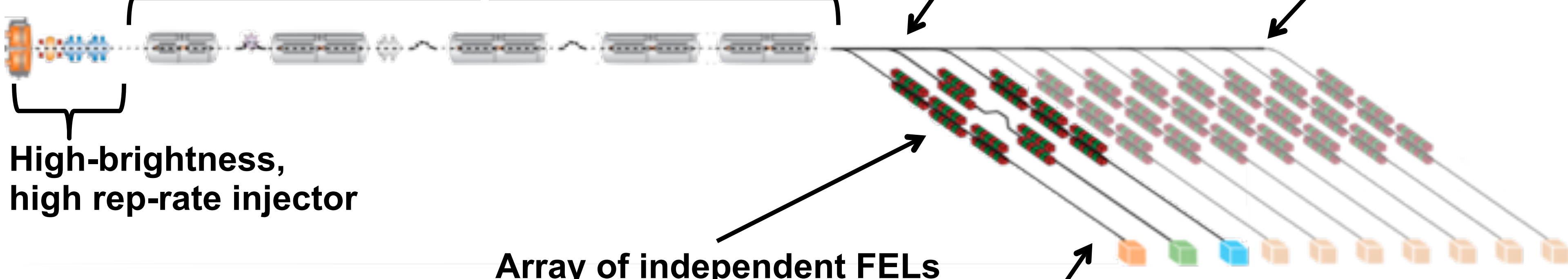

High repetition rate soft X-ray laser array
- **Up to 10^6 pulses per second**
- **Average coherent power up to ~100 W**

Spatially and temporally coherent X-rays (seeded)
- **Ultrashort pulses from ≤1 fs to ~300 fs**
- **Narrow energy bandwidth to 50 meV**

Tunable X-rays
- **Adjustable photon energy from 100 eV – 1.25 keV, 2 keV achievable**
- **Moderate to high flux with 10^{10} – 10^{12} photons/pulse**

Expandable
- **Capability (e.g. repetition rate, pulse duration, tuning range)**
- **Capacity (additional FEL beamlines)**

Courtesy J. Corlett

Superconducting LINAC : Toward higher multiple FEL lines

NGLS performance

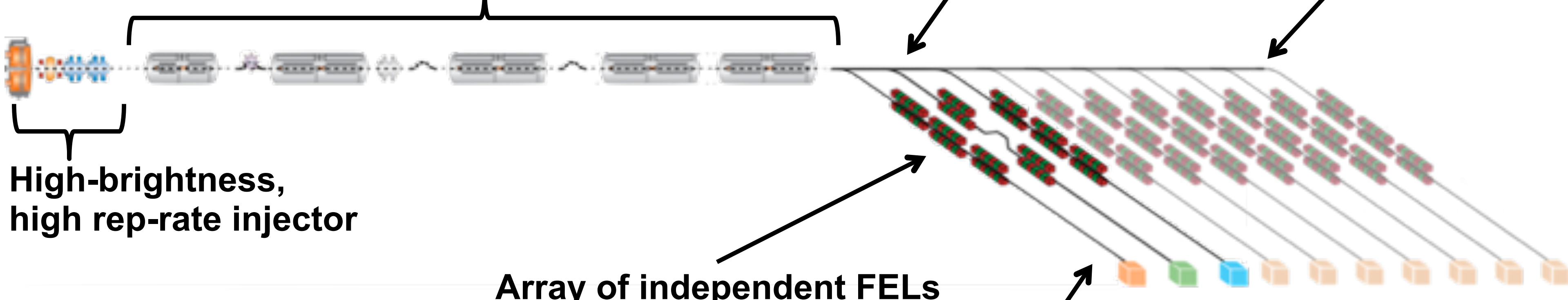

High repetition rate soft X-ray laser array
- Up to 10^6 pulses per second
- Average coherent power up to ~100 W

Spatially and temporally coherent X-rays (seeded)
- Ultrashort pulses from ≤1 fs to ~300 fs
- Narrow energy bandwidth to 50 meV

Tunable X-rays
- Adjustable photon energy from 100 eV – 1.25 keV, 2 keV achievable
- Moderate to high flux with 10^{10} – 10^{12} photons/pulse

Expandable
- Capability (e.g. repetition rate, pulse duration, tuning range)
- Capacity (additional FEL beamlines)

- A CW SCRF linac provides a "backbone" for delivering high-brightness electron beam to an array of independent FELs
- Nominal high-level linac parameters
  - 300 pC
  - 1 MHz
  - 2.4 GeV
  - 16 MV/m
  - 500 A
  - 300 fs

NGLS next generation light source

Courtesy J. Corlett

SOLEIL SYNCHROTRON LUNEX5

XFEL on low emittance ring

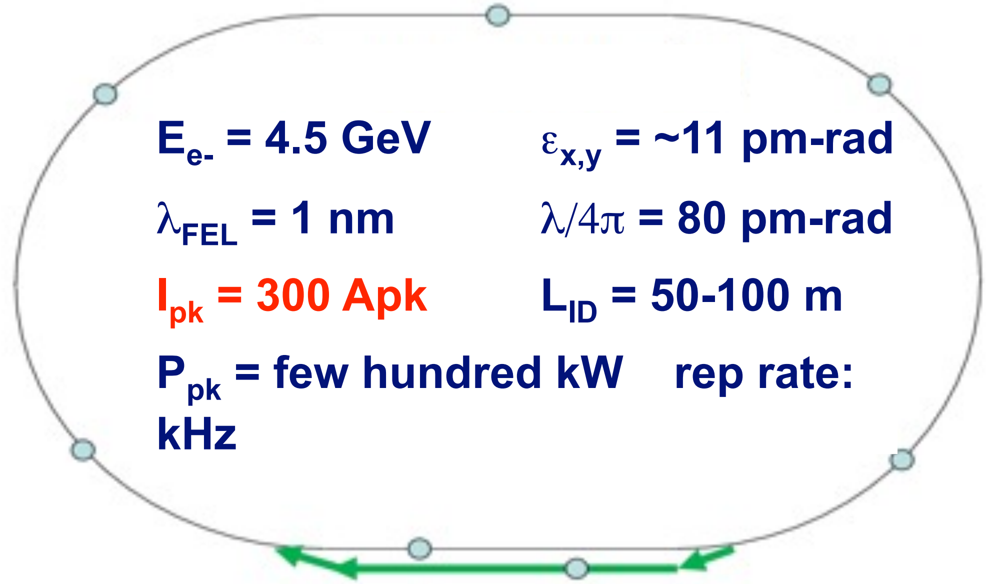

Soft X-ray FEL in switched by-pass

A.S. Fischer et al. 40 Å designs for the PEP storage ring, NIM 318 (1992)730-735

Can inject special short, high peak current bunch to lase for a few turns

Soft X-ray partial lasing with stored beam in PEP-X

Z. Huang, C. Pellegrini et al.

SASE with Transvers eGradient Undulator

Z. Huang, Y. Cai, Y. Ding

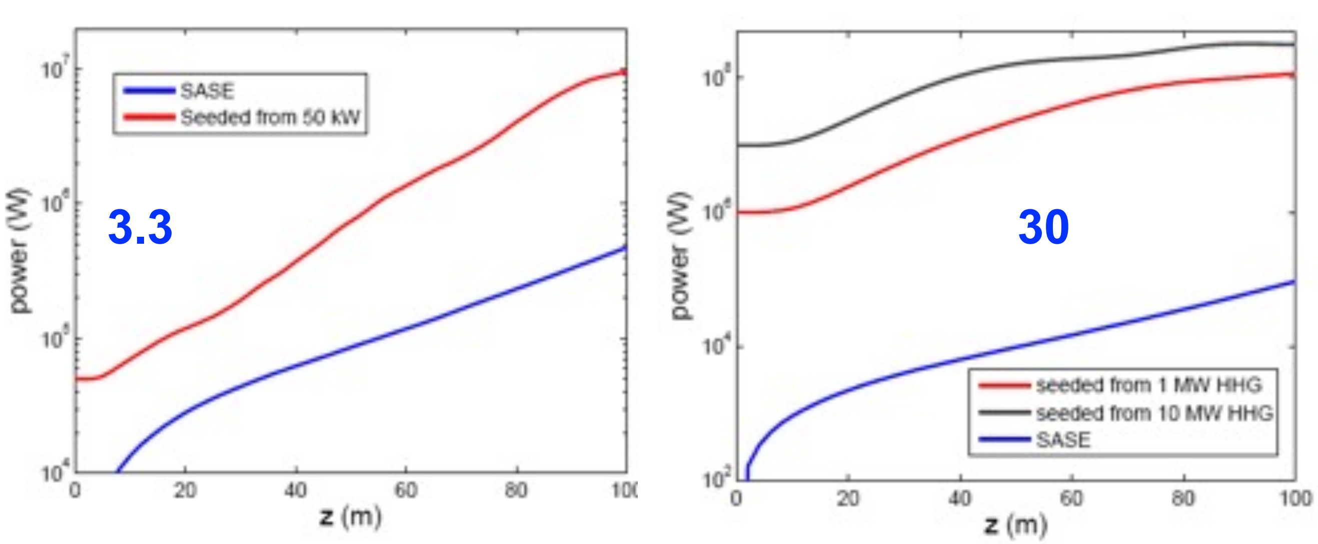

E = 4.5 GeV $\varepsilon_{x/y}$=160 / 1.6 pm $\delta E/E = 1.6\times10^{-3}$ rms σ_z=1ps Q = 0.75 nC

I_{pk} = 300 A

η_y = 0.05 m $\beta_{x/y}$ = 16 / 50 m σ_β = 52 mm σ_η = 78 mm

vertical undulator: λ_u = 3 cm K = 3.7 **λ_{ph} = 1.5 nm**

XFEL on low emittance ring

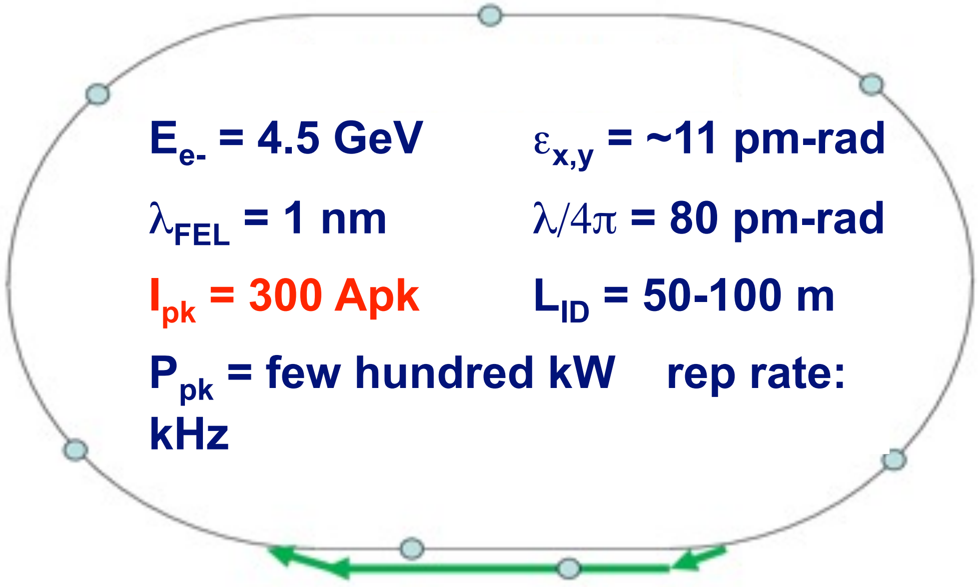

Soft X-ray FEL in switched by-pass

A.S. Fischer et al. 40 Å designs for the PEP storage ring, NIM 318 (1992)730-735

Can inject special short, high peak current bunch to lase for a few turns

Soft X-ray partial lasing with stored beam in PEP-X

Z. Huang, C. Pellegrini et al.

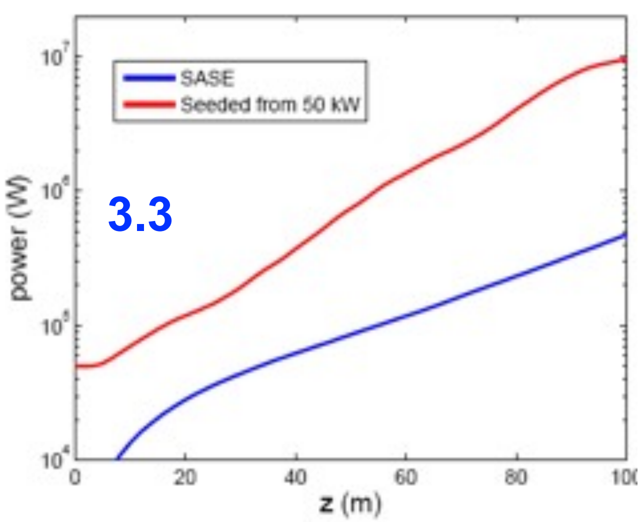

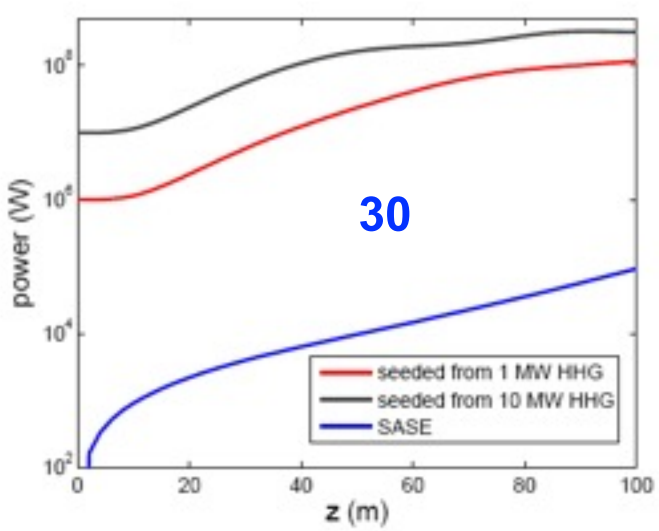

E = 4.5 GeV $\varepsilon_{x/y}$=160 / 1.6 pm $\delta E/E$ = 1.6x10^{-3} rms σ_z=1ps Q = 0.75 nC I_{pk} = 300 A

η_y = 0.05 m $\beta_{x/y}$ = 16 / 50 m σ_β = 52 mm σ_η = 78 mm

vertical undulator: λ_u = 3 cm K = 3.7 **λ_{ph} = 1.5 nm**

SASE with Transvers eGradient Undulator

Z. Huang, Y. Cai, Y. Ding

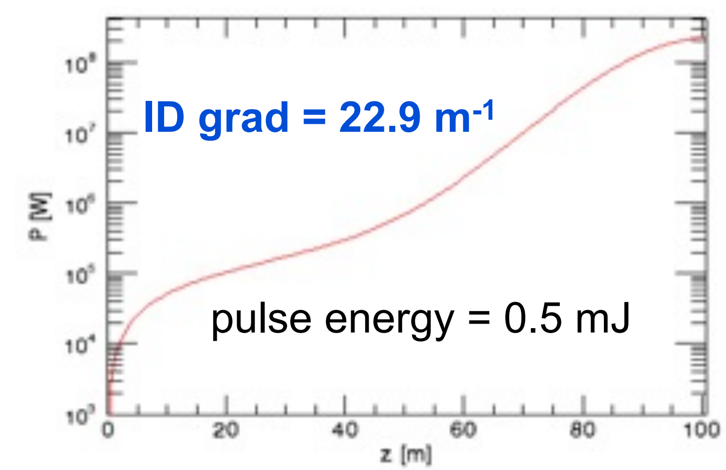

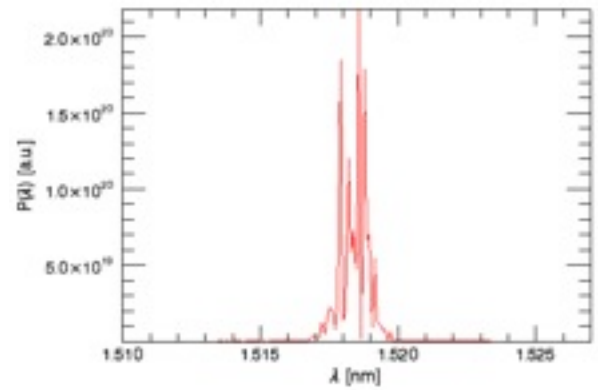

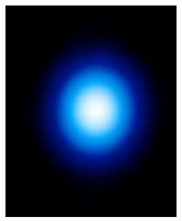

Laser Wakefield Accelerator

Intense laser focused in a gas jet / cell / capillary
=> ions : accelerator electric field

LWFA beam

- Very short
- Strongly diverging (1 mrad)
- Small size
- Large relative energy spread (1 %)

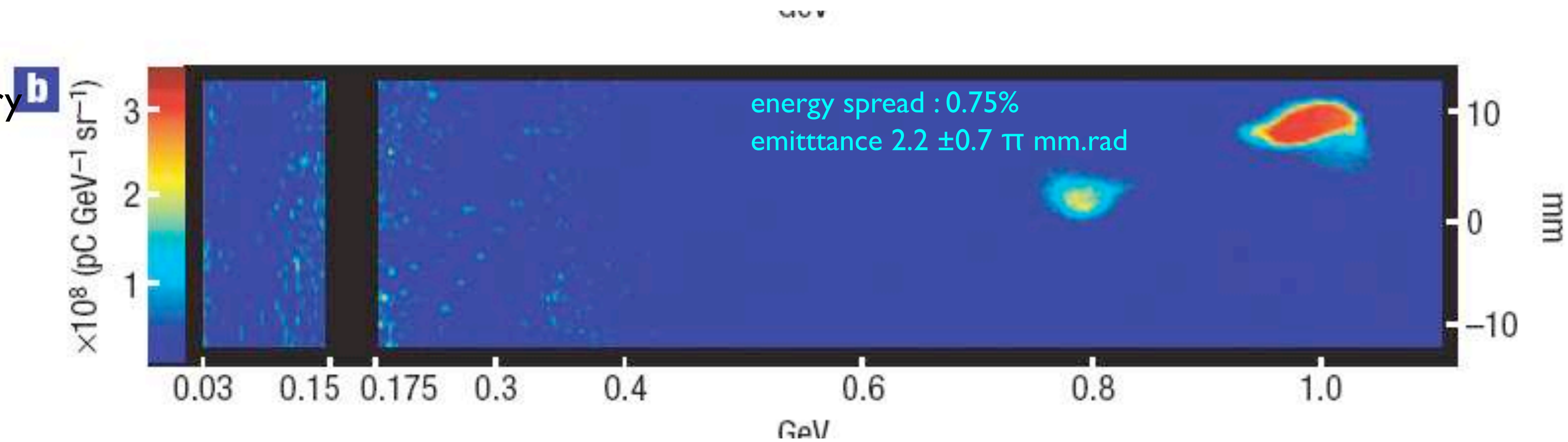

W. P. Leemans et al. , Nature Physics 418, 2006, 696

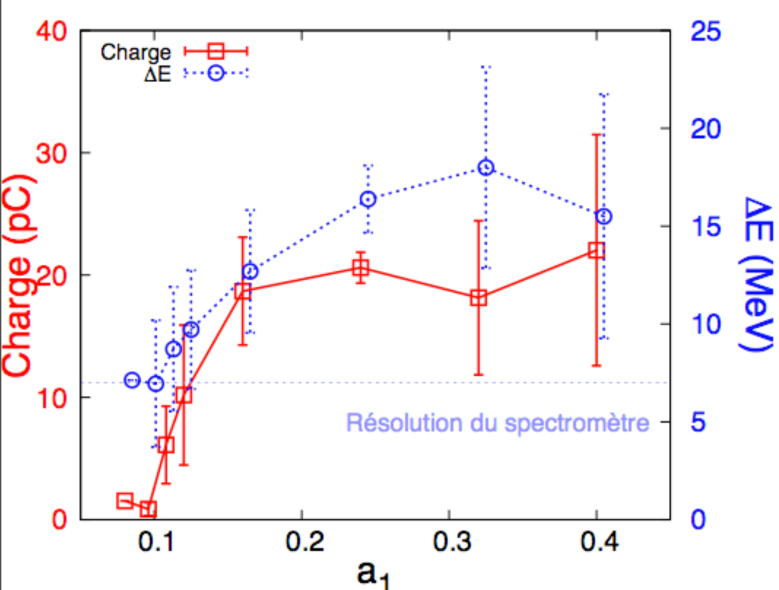

C. Rechatin et al., Phys. Rev. Lett. ***102****, 194804 (2009)*

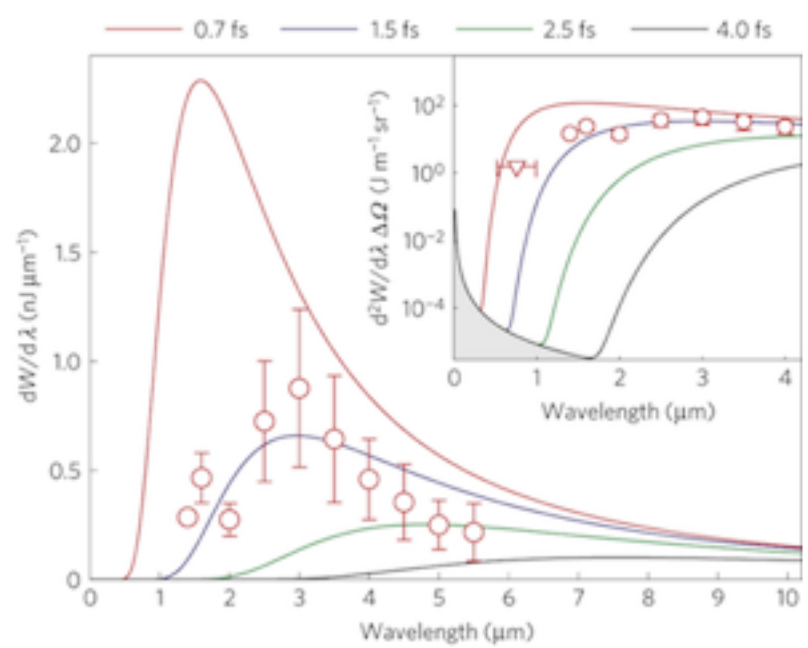

1.5 fs RMS duration : Peak current of 4 kA

O. Lundh et al. Nature Physics,

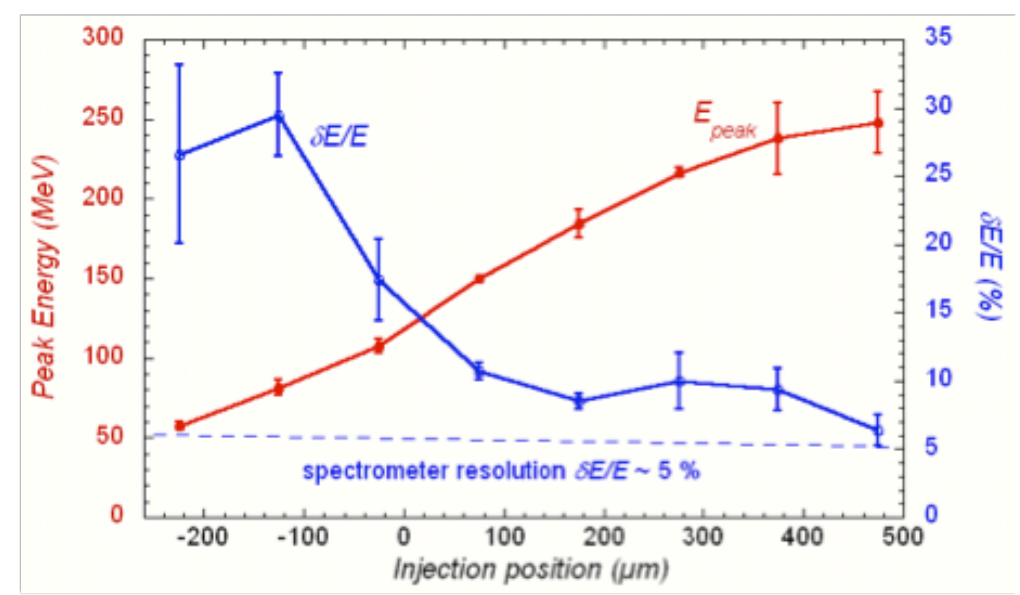

	2002	2004	2009
Energy spread (%)	100	5	1

below : *C. Cipiccia et al. Nature Physics, 2011*

Laser Wakefield Accelerator

Production or radiation :
- betatron radiation
- Thomson scattering
- undulator spontaneous emission
- FEL?

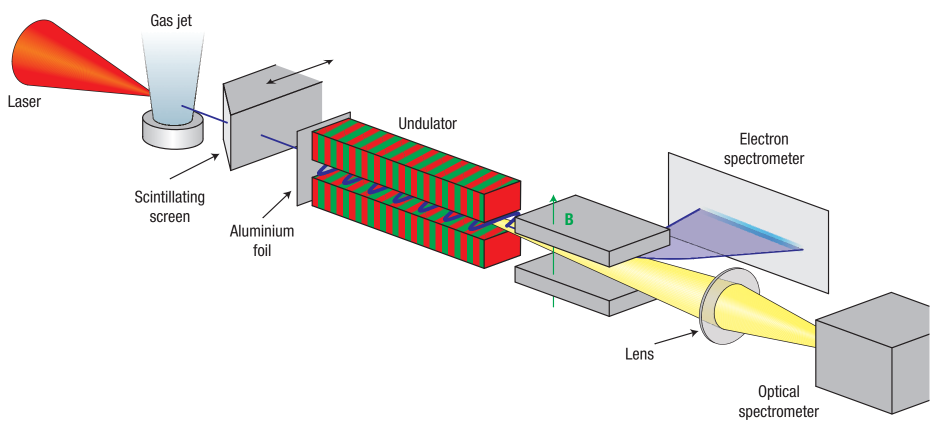

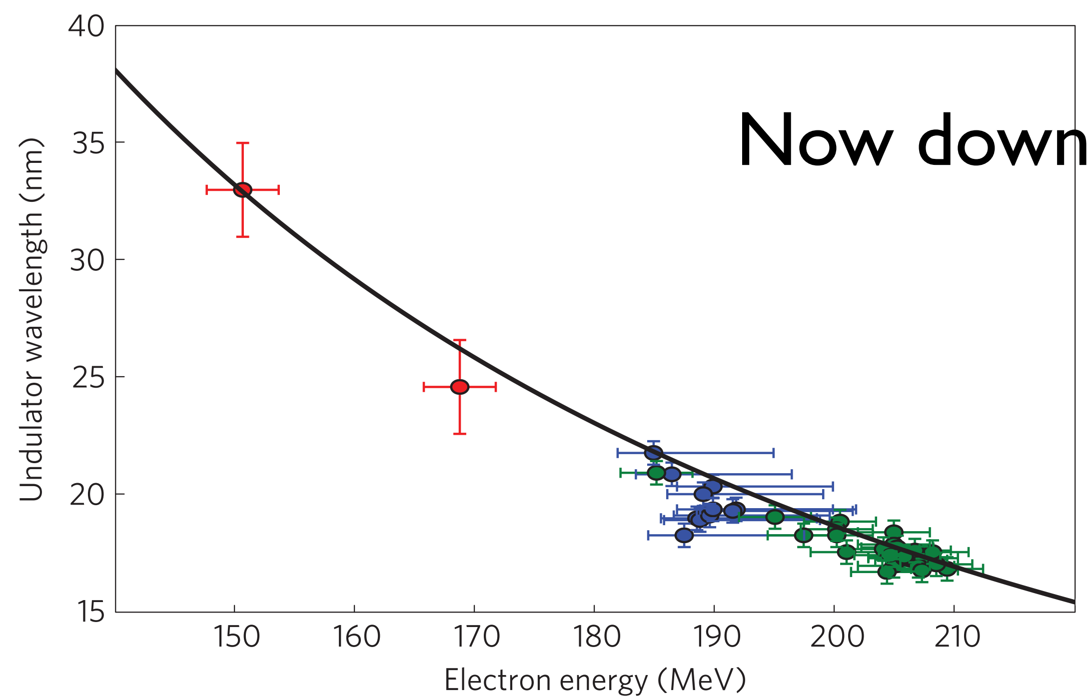

Now down to 4 nm

M. Fuchs et al. 5, 2009, 826

LWFA based FEL

- Energy spread : 1 %, divergence 1 mrad

=> strong focusing + **chicane decompression** + chromatic matching

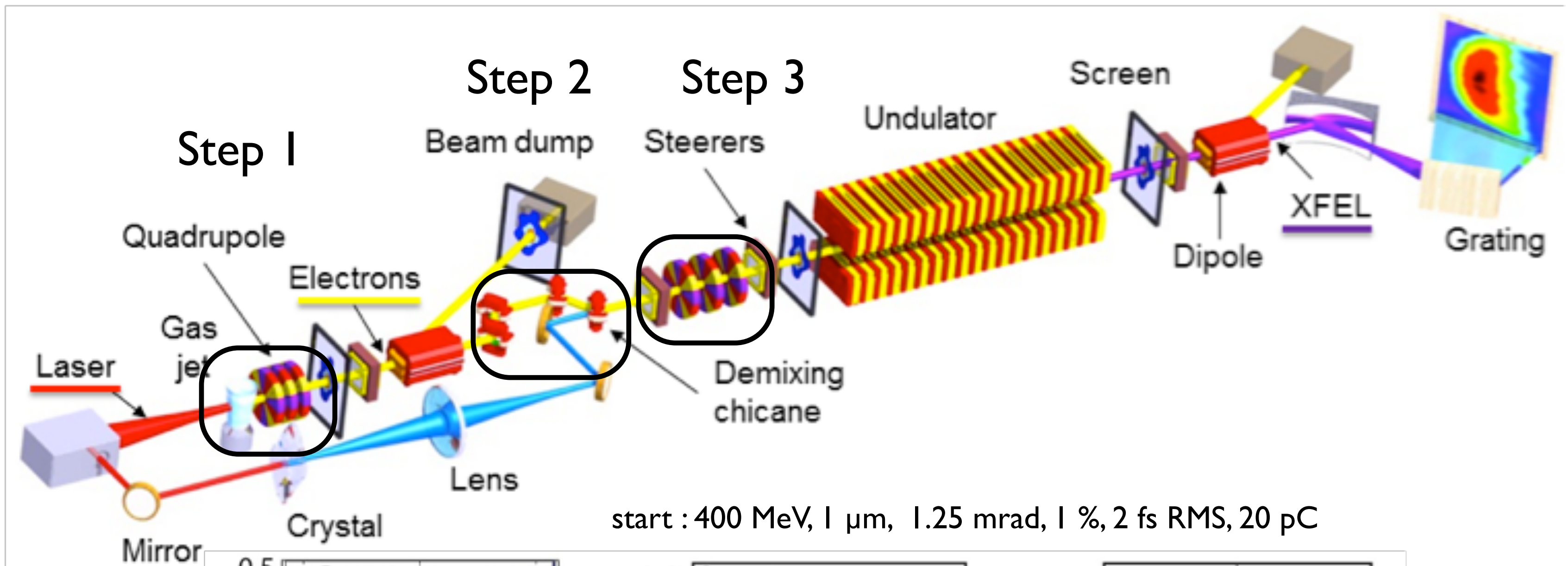

start : 400 MeV, 1 µm, 1.25 mrad, 1 %, 2 fs RMS, 20 pC

Step 1

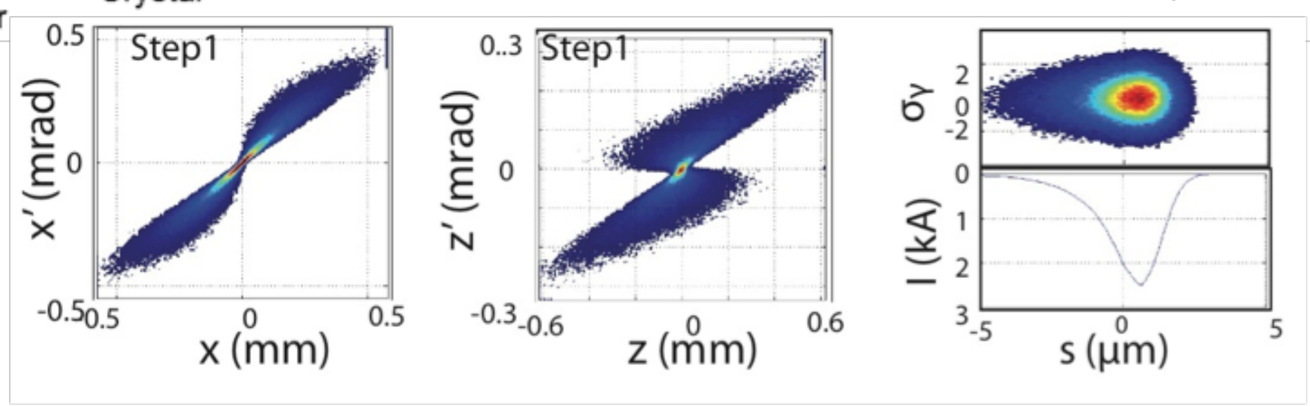

Step 2

before the chicane (2.2 kA, 4 fs RMS)

after the chicane (180A, 40 fs RMS

FEL power

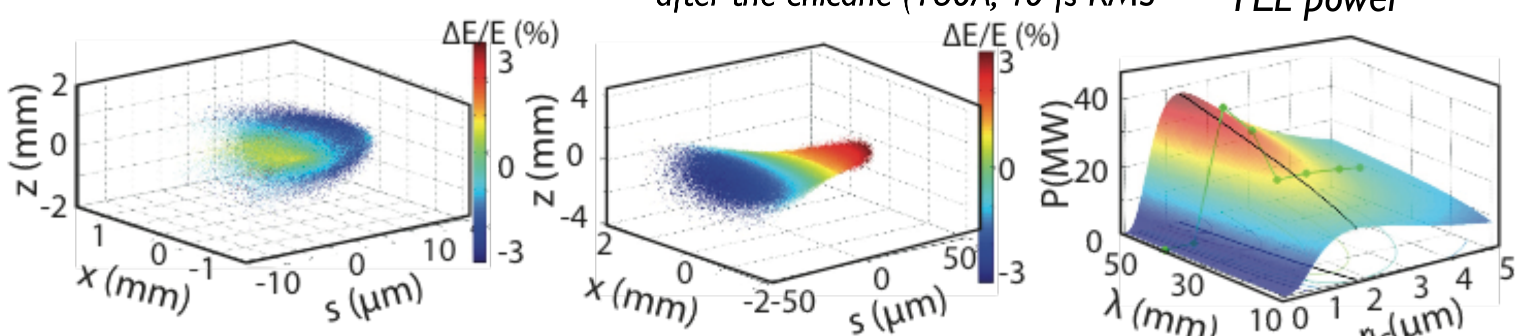

A. R. Maier et al., Phys. Rev. X 2, 031019 (2012)

Step 3

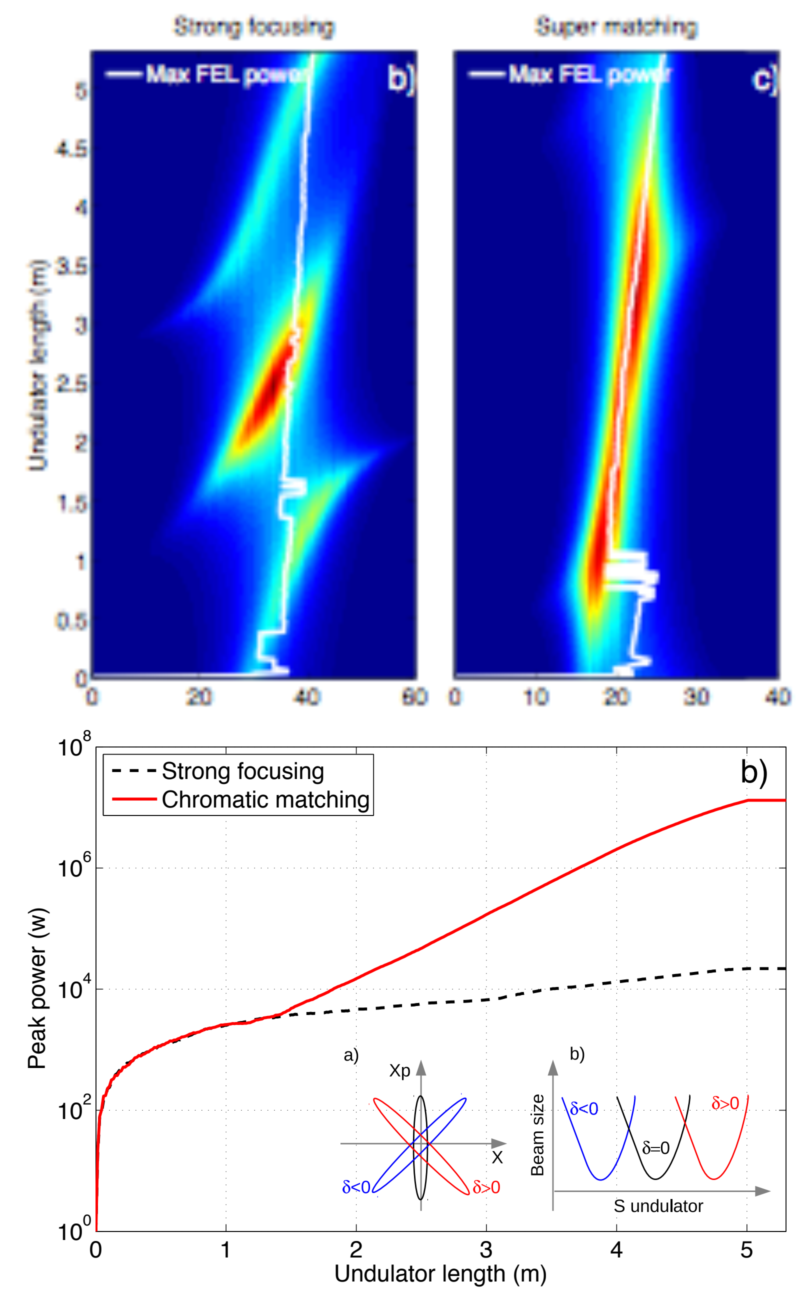

A. Loulergue et al. sub. PRL

LWFA based FEL

Example of LUNEX5 : free electron **L**aser **U**sing a **N**ew accelerator for the **E**xploitation of **X**-ray radiation of **5**th generation :

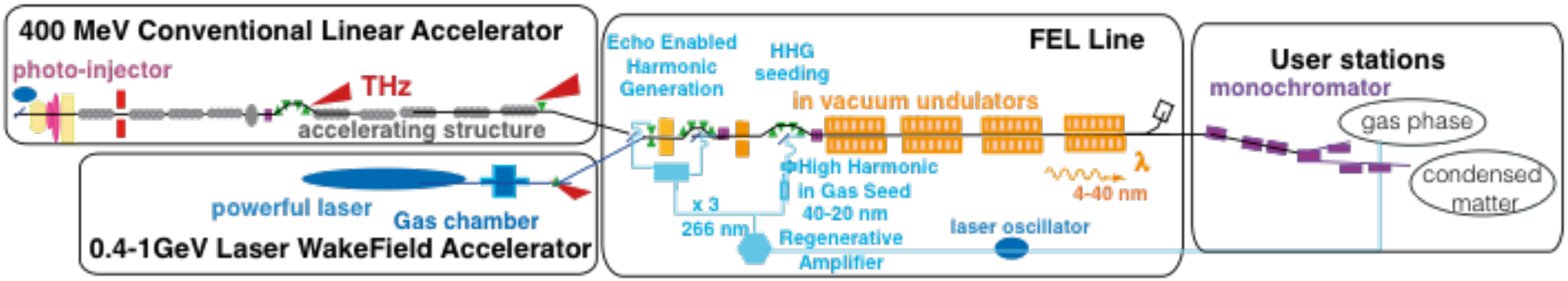

40-4 nm, 20 fs and shorter

4G+ : towards full temporal and transverse, short pulses, multi-FEL lines to be validated by,

5G: (Conventional Linac replaced by a LWFA), FEL being viewed as an qualifying LWFA application

pilot user experiments

electron beam transport for FEL amplification

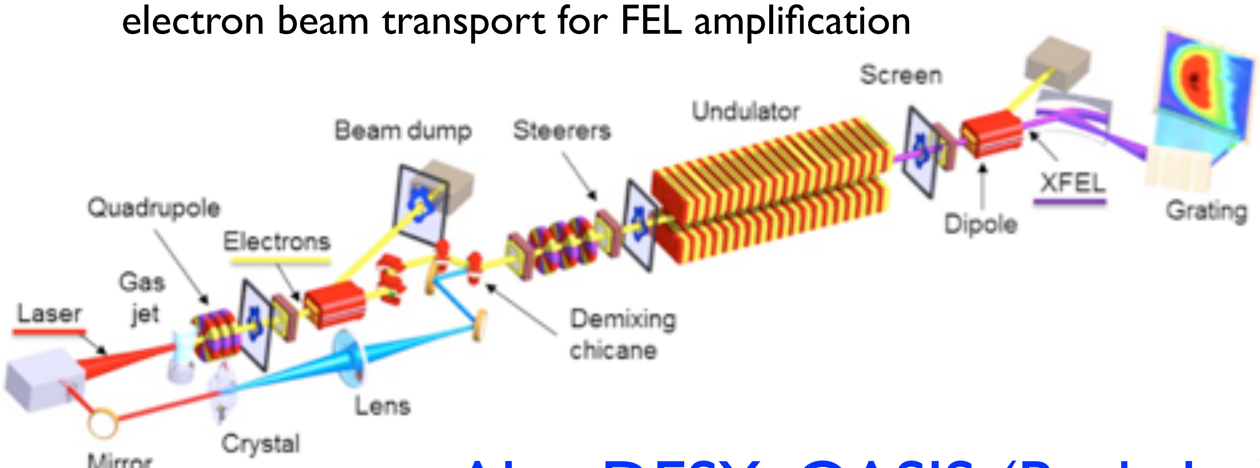

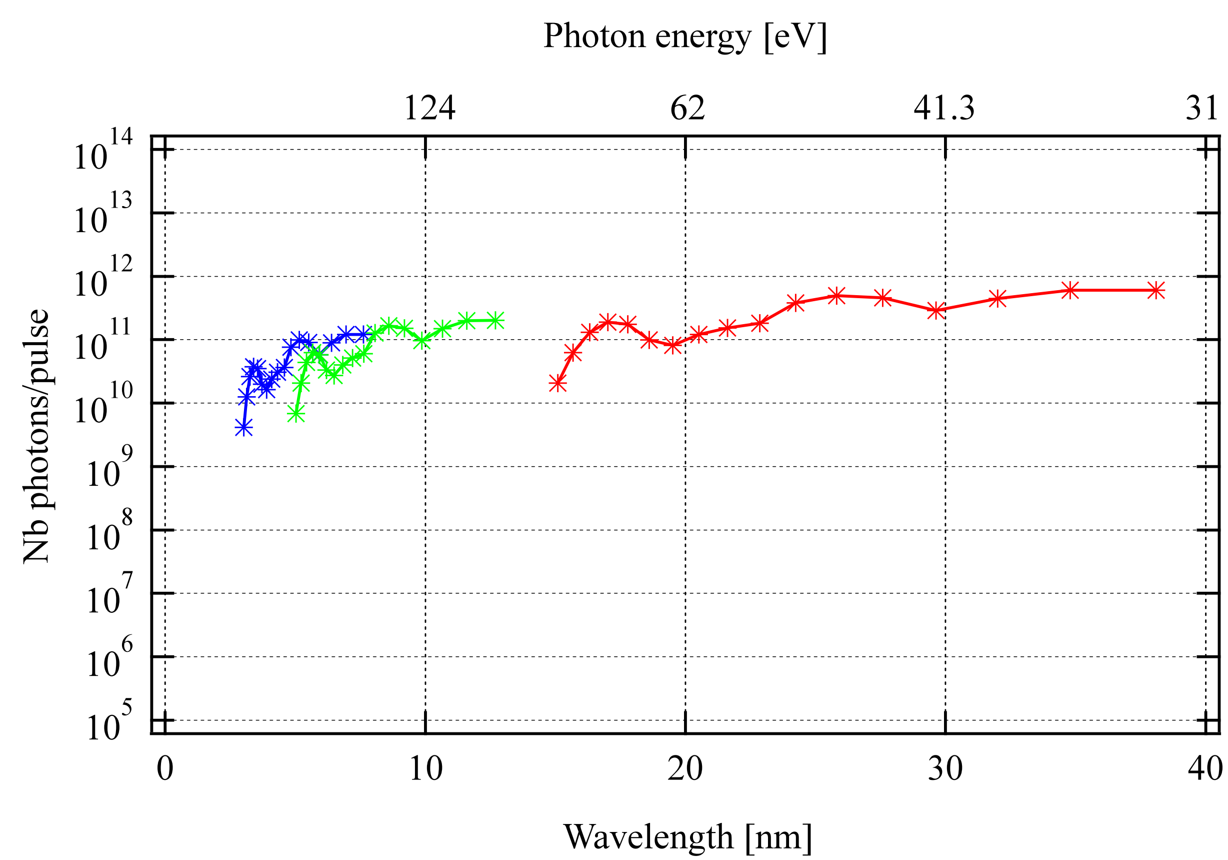

Also DESY,, OASIS (Berkeley), Stratclyde et al.

LWFA based FEL

• Energy spread : 1 % too large for FEL amplification
=> chicane decompression / **transverse gradient undulator**

$$\frac{\Delta K}{K_0} = \alpha x. \qquad \eta = \frac{2 + K_0^2}{\alpha K_0^2}$$

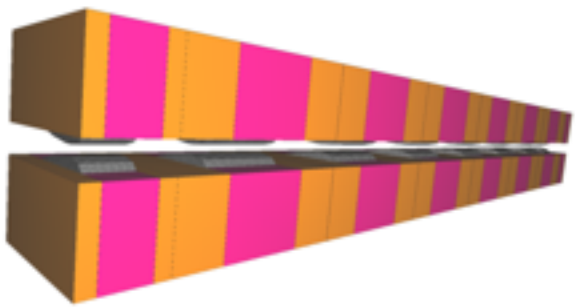

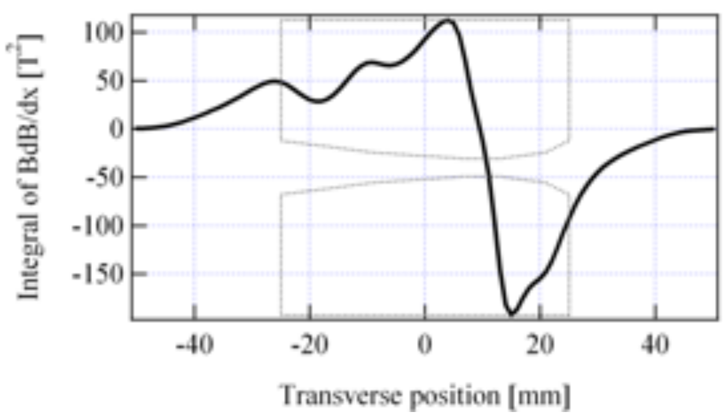

Gap	6 mm
B_{max}	-2.5 T
Int[BdB/dX]	193 T²
Period length	164 mm
No. of periods	12

H. Abualrob, P. Brunelle, M-E. Couprie, O. Marcouillé, A. Nadji, L. Nadolski, R. Nagaoka, SOLEIL emittance reduction using a Robinson wiggler, IPAC12, Louisiana, La Nouvelle Orleans 20-25 Mai 2012

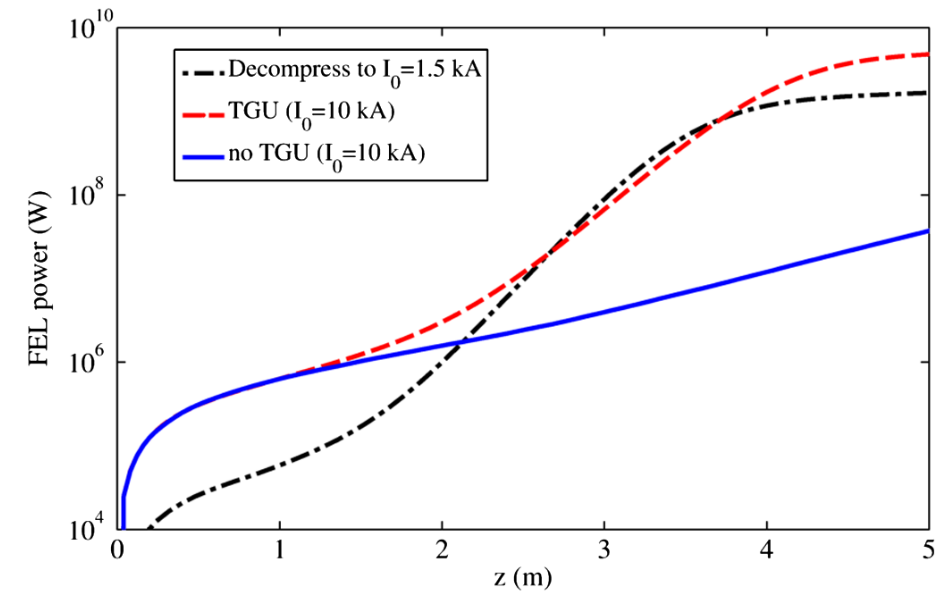

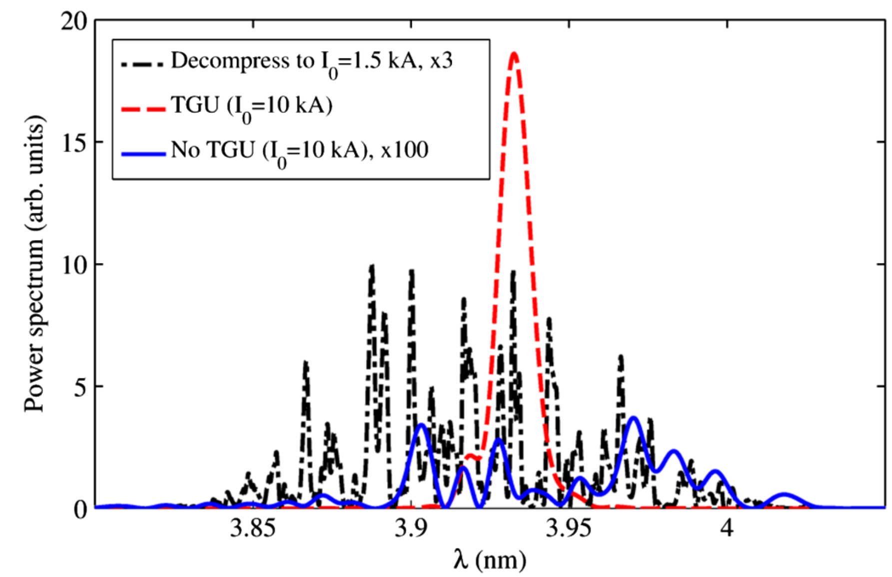

Z. Huang et al., Phys. Rev. Lett. 109, 204801 (2012)
T. Smith, J. M. J. Madey, L. R. Elias, and D.A. G. Deacon, J. Appl. Phys. 50, 4580 (1979)

Dielectric accelerator

μ-quadrupole

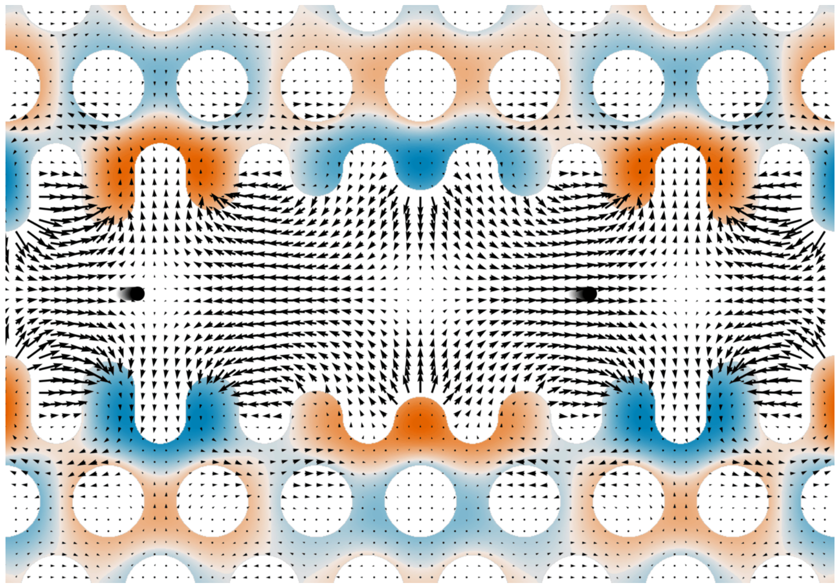

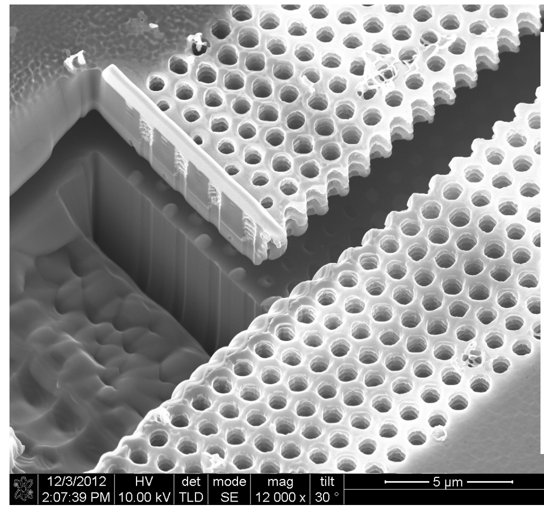

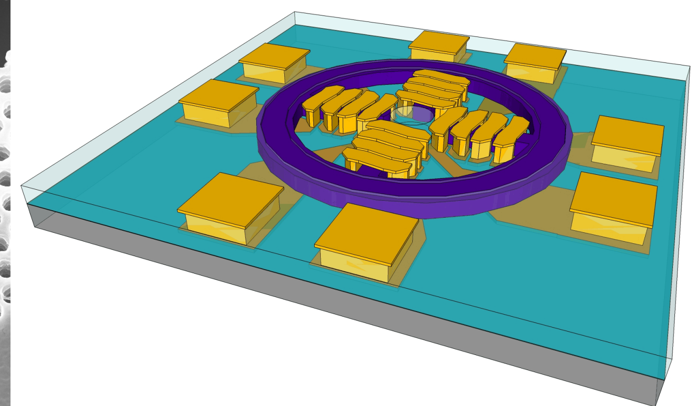

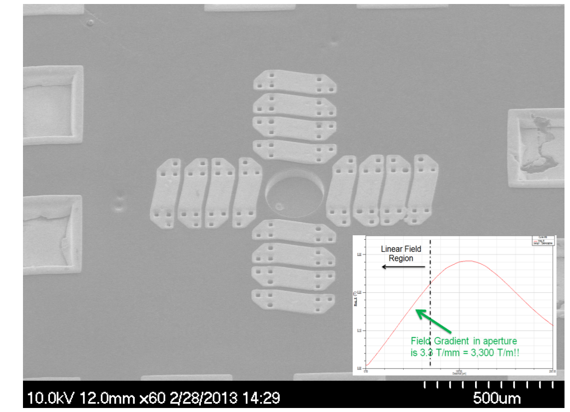

[Max Ho, UCLA Nanolab]

B. Naranjo, A. Valloni, S. Putterman, J. B. Rosenzweig, stable charge-particle accleration and focusing in an laser accelerator using spatial harmonics, Phys. Rev. Lett. 109, 176803 (2012)

R. Candler et al. High brightness electron beam workshop, Porto-Rico, 2013

- Resonant spatial harmonic provides acceleration
- non resonant spatial harmonics provides focusing
- hole diameter typically 800 nm

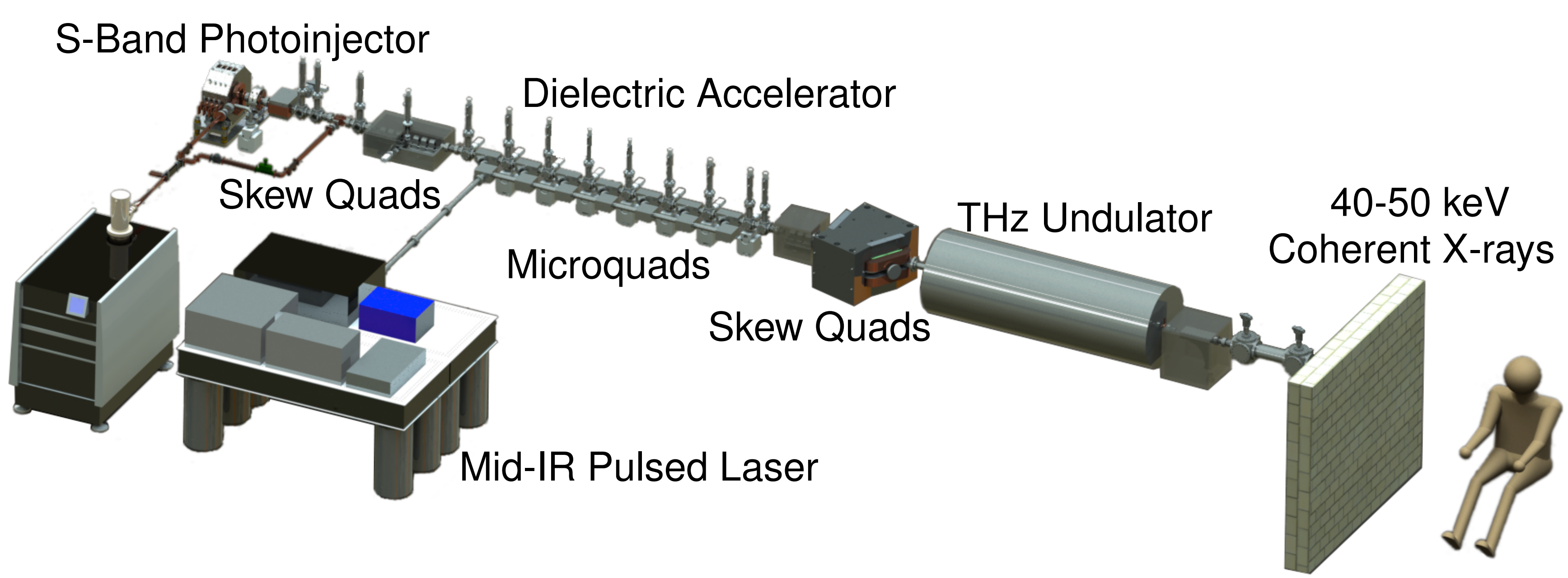

Example of GALAXIES project UCLA

The inverse FEL

In an FEL energy in the e-beam is transferred to a radiation field

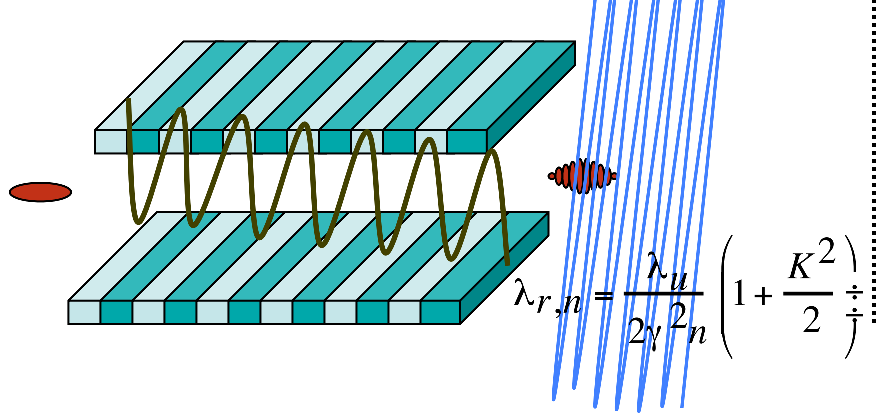

In an IFEL the electron beam absorbs energy from a radiation field.

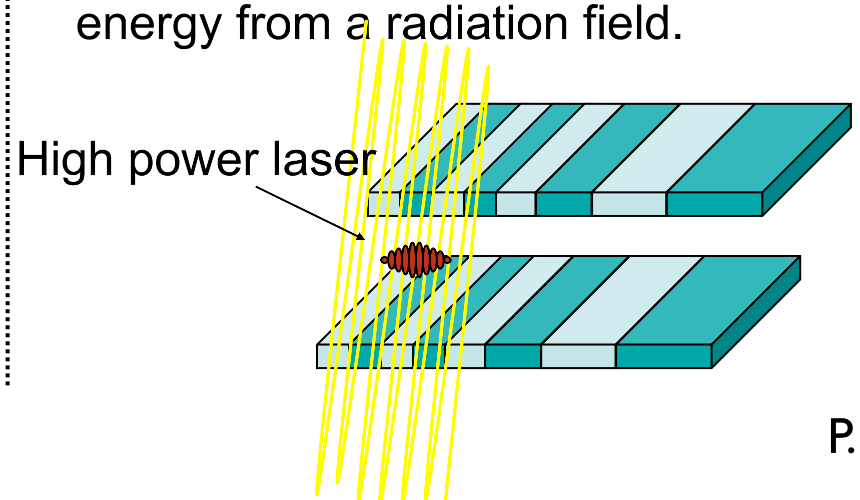

$$\gamma_r^2 \cong \frac{\lambda_w}{2 \times \lambda} \cdot \left(1 + \frac{K^2}{2}\right)$$

P. Musumeci

STELLA 2 : gain of 17% of the energy — *W. Kimura et al. PRL92, 154801 (2004)*

IFEL @ UCLA : 15 => 35 MeV in 25 cm (0.5 TW @ 10.6 μm), 70 MeV / m — *P. Musumeci et al. PRL94, 154801 (2005)*

RUBICON, LLNL : 105 MeV achieved recentyly — *P. Musumeci EAAC , Elba, May 2013*

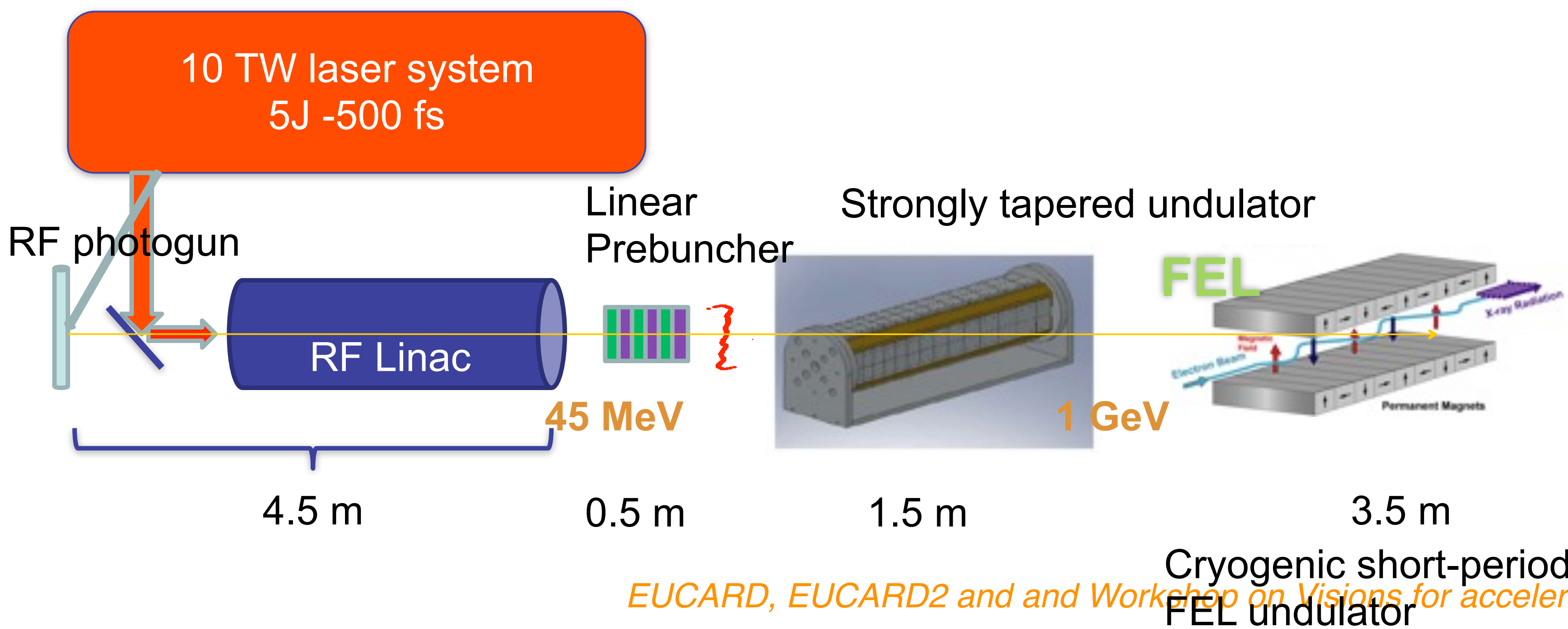

towards high rep. rate LWFA based FEL

Towards 100 TW to PW laser peak power, with MW average power
with an improve efficiency (target : 30 %)

- Yb doped single mode fiber (fiber noise)
- µm precision fiber assembly
- fiber to fiber phase shift measurement :
quadriwave lateral shearing interefrometer

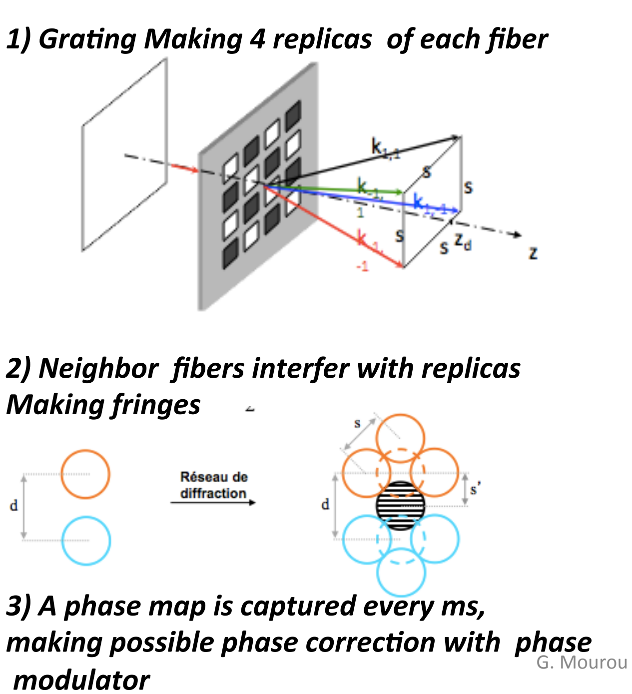

J. Primot (ONERA)

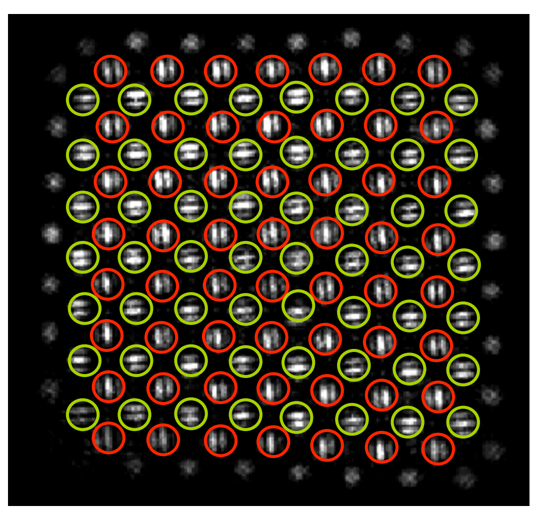

Only 6 pixels are necessary to reach λ/60 precision.

33

G. Mourou EEAC, May 2013, Elba

- phase correction by optical modulator :
64 fibers locked in 2011 !

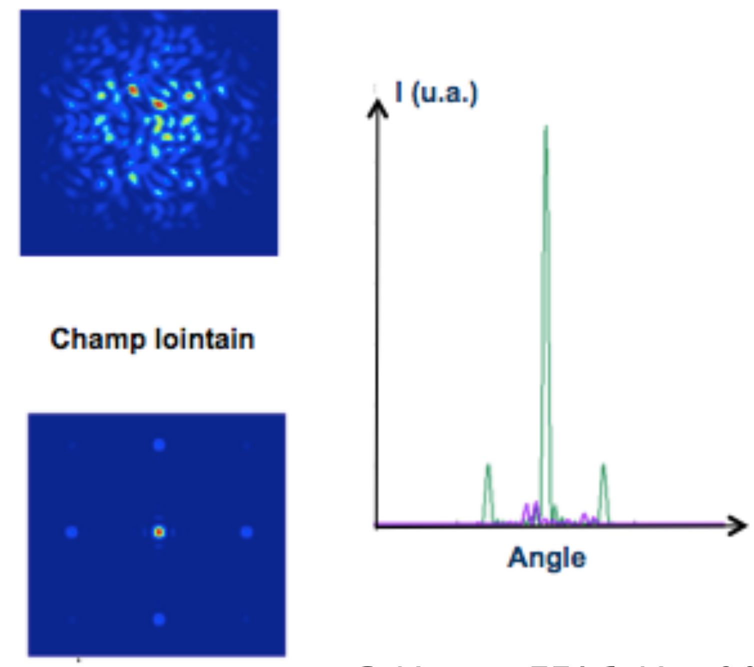

G. Mourou EEAC, May 2013, Elba

- non linear effects
phase locking of 8 fiber amplifiers : 3.1 µJ, 50 fs, 1 MHz

L. Daniault et al., Opt. Expr. 20, 21627 (2012)

A wide landscape

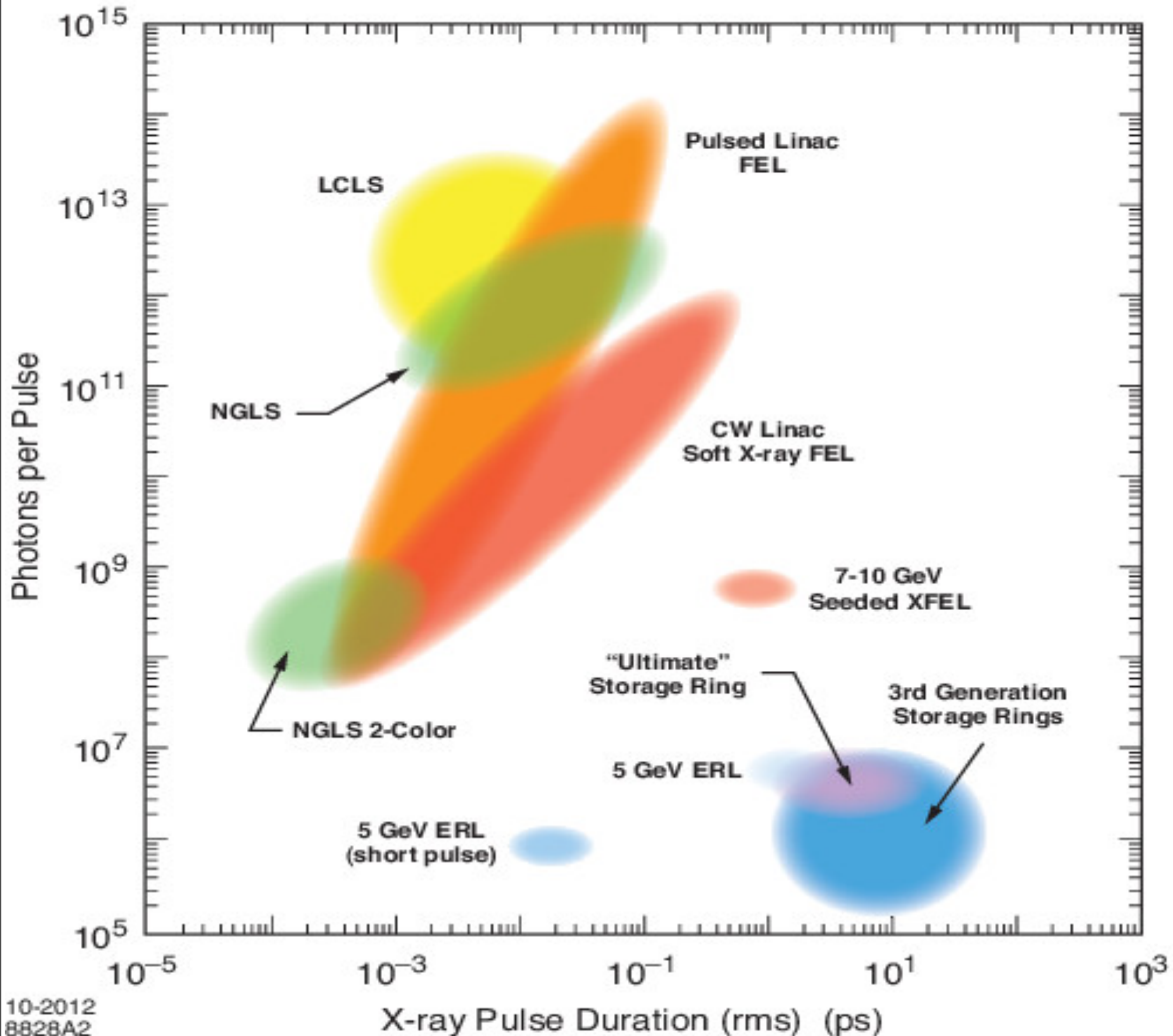

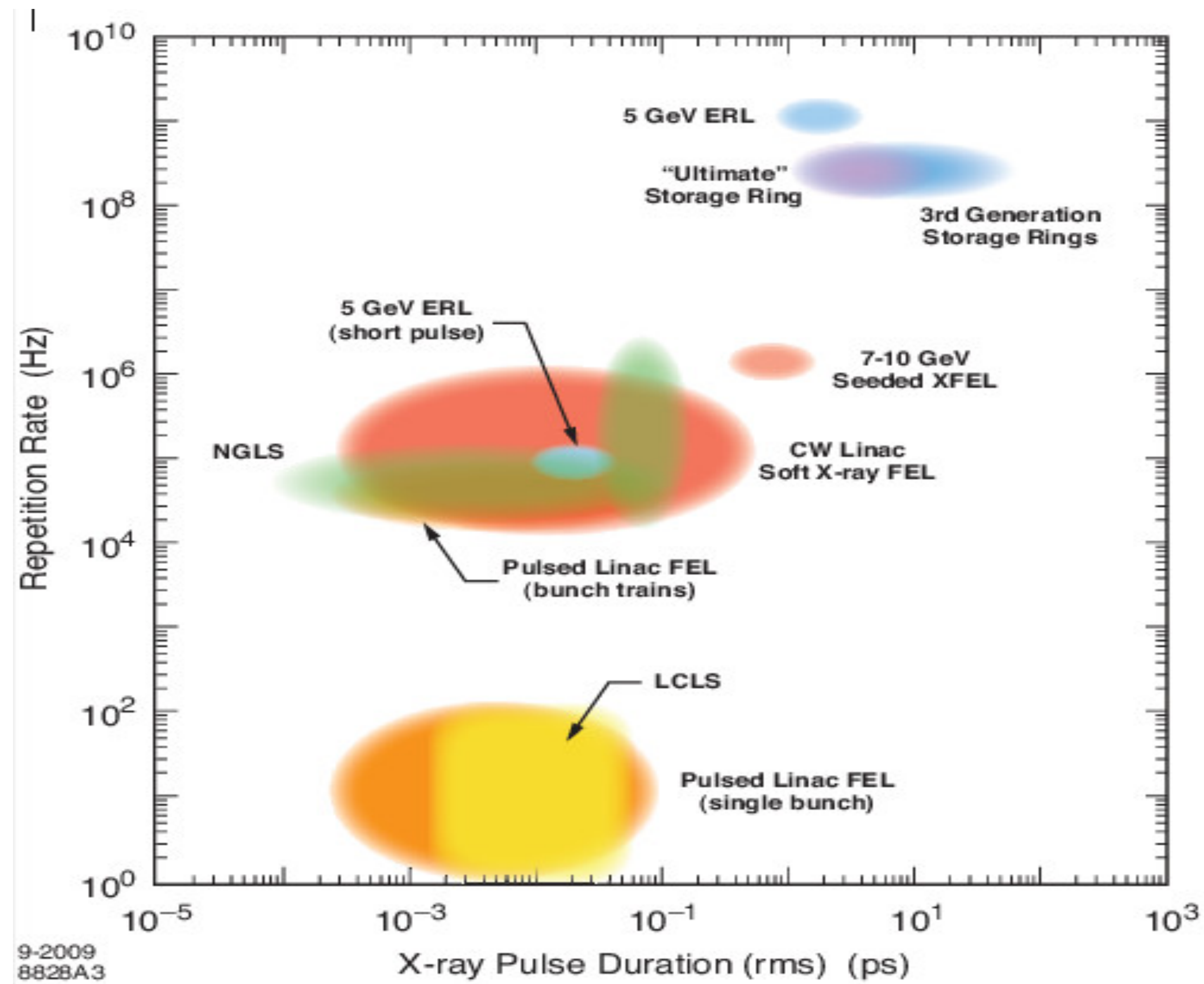

B. Hettel, Ultimate storage ring light sources, design and performances objectives, USR Accelerator R&D Workshop, Huairou (Beijing), China, October 30, 2012

A wide landscape

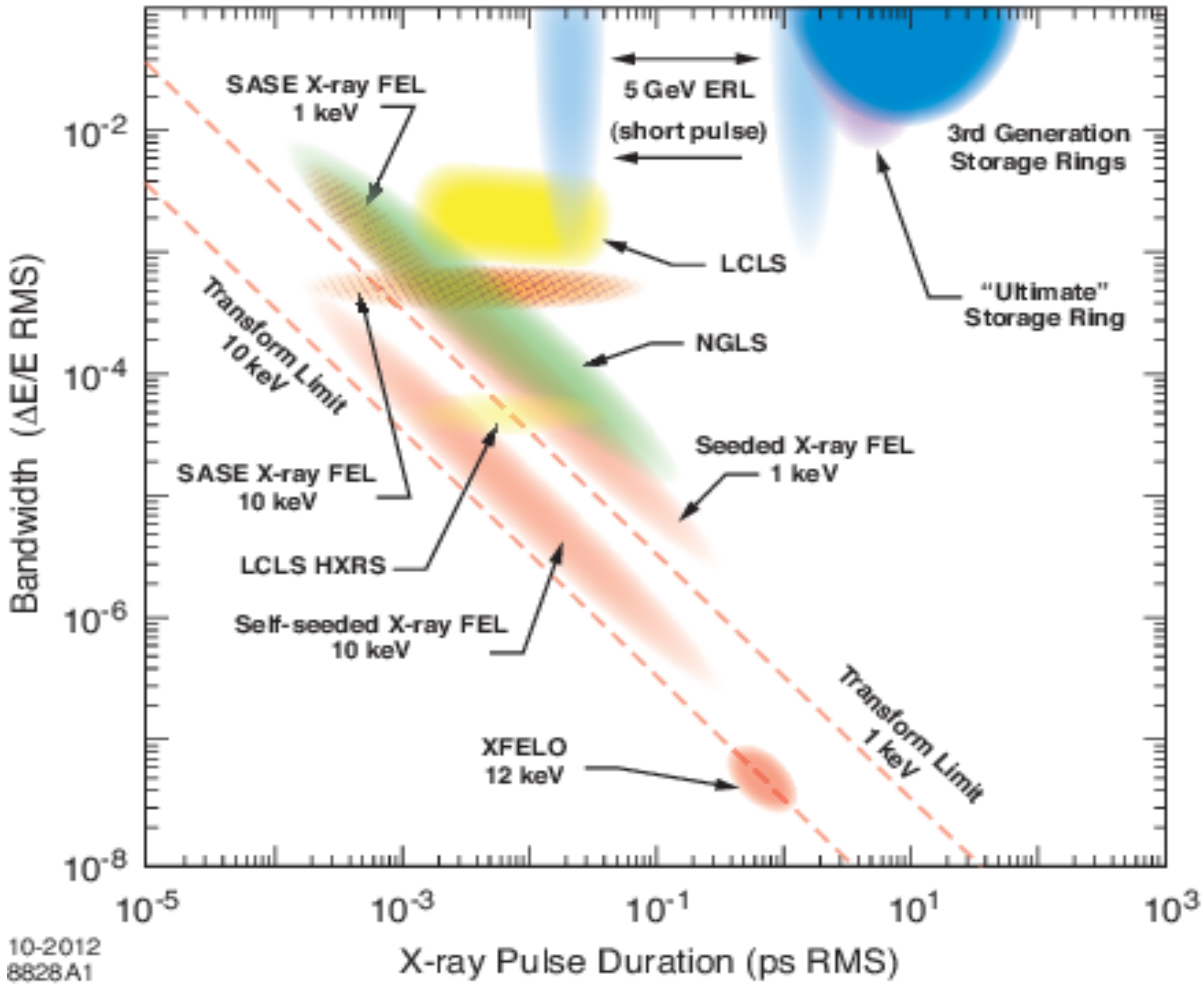

B. Hettel, Ultimate storage ring light sources, design and performances objectives, USR Accelerator R&D Workshop, Huairou (Beijing), China, October 30, 2012

Conclusion

For the next 50 years ....

Sources complementarity and more flexibility on light source properties
Further synergy / interplay with laser

- Storage ring based : mature, towards transverse coherence (USR) and tailored bunches but still rather long bunches and rather large energy spreads

- ERL : Test facility, towards X-ray user facilities

FEL provides longitudinal coherence in X-ray range
- Linac based SASE :
Now LCLS has acheived a 95% photon avalaibility, equivalent to what is provided on synchrotron light sources
It evolves towards advanced «tailored» charactristics with muti-color, , adjustable polarisation, higher powers and energies...
harmonic production (to which number? when?)
Emergence of new accelerator schemes and related technologies
need of demo experiments, improvement of stability and relaibility

+ New ideas.....

Overview of short wavelength FEL

	LCLS	LCLS II	Eu-XFEL	SACLA	FLASH	FLASH II	FERMI	SwissFEL	PAL XFEL	Shanghai XFEL	NGLS	MaRIE
Shortest wavelength	1.5 Å	1 Å	0.5 Å	1 Å	40 Å	40 Å	40 Å	1 Å	1 (0.6) Å	1 Å	10 Å	0.3 Å
Undulator type hard X-ray.	Fixed gap	Variable gap	Variable gap	In-vacuum Var. gap	n.a.	n.a.	n.a.	In-vacuum var. gap	Variable gap	Variable gap	n.a.	?
Undulator type soft X-ray.	n.a.	Variable gap	Variable gap	n.a.	Fixed gap	Variable gap	Apple II	Apple II	Apple II	?	Var. gap & Apple	n.a.
Injector	S-band RF gun	S-band RF gun	L-band RF gun	Pulsed Diode	L-band RF gun	L-band RF gun	S-band RF gun	S-band RF gun	S-band RF gun	S-band RF gun	VHF c.w. RF Gun	?
Cathode	Cu	Cu	Cs_2Te	CeB_6 (thermionic)	Cs_2Te	Cs_2Te	Cu	Cu	Cu	Cu	K_2CsSb	?
Main linac technology	n.c. Pulsed	n.c. pulsed	s.c. pulsed	n.c. pulsed	s.c. pulsed	s.c. pulsed	n.c. pulsed	n.c. pulsed	n.c. pulsed	n.c. pulsed	s.c. c.w.	n.c. pulsed
RF frequency	S-band	S-band	L-band	C-band	L-band	L-band	S-band	C-band	S-band	C-band	L-band	S–band
RF Rep. rate	120 Hz	120 Hz	10 Hz	60 Hz	10 Hz	10 Hz	10-50 Hz	100 Hz	120 Hz	60 Hz	n.a.	60 Hz
FEL pulses/RF pulse	1	1	2700	1	2700	2700	1	2	1	1	1 MHz c.w.	100
max. bunch charge	0.25 nC	0.25 nC	1 nC	0.2 nC	1 nC	1 nC	0.5 nC	0.2 nC	0.2 nC	0.2 nC	0.3nC	0.1 nC
max. electron energy	13.6 GeV	14 GeV	17.5 GeV	8 GeV	1.2 GeV	1.2 GeV	1.5 GeV	5.8 GeV	10 GeV	6.4 GeV	2.4 GeV	12 GeV
No. RF stations	81	81	29	69	5	5	15	34	49	?	?	?
Approx. facility length	1.7km	1.7km	3.4 km	0.8km	0.32 km	0.32 km	0.5 km	0.7km	1.1 km	0.6 km	?	1.0 km
Start operation	2009	2017	2015	2011	2005	2013	2010	2016	2015	2019	2023	?

towards high rep. rate LWFA based FEL

Towards 100 TW to PW laser peak power, with MW average power with an improve efficiency (target : 30 %)

G. Mourou et al. The future is fiber accelerator, Nature Photonics 7, 2013, 258

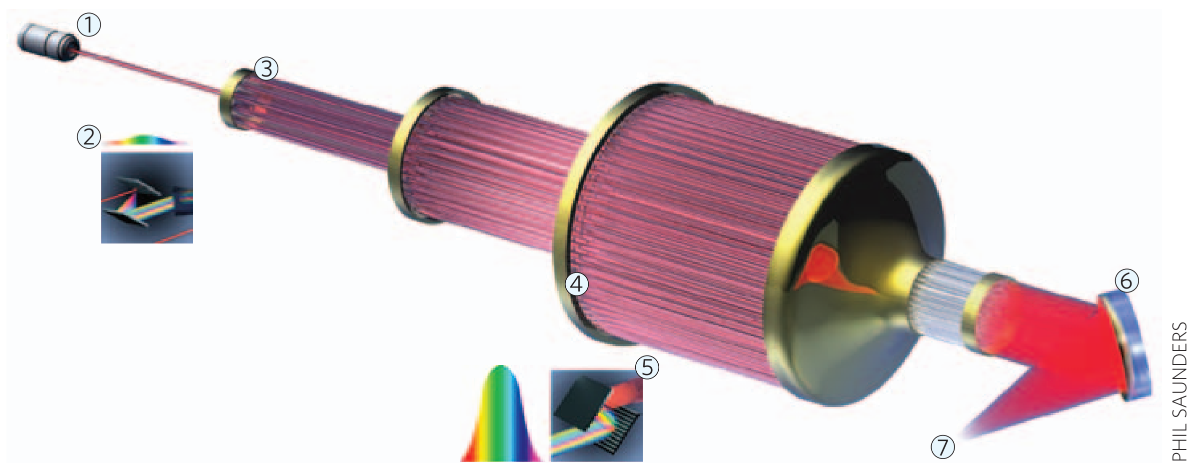

Reduction of the number of fibers by cavity enhancement

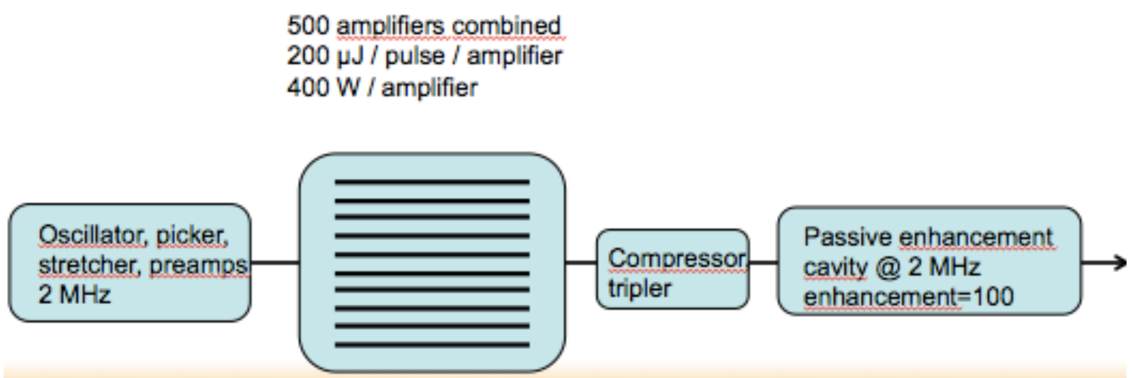

T. Eidam et al., Fiber chirped--pulse amplitification system emitting 38 GW peak power, Optics Express 19, 255, (2010)

J. Limpert, EEAC workshop, ELBA, 2013

- Yb doped single mode fiber (fiber noise)
- µm precision fiber assembly
- fiber to fiber phase shift measurement : quadriwave lateral shearing interefrometer
- phase correction by optical modulator : 64 fibers locked in 2011 !
- non linear effects
  phase locking of 8 fiber amplifiers : 3.1 µJ, 50 fs, 1 MHz

L. Daniault et al., Opt. Expr. 20, 21627 (2012)

Synchrotron Radiation

Astrophysics

The sun : Hydrogen, loops of magnetic field
visible synchrotron radiation emitted in the center,
X-ray on the edges

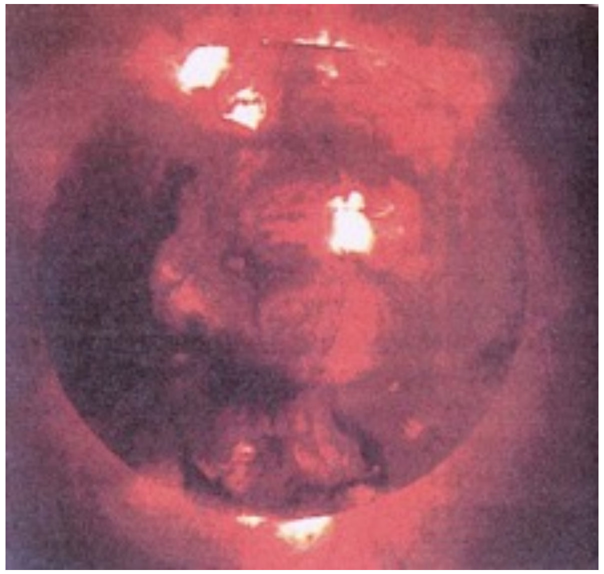

Particle accelerators

- Bending magnets in storage rings

- Undulators

Create a (quasi-) periodic (permament) magnetic field